

**UCSF**

**UC San Francisco Electronic Theses and Dissertations**

**Title**

Novel molecular insights into Epstein-Barr virus reactivation

**Permalink**

<https://escholarship.org/uc/item/9pj8j82t>

**Author**

Moquin, Stephanie Anne

**Publication Date**

2017

Peer reviewed|Thesis/dissertation

Novel molecular insights into Epstein-Barr virus reactivation

by

Stephanie Moquin

DISSERTATION

Submitted in partial satisfaction of the requirements for the degree of

DOCTOR OF PHILOSOPHY

in

Biomedical Sciences

in the

GRADUATE DIVISION

of the

UNIVERSITY OF CALIFORNIA, SAN FRANCISCO



## **Acknowledgements**

There are so many people that have contributed to my success as a scientist and as a person. I would like to start by thanking by my mentor, JJ Miranda, for his scientific guidance, compassion, and patience. I have grown so much as a scientist and a person as a member of your lab. Thank you to my thesis committee – Melanie Ott, Barbara Panning, and Katie Pollard, who were there from the beginning, asking important questions that helped guide the direction of my thesis work. Thank you to the members of the Miranda Lab over the years, Kristin, Sam, Delsy, and Amanda, who taught me so much and made lab such a great place to be. To all the incredible scientists I had the opportunity to interact with during my time at UCSF – thank you for your brilliance and willingness to help. Thank you to my undergraduate mentors – Ursula Shepherd and Christina Takacs-Vesbach, who introduced me to science and made me fall in love with it.

Thanks to all my friends who made San Francisco feel like home – both the contingent of New Mexican friends that fortuitously ended up in the Bay Area and my new-found friends and classmates. Thanks to everyone who dressed up in ridiculous costumes, shredded mountains, camped under the stars, ate delicious food, and drank delicious beer with me – you made graduate school so much more fun. Thanks to my extended family, who, despite that we are spread all around the world, manage to sometimes be in the same place at the same time, to great joy and celebration. Thank you to my siblings, Lilly and Dan, for their love and support. To my parents, Niki and Andre, thank you for being such incredible parents and for supporting me no matter what I decided to do. Thanks to the Coffmans: John, Connie, Erin, Tim, JM, TA, and Emily, who have made me feel like a member of their family from day one. And last but not least, to my husband, Phil, my adventure buddy, partner in crime, and my rock: thank you for everything that you do. You are the best.

## **Contributions**

**The contents of Chapter II are modified and reproduced from the following manuscript, which has been published as a preprint on bioRxiv and is currently under review at**

**Journal of Virology:**

Moquin S.A., Thomas S., Warburton A., Whalen S., Fernandez S., McBride A., Pollard K.S., and Miranda, J.L. 2017. The Epstein-Barr virus episome maneuvers through human chromatin during reactivation. bioRxiv. **doi:** <https://doi.org/10.1101/177345>.

**The contents of Chapter III are modified and reproduced from the following publication:**

Keck, K.M., Moquin, S.A., He, A., Fernandez, S.G., Somberg, J.J., Liu, S.M., Martinez, D.M., and Miranda, J.L. 2017. BET inhibitors block the Epstein-Barr virus lytic cycle at two distinct steps. *Journal of Biological Chemistry* 292(32), 13284-13295.

## **Novel molecular insights into Epstein-Barr virus reactivation**

**Stephanie Anne Moquin**

### **Abstract**

Epstein-Barr Virus (EBV) is a herpesvirus responsible for approximately 1% of cancers worldwide, including African Burkitt lymphoma, Hodgkin lymphoma, lymphomas in immunosuppressed patients, and nasopharyngeal and gastric carcinoma. Interestingly, the development of different cancers is mainly due to expression of the latent EBV proteins, although expression of lytic genes has recently been shown to play a role. Many of the molecular mechanisms behind EBV reactivation have been revealed, however, the contribution of chromatin dynamics to EBV reactivation is not well understood. A better understanding of how the switch between the latent and lytic cycle is regulated could have implications in treating disease. Here we investigate the contribution of chromatin dynamics to EBV reactivation in the context of i) nuclear localization and contacts with the human genome, and ii) the chromatin-reading protein BRD4. We used in situ Hi-C to show that the Epstein-Barr virus associates with repressive compartments of the nucleus during latency, and non-repressive compartments of the nucleus during reactivation. This adds 3D re-localization as a novel component to the molecular events that occur during EBV reactivation. Furthermore, we show that the protein BRD4 plays an important role in EBV lytic reactivation. BRD4 binds to the lytic origins of replication and inhibition of BRD4 by JQ1 inhibits the lytic cycle at two different steps. In summary, this work has led to a better understanding of how the latent-lytic switch of EBV is regulated.

## Table of Contents

<b>Chapter I: Introduction.....</b>	<b>1</b>
<b>EBV latency .....</b>	<b>1</b>
Genome structure .....	2
Regions of the genome important for maintaining latency.....	3
Establishment of latency and different transcriptional programs .....	3
Latent proteins and non-coding RNAs .....	4
<b>EBV reactivation.....</b>	<b>6</b>
Reactivation stimuli .....	7
Transcription of immediate early genes and early genes.....	7
Replication, late gene expression, packaging and egress .....	8
<b>EBV and disease.....</b>	<b>9</b>
Lytic diseases .....	9
Latent diseases .....	9
<b>The latent to lytic transition: translational implications.....</b>	<b>12</b>
Induce the lytic cycle: using the virus as a marker for malignant cells .....	12
Repress the lytic cycle: a role for the lytic cycle in EBV malignancies .....	13
<b>Investigation of chromatin dynamics in EBV reactivation .....</b>	<b>14</b>
3D structure of the human genome.....	14
Rationale: How does EBV interact with the 3D structure of the human genome?.....	15
BET proteins .....	16
Rationale: How do BET inhibitors affect a ubiquitous latent virus? .....	17
<b>Chapter II: The EBV episome maneuvers between nuclear chromatin compartments</b>	
<b>during reactivation.....</b>	<b>18</b>
<b>Introduction.....</b>	<b>18</b>
<b>Results .....</b>	<b>20</b>
Association of the EBV episome with the host genome depends on chromosome gene	
density .....	20
Preferential EBV chromosome associations require episomal genomes .....	21

Chromosome association preferences are conserved among some but not all episomal viruses .....	22
OriP and EBNA1 sufficiently reconstitute preferential EBV chromosome associations .....	22
EBV interacts with gene-poor human chromatin distant from transcription start sites .....	24
The EBV episome switches contacts from human heterochromatin to euchromatin during reactivation.....	24
<b>Discussion .....</b>	<b>26</b>
<b>Materials and methods .....</b>	<b>29</b>
Cell culture and plasmids.....	29
In situ Hi-C .....	30
Analysis of interchromosomal interactions .....	30
ChIP-seq.....	31
Analysis of viral-human contact regions .....	31
shRNA-mediated EBNA1 knockdown.....	32
Viral reactivation .....	33
LAD state predictions .....	33
Accession codes .....	34
<b>Chapter III: BET inhibitors block the EBV lytic cycle at two distinct steps .....</b>	<b>35</b>
<b>Introduction.....</b>	<b>35</b>
<b>Results .....</b>	<b>36</b>
BET inhibitors block immediate-early transcription .....	36
BET proteins localize to the lytic origins of replication.....	38
BET inhibitors prevent lytic DNA replication.....	39
<b>Discussion .....</b>	<b>41</b>
<b>Materials and methods .....</b>	<b>43</b>
Cell culture and treatment.....	43
Staining and flow cytometry.....	44
Western blotting.....	44
RNA-seq .....	44
ChIP-seq.....	45
EBV DNA quantitation.....	47



Replication fragment mapping.....	47
Accession codes .....	47
<b>Chapter IV: Discussion .....</b>	<b>48</b>
<b>References .....</b>	<b>51</b>

**List of Tables**

**Table 1.** EBV genes differentially regulated by JQ1 during viral reactivation..... 75

**Table 2.** EBV genes differentially regulated by I-BET during viral reactivation. .... 76

## List of Figures

<b>Figure 1.</b> EBV and its latent genes in 2016.....	77
<b>Figure 2.</b> EBV latency gene expression in different latency states.....	79
<b>Figure 3.</b> Episomal EBV genomes associate with the human genome in correlation with chromosomal gene density.....	80
<b>Figure 4.</b> KSHV but not HPV genomes associate with the human genome in correlation with chromosomal gene density.....	82
<b>Figure 5.</b> OriP-bound EBNA1 is sufficient to reconstitute chromosome association preferences of full-length EBV.....	83
<b>Figure 6.</b> EBNA1 is not necessary to reconstitute chromosome association preferences of full length EBV.....	84
<b>Figure 7.</b> EBV episomes contact gene-poor human chromatin distant from transcription start sites. ....	86
<b>Figure 9.</b> Predicted association of the EBV genome with LADs during latency and reactivation in the Akata ZTA cell line.....	89
<b>Figure 10.</b> Schematic of the EBV lytic cycle and BET inhibitor points of intervention. ....	90
<b>Figure 11.</b> BET inhibitors suppress BZLF1 expression.....	91
<b>Figure 12.</b> BET proteins bind the lytic origins of replication. ....	93
<b>Figure 13.</b> BET inhibitors suppress lytic DNA replication.....	94
<b>Figure 14.</b> JQ1 prevents BRD4 recruitment to the lytic origins of replication.....	96

## **Chapter I: Introduction**

EBV was the first human oncogenic virus to be discovered. In 1961, a young pathologist, Anthony Epstein, attended the talk of Denis Burkitt, a surgeon working in Uganda. Burkitt was studying an unusual tumor with high prevalence in Africa, which would later be named after him. Burkitt had traced the distribution of the lymphoma across Africa, and had determined that the distribution was related to temperature and rainfall, suggesting a role for an infectious agent. Epstein had previously been working with a chicken cancer virus, so was primed to the idea that a virus could cause cancer. He was extremely excited by Burkitt's talk, and Burkitt agreed to send Epstein lymphoma samples. After several years of failing to isolate a virus from the lymphomas, Epstein began to try to culture the lymphoma cells. Working with Yvonne Barr and Bert Achong, Burkitt was able to culture lymphoma explants, and after examination under the electron microscope, they saw virus particles. The particles resembled known herpesviruses at the time, but were smaller. Further studies confirmed the discovery of a new herpesvirus, which was named Epstein-Barr virus, as well as the role of the virus in Burkitt lymphoma and other malignancies.

EBV is currently the most transforming agent known to man, and can transform B cells in vitro. It infects greater than 95% of people worldwide (Thompson and Kurzrock, 2004). EBV belongs to the gammaherpesvirus family. The family name is derived from the Greek word *herpein*, which means "to creep." Fitting to its name, once a host is infected, the virus establishes a life-long infection in the B cells of its host, with occasional spontaneous reactivation. EBV is transmitted via saliva and is generally acquired asymptotically in the first few years of life, especially in non-developed countries. In more developed countries, infection with EBV can be delayed into adolescence, sometimes resulting in infectious mononucleosis (IM). EBV also infects epithelial cells.

### **EBV latency**

EBV has three main latent transcription programs, latency I, II, and III, though recent studies have identified several latency subtypes (see below for a more thorough description). The latency gene expression programs are designed to drive differentiation of a naïve B cell into a memory B

cell, a long-lived cell type. Once latency is established, EBV occasionally reactivates to produce virions.

### **Genome structure**

The virus is an enveloped virus with a circular double-stranded DNA genome (Figure 1). The genome is ~180 kb long, and expresses 1-10 proteins during latency and >80 proteins during the lytic cycle. EBV infects cells via the CD21 receptor. Subsequently, the viral genome enters the nucleus as naked linear DNA, as no histone proteins are detected by mass spectrometry (Johannsen et al., 2004). The linear DNA then forms a closed episome via its terminal repeats. Each infection results in a different number of repeats in the genome, allowing detection of clonality in cancer isolates. Once the episome is closed, the genome is heavily CpG methylated, with the exception of OriP, Cp, Qp and the EBER promoters. Interestingly, the transactivating immediate early protein BZLF1 binds preferentially to CpG methylated DNA (Kalla et al., 2011). The lack of methylation on the incoming genome may therefore contribute to abortion of the lytic cycle and establishment of latency after initial infection.

Histones also bind the viral genome. Interestingly, activating histone marks can be found on the viral genome, but repressive histone marks (H3K27m3 and H3K9m3) are largely absent or have very low enrichment. H3K4m1, H3K4m2 and H3K4m3 are enriched at the EBER-OriP-Cp locus, the BART transcript promoter region (BARTp) and the LMP2-LMP1 promoter locus. Acetylated histones (H3K9ac and H3K27ac) are enriched at sites of transcription initiation at Cp, BARTp, LMP1p, and LMP2a promoter region (Arvey et al., 2013). By ChIP-seq, there is enrichment of the repressive mark H3K9m3 at the FR region of OriP and modest H3K27m3 enrichment at BHLF1 (Arvey et al., 2013).

Furthermore, CTCF and cohesin, proteins that ubiquitously bind the human genome to demarcate chromatin boundaries, bind across the EBV genome as well (Arvey et al., 2013; Chau et al., 2006; Day et al., 2007; Holdorf et al., 2011). CTCF binding at latency promoters Cp and Qp prevents spread of repressive chromatin to Qp (Tempera et al., 2010). These binding sites also mediate chromatin loops to promote latency type-specific promoter usage (Tempera and Lieberman, 2010; Tempera et al., 2011).

### **Regions of the genome important for maintaining latency**

OriP is the origin of replication for the viral genome. This 1.7 kb region is also important for maintaining viral episomes in daughter cells during cell division. These two functions are mediated by binding of the viral protein EBNA1 to two main elements, dyad symmetry (DS) and family of repeats (FR). The DS element mediates replication of the viral genome. DS contains four binding sites for EBNA1, which recruits cellular DNA replication machinery. The FR contains 20 binding sites for EBNA1 and its main role is plasmid maintenance during cell division. This is accomplished by binding of EBNA1 to the FR via its C-terminal domain, and binding of EBNA1 to mitotic chromosomes via the chromosome binding domain, which binds AT-rich DNA.

OriP also acts as an enhancer for the Cp and LMP1 promoters (Gahn and Sugden, 1995; Nilsson et al., 2001; Puglielli et al., 1996). 3C data shows that OriP forms loop with different promoters based on expression pattern – OriP is in close physical space with the Qp promoter during latency I and in close physical space with the Cp promoter during latency III (Tempera et al., 2011).

### **Establishment of latency and different transcriptional programs**

See Figure 2. The most well accepted model for how latency is established in memory B cells is that EBV infects naïve B cells, and expresses a complex transcriptional program that drives differentiation through a germinal center reaction and into a memory B cell. Within several hours after circularization and chromatinization of the genome, there is a burst of expression of EBV lytic genes without full lytic replication. This includes the immediate early protein BZLF1 (Wen et al., 2007), and the viral Bcl-2 homologues BHRF1 and BALF1 (Altmann and Hammerschmidt, 2005), which prevent apoptosis and are critical for establishing latency. Along with the burst of lytic genes, the latent proteins EBNA2 and EBNA-LP are expressed from the Wp promoter. This state is referred to as pre-latency. EBNA2 and EBNA-LP are transcription factors, and together, they activate the upstream promoter, Cp, leading to the expression of all 6 EBNA proteins from a single, alternatively-spliced transcript. The viral BART miRNAs as well as the non-coding EBER RNAs are expressed. The LMP proteins are only expressed at low levels during this stage of infection, which has been termed latency Iib. Subsequently, latency III

is observed, which is characterized by expression of all EBNA and all LMP proteins, and the BARTs and EBERs. LMP1 mimics a constitutively active host CD40 (Mosialos et al., 1995) and is a highly transforming protein.

After EBV infection *in vitro*, latency III is the final gene expression pattern that is observed in transformed lymphoblastoid cell lines (LCLs). However, *in vivo*, latency III is highly immunogenic, and epitopes from these proteins are recognized by cytotoxic T lymphocytes (CTLs), leading to killing of infected cells. This immune pressure likely leads to the more restricted forms of latency. Latency IIa is characterized by expression of EBNA1 from the Qp promoter, and expression of LMP1 and LMP2A, as well as the BARTs and EBERs. Finally, the latent expression pattern is fully restricted to latency 0, where no viral proteins are expressed, or latency I, where only EBNA1 is expressed in order to ensure equal division of the viral episome to daughter cells during cell division. During both latency 0 and I, both the BARTs and EBERs are expressed. Since EBNA1 inhibits antigen presentation of itself (Levitskaya et al., 1995; 1997), cells in latency 0 or I evade immune detection. Thus, the majority of EBV latently infected cells *in vivo* are peripheral blood class-switched memory cells (Babcock et al., 1998) expressing latency 0 or I. While this sequence of events and transcriptional programs has been determined using mostly *in vitro* models, evidence from *in vivo* models support these conclusions, as different forms of EBV-associated cancers display these different transcription programs (see below).

### **Latent proteins and non-coding RNAs**

EBNA1. Expressed during all forms of latency, EBNA1 is a sequence-specific DNA-binding protein required for replication and maintenance of the genome. EBNA1 binds at the FR and DS regions of OriP and also at the Qp promoter. EBNA1 binds the viral genome in a sequence-specific manner via its C-terminal DNA-binding domain (DBD). This DBD has structural similarity to the KSHV protein LANA-1 and the HPV protein E2, which also tether viral genomes to the human genome (Bochkarev et al., 1995). EBNA1 has two chromatin-binding domains (CBDs), which attach to metaphase chromatin in a sequence-independent manner. The CBDs have been found to interact with AT-rich DNA, G-quadruplex RNA, histone H1, EBP2, and nucleosome core particles (Hung et al., 2001; Kanda et al., 2013; Norseen et al.; Sears et al.,

2004). Thus, EBNA1 binds the viral genome in a sequence-specific manner via its DBD, and tethers the viral genome to metaphase chromosomes via interactions with its two CBD domains.

EBNA2. Together with EBNA-LP, EBNA2 is one of the first latent proteins expressed after infection of a cell (pre-latent phase), and during latency IIb and latency III. It is a transcriptional coactivator that mainly serves to up-regulate the expression of viral EBNA proteins from the Cp promoter. It also upregulates cellular genes, such as *CD23* (surface marker of activated B cells), and *c-myc* (a cellular proto-oncogene).

EBNA-LP. Together with EBNA-2, EBNA-LP is one of the first latent protein expressed after infection of a cell (pre-latent phase), and during latency IIb and latency III. It interacts with EBNA-2 to drive resting B lymphocytes into the G1 phase of the cell cycle by binding and inactivating cellular *p53* and *retinoblastoma* protein tumor suppressor gene products.

EBNA-3A, EBNA-3B, and EBNA-3C. Expressed during latency IIb and latency III, the EBNA3 proteins are transcriptional regulators. EBNA-3A and EBNA-3C are critical for transformation (Tomkinson et al., 1993). EBNA-3C increases the production of LMP-1 in some conditions, and also may overcome the *retinoblastoma* tumor suppressor gene checkpoint in the G1 phase of the cell cycle. All three EBNA3 proteins also interact with CBP1/RBP-Jk, which is involved in the Notch signaling pathway.

LMP-1. Expressed during latency III and latency IIa, LMP1 is essential for EBV immortalization (Kaye et al., 1993) and is a classical oncogene (Wang et al., 1985). LMP-1 is a membrane protein that acts as a constitutively active receptor similar to CD40, mimicking cellular growth signals. At least four diverse signaling cascades are implicated in the function of LMP-1: NF- $\kappa$ B, JNK signaling, p38 MAP kinase, and the JAK/STAT pathway. These activating cascades lead to increased expression of B cell adhesion molecules, B cell activation markers, and anti-apoptotic proteins such as Bcl-2 and A20.

LMP-2A and LMP-2B. Expressed during latency III and latency II, LMP-2A and LMP-2B are both membrane proteins. LMP2A is a B cell receptor (BCR) mimic that can prevent apoptosis of



BCR-negative cells (Caldwell et al., 1998). Therefore LMP-2A can promote the survival of cells that would otherwise die of apoptosis due to lack of BCR signaling.

BHRF1. Expressed during pre-latency, latency IIb and latency III, BHRF1 is Bcl-2 homologue (Henderson et al., 1993; Pearson et al., 1987), which protects B cells from programmed cell death (Henderson et al., 1983). Originally thought to be a lytic protein, has now been shown to be expressed early in infection to prevent apoptosis (Altmann and Hammerschmidt, 2005; Kelly et al., 2009).

BARF1. Originally described as a lytic gene, BARF1 has been shown to transform cells (Wei and Ooka, 1989; Wei et al., 1994); highly expressed in NPC and GC in the absence of other lytic genes (Seto et al., 2005).

EBER1 and EBER2. Expressed in all forms of latency, these two RNAs are thought to form secondary structures to interact with a variety of proteins in order to modulate innate immunity (reviewed in (Iwakiri and Takada, 2010)). They have been shown to be excreted in exosomes (Ahmed et al., 2014) and are highly expressed in NPC.

BamHI-A rightward transcript (BART) miRNAs. Expressed in all forms of latency, there are 44 verified BART miRNAs to date (Kozomara and Griffiths-Jones, 2014). These miRNAs maintain latency by targeting EBV lytic genes and pro-apoptotic proteins, regulating LMP1 expression, impairing host immune responses and inactivating tumor suppressor genes (Hsu et al., 2014; Kanda et al., 2015; Kang et al., 2015; Lei et al., 2013; Marquitz and Raab-Traub, 2012; Shinozaki-Ushiku et al., 2015; Vereide et al., 2014). They are highly expressed in NPC.

### **EBV reactivation**

EBV spends the majority of its lifecycle in the latent phase. Occasionally, the virus reactivates, switching from a latent transcription pattern of 1-10 proteins plus RNAs, to the full 80+ proteins required for replication, packaging, and egress of new virions.

## **Reactivation stimuli**

*In vivo*, it is likely that EBV is reactivated by differentiation signals in B cells (Tovey et al., 1978), specifically, stimulation of the B cell receptor and differentiation into plasma cells (Laichalk and Thorley-Lawson, 2005). Differentiation also reactivates epithelial cells (Young et al., 1991). Similarly, *in vitro*, anti-IgG activation of the B cell receptor cells can reactivate the virus. This is thought to be the most physiologically relevant form of reactivation. Other stimuli including phorbol esters such as TPA (Gao et al., 2001), TGF $\beta$  (di Renzo et al., 1994a; 1994b; Fahmi et al., 2000; Iempridee et al., 2011), hypoxia (Jiang et al., 2006), calcium ionophores (Faggioni et al., 1986), 5-azacytidine (Ben-Sasson and Klein, 1981), and various agents that induce DNA damage such as irradiation (Roychowdhury et al., 2003; Westphal et al., 2000) and chemotherapeutic drugs (Feng et al., 2004; 2002a; Fernandez and Miranda, 2016) also reactivate EBV. Additionally, histone deacetylase (HDAC) inhibitors such as sodium butyrate, trichostatin A, and valproic acid induce lytic EBV gene transcription in some cell lines (Davie, 2003). These agents likely function by increasing the histone acetylation state of the two viral immediate early gene promoters. Treatment with reactivating agents leads to activation of signal transduction pathways including PI3 kinase, p38 kinase, ERK kinase, and protein kinase C. During anti-IgG reactivation, calcium-dependent mechanisms are also important (Kenney, 2007).

## **Transcription of immediate early genes and early genes**

Ultimately, treatment with reactivating agents and activation of signaling cascades leads to binding of host transcription factors to the promoters of the immediate early (IE) proteins BZLF1 and BRLF1 and their subsequent transcription, reviewed in (Kenney and Mertz, 2014). A variety of cellular transcription factors both negatively and positively regulate the promoters of BZLF1 and BRLF1 (Kenney, 2007). These two proteins then bind to promoters of the early EBV genes and start the lytic cascade; however, BZLF1 on its own is sufficient to activate the lytic cycle (Countryman and Miller, 1985).

Once BZLF1 is transcribed, it transcriptionally activates the early viral genes by directly binding to DNA at BZLF response elements (ZREs) (Kenney, 2007). Interestingly, BZLF1 preferentially binds methylated promoters (Bhende et al., 2004), allowing the virus to circumvent the normally repressive effects of DNA methylation. Along with activating several cellular genes (Kenney,

2007), many of the EBV early proteins that BZLF1 activates are those involved in replication: the viral DNA polymerase (BALF5), the DNA polymerase processivity factor (BMRF1), the single-stranded DNA binding protein (BALF2), a helicase (BBLF4), a primase (BSLF1), a primase-associated protein (BBLF2/3), and the viral thymidine kinase (BXLF1), which makes nucleotides available for replication. EBV expresses another early kinase, BGLF4. BGLF4 phosphorylates a variety of host proteins, resulting in chromatin condensation (Lee et al., 2007) and disassembly of the nuclear lamina (Lee et al., 2008). Other early genes include the transcription factor that activates the lytic origin of replication (OriLyt) (BMRF1), a protein that regulates RNA stability (SM), and proteins that inhibit apoptosis (BHRF1) and promote immune evasion (BARF1).

### **Replication, late gene expression, packaging and egress**

Replication of the viral genome during the lytic cycle occurs through a rolling circle mechanism. This results in concatamers of head-to-tail copies of the viral genome, which are cleaved at the terminal repeats and packaged into virions. Lytic replication requires the six viral core replication proteins and BZLF1, which directly interacts with several core replication proteins.

EBV late genes are expressed after replication. Late genes promoters do not contain BZLF binding sites; instead, they have non-canonical TATA boxes, with a thymidine in the fourth position (TATT). These sequences are bound by a complex of six viral proteins (BcRF1, BDLF3.5, BDLF4, BFRF2, BGLF3, and BVLf1) to promote late gene transcription (Djavadian et al., 2016). The late genes are mostly structural proteins, including tegument and nucleocapsid proteins, and glycoproteins. Two non-structural late proteins of note are BCLF1 and BALF1. BCLF1, or viral IL-10 (vIL-10), is a homologue of host IL-10, which potently represses the cytotoxic T cell response (Hsu et al., 1990). BALF1 is a Bcl-2 homologue, though it is unclear whether it promotes or prevents apoptosis (Bellows et al., 2002; Marshall et al., 1999).

The viral genome is packaged into nucleocapsids. The nucleocapsids escape the nucleus by budding through the inner nuclear membrane into the perinuclear space, and then fusing with the outer nuclear membrane in order to enter the cytoplasm. Once in the cytoplasm, the nucleocapsid acquires the rest of the tegument proteins and its final envelope by budding through a

cytoplasmic compartment, likely the trans-golgi network, and exits the cell via exocytosis (reviewed in (Mettenleiter, 2002)).

## **EBV and disease**

### **Lytic diseases**

There are two main forms of EBV-associated disease are associated with the lytic cycle of the virus – infectious mononucleosis (IM) and oral hairy leukoplakia (OHL). During IM, after infection with EBV, there is an initial stage of B cell proliferation; however after a few weeks the B cells begin to die. This death is mediated by CD4+ and CD8+ T cells, which recognize viral epitopes and kill the lytic B cells (Moss et al., 1988). OHL is a hyperproliferative lesion seen only in severely immunocompromised patients, but it is easily treatable by antiviral agents that inhibit the lytic cycle of EBV (Walling et al., 2003). Furthermore, lytic genes have been shown to play a role in the development post-transplant lymphoproliferative disease (Hong et al., 2005b).

### **Latent diseases**

Unlike alpha and beta-herpes viruses, which cause disease during the lytic phase of the viral lifecycle, most EBV-associated diseases are associated with the latent phase of the viral lifecycle. There are several types of latency during which 1-10 latent viral proteins and several small RNAs are expressed (see above); different types of cancer are associated with different forms of latency. Despite EBV's strong ability to transform cells *in vitro*, its role in each type of cancer is different. In some cancers, strong evidence points to EBV as the oncogenic driver, while in other cancers, EBV seems to be a secondary agent, infecting cells that are predisposed to a cancerous phenotype, and contributing the final molecular events to proceed with oncogenesis. Below is a non-exhaustive description of the most significant and well-understood cancers that have been linked to EBV.

### **Burkitt lymphoma (BL)**

There are two forms of Burkitt lymphoma – endemic, which is found in sub-saharan Africa, and sporadic, which occurs around the rest of the world. Interestingly, while 90-95% of BL is sub-saharan Africa is EBV-positive, there are also sporadic EBV-negative BL tumors found

worldwide. Thus, BL is not characterized by the presence of EBV, rather it is characterized by translocation between the MYC gene on chromosome 14, and an immunoglobulin enhancer, most commonly the IgH enhancer on chromosome 8 (Bernheim et al., 1980; Erikson et al., 1983).

The distribution of endemic Burkitt lymphoma in accordance with temperature and rainfall led to the hypothesis that an arthropod-borne vector may be involved. Though EBV is not arthropod-borne and acquired early in life by most of the human population, a contribution from the malaria parasite, *Plasmodium falciparum*, whose distribution is related to temperature and rainfall, has long been suspected. Recently, the mechanisms behind this contribution are becoming clearer. Infection with *P. falciparum* likely induces an expansion of memory B cells, increasing the pool of EBV-infected cells. Furthermore, the parasite can increase expression of the enzyme activation-induced cytidine deaminase (AID) (Torgbor et al., 2014), an enzyme normally expressed in germinal center cells and important for creating antibody diversity. Increased expression of AID may promote translocations, including the MYC translocation that is a hallmark of BL. Normally, high levels of MYC expression would lead to death of the cell by apoptosis; however, evidence suggests that expression of EBV proteins provide resistance to this apoptosis (Kelly et al., 2009). Thus, the combination of the two agents leads to an increased prevalence of BL in sub-Saharan Africa. In summary, the malaria parasite induces B cell proliferation, increasing the pool of EBV-infected cells. The parasite also deregulates the expression of AID, increasing the probability of a MYC translocation. EBV then provides resistance to apoptosis usually induced by high MYC levels. Thus, the synergistic effect of malaria and EBV lead to the high prevalence of BL in sub-saharan Africa. In sporadic BL seen across the rest of the world, other mutations help cells survive MYC over-expression.

#### Post-transplant lymphoproliferative disorder (PTLD)

Normally, cells infected with EBV that express latency III or lytic proteins are killed by surveilling T cells. However, in immunocompromised patients, these circulating cells are reduced and lymphomas can develop. This heterogeneous group of tumors generally express latency III and are collectively referred to as post-transplant lymphoproliferative disorder (PTLDs). Reduction of immune suppression is the first mode of treatment, followed by the drug

rituximab, chemotherapy or radiotherapy. Furthermore, as PTLDs express all latent proteins, they are sensitive to EBV-specific T lymphocytes, and CTL therapy has been successful in treating them.

### Hodgkin lymphoma (HL)

HL is an unusual tumor comprised of Hodgkin-Reed-Sternberg cells (HRS), which are large and often binucleated. They are surrounded by various non-malignant inflammatory cells including T cells, macrophages and fibroblasts. HRS cells are extensively somatically hypermutated, and often contain a non-functional immunoglobulin gene, which normally would lead to apoptosis. Thus, HL cells generally express latency IIa, and it is believed that LMP1 and LMP2A provide the anti-apoptotic signal for these cells by mimicking the CD40 receptor and BCR functions, respectively (Alber et al., 1993; Klein, 1983; Pallesen et al., 1991).

### Burkitt lymphoma in HIV-infected patients

BL in HIV patients contains the canonical *MYC* translocation, and occurs when CD4 T cell counts are still relatively normal. In the same way that malaria is thought to contribute to BL, HIV is thought to increase the pool of EBV-infected B cells that carry an accidental *MYC* translocation.

### EBV and epithelial cancers

In contrast to the infection of B cells by EBV, which use the CD21 receptor to gain entry into the cell, the infection route for epithelial cells is thought to occur via cell-to-cell transmission (Imai et al., 1998; Shannon-Lowe and Rowe, 2011). Epithelial cancers express latency II, or a variant thereof (Imai et al., 1994; Young et al., 1988), though contribution of EBV genes to oncogenesis in epithelial cancers is less well understood.

Nasopharyngeal carcinoma (NPC) is a cancer of the nasopharynx, which has a high prevalence in parts of south China. Evidence points to both genetic and environmental factors as risks for NPC, as descendants of Chinese immigrants in California have lower risk than their parents, but still have an elevated risk compared to the non-Chinese population. It is believed that the contribution of EBV to NPC is a relatively late event in development of cancer (Hausen et al.,

2004). The current hypothesis is that premalignant lesions form (Tsao et al., 2015; Young and Rickinson, 2004), possibly as a result of exposure to carcinogenic nitrosamines in foods such as salted fish or other preserved food, as well as smoking (Jia and Qin, 2012). These lesions then become susceptible to EBV infection, and EBV provides growth and survival benefits, resulting in the development of NPC.

As in NPC, EBV is thought to play a late role in gastric cancer (GC), as demonstrated by the absence of EBV in premalignant lesions (Hausen et al., 2004). Approximately 10% of gastric cancers are EBV positive (Tsao et al., 2015), and EBV positive GC are distinct from EBV-negative GC (Cancer Genome Atlas Research Network, 2014; Lee et al., 2004; Schneider et al., 2000; Ushiku et al., 2007; van Rees et al., 2002; Wang et al., 2014).

### **The latent to lytic transition: translational implications**

A deeper understanding of the EBV latent-lytic switch could have implications in treating disease.

### **Induce the lytic cycle: using the virus as a marker for malignant cells**

Acyclovir and its more broad and potent cousin, ganciclovir (GCV) are nucleoside analogs commonly used to treat lytic infections of herpesviruses (Cheng et al., 1983). Both acyclovir and ganciclovir are converted to their monophosphate form by the viral thymidine kinase. Host kinases do not phosphorylate ganciclovir, making this drug specific to cells infected with the virus. The monophosphate forms are then converted to the triphosphate form by cellular enzymes, and are subsequently incorporated into the growing chain of viral DNA. Since these analogs lack the 3'-OH group required for chain elongation during DNA synthesis (Furman et al., 1979), this leads to premature termination of viral replication (Lin et al., 1984). This results in double-stranded DNA breaks and subsequent cell death by apoptosis (Tomicic et al., 2002). Death of "bystander" cells can also be induced by GCV (Freeman et al., 1993), because the converted monophosphate form diffuses to other cells.

Though nucleoside analogs are effective against the lytic EBV disease oral hairy leukoplakia (Newman and Polk, 1987; Resnick et al., 1988), they are not effective against EBV-associated

malignancies, because the viral thymidine kinase is only expressed during the lytic cycle, and most EBV-associated malignancies express only latent proteins. Accordingly, scientists have proposed lytic induction therapy (Ambinder et al., 1996; Feng et al., 2004; 2002b; Gutiérrez et al., 1996; Kenney et al., 1998; Mentzer et al., 1998; 2001), where patients would be given with drugs that reactivate the lytic cycle, such as the chemotherapeutic drugs gemcitabine and doxorubicin, in combination with GCV. Reactivation of the virus leads to expression of immediate early protein BZLF1 as well as the rest of the lytic proteins including the viral thymidine kinase. The thymidine kinase phosphorylates GCV and converts it to a cytotoxic form, killing the EBV-infected cancer cells. Chemotherapeutics plus GCV have been shown to be more effective than chemotherapeutics alone.

Lytic induction therapy, also known as cytolytic virus activation (CLVA), has been shown to be effective in mouse models of lymphoproliferative disorder (Feng et al., 2004) and gastric carcinoma (Feng et al., 2002a). In humans, this strategy has been tested on six patients with EBV-associated lymphoma or PTLDs – with 4 of 6 showing complete clinical response, and a fifth showing a partial response (Mentzer et al., 2001). Ten of 15 patients with EBV-associated malignancies showed significant anti-tumor responses, though 3 patients experienced complications from rapid tumor lysis (Perrine et al., 2007). In three patients with late-stage NPC, treatment with gemcitabine and valproic acid in conjunction with GCV resulted in clear improvement in clinical condition – patients with progressive disease became stable (Wildeman et al., 2012). Further studies with larger cohorts and different types of EBV-positive malignancies need to be tested to determine the effectiveness of this approach.

### **Repress the lytic cycle: a role for the lytic cycle in EBV malignancies**

Surprisingly, although most EBV-related malignancies express latent genes, it has now been demonstrated that the lytic proteins play an important role in establishment of both lymphoproliferative disease in SCID mice (Hong et al., 2005a; 2005b) as well as the development of B cell lymphomas in immunocompetent mice (Ma et al., 2011). LCLs derived from viral genomes lacking either of the immediate early genes BZLF1 or BRLF1 are impaired in growth in SCID mice compared to LCLs derived from WT genomes (Hong et al., 2005b). These tumors 1) express dramatically less of the lytic protein BHRF1, which encodes a Bcl-2



homologue (Hong et al., 2005b), 2) express less paracrine growth factors such as IL-6, IL-10 and viral IL-10 (Hong et al., 2005b), which have been shown to enhance the growth of LCLs (Scala et al., 1990; Vockerodt et al., 2001) and survival of some EBV-positive lymphoma explants (Masood et al., 1995), and 3) express less vascular endothelial growth factor, which is an angiogenesis factor (Hong et al., 2005a). Thus, the lytic cycle seems to be important early in the establishment of EBV-associated tumors via production of paracrine growth factors that promote cell growth and survival, angiogenesis factors, and anti-apoptotic proteins. In this way, suppressing the lytic cycle could possibly prevent the development of malignancies.

### **Investigation of chromatin dynamics in EBV reactivation**

#### **3D structure of the human genome**

The chromatin of a human interphase nucleus is structurally and functionally organized. Recent technical advances such as in situ Hi-C have allowed us to look at the 3D structure of the human genome at very high resolution—as small as 1-kb scale. This data shows that chromosomes are subdivided into what have been called topologically associated domains (TADs). TADs are defined as structural genomic units characterized by sharp boundaries, which promote long-range interactions within but not between different domains (Dixon et al., 2015). TADs on average measure ~200 kb each (Rao et al., 2014), and fold into discrete globules in three-dimensional space (Boettiger et al., 2016). TADs can be classified into two main groups – compartment A, which replicates early and contains chromatin marks consistent with traditionally defined euchromatin, and compartment B, which replicates late and contains chromatin marks consistent with traditionally defined heterochromatin (Lieberman-Aiden et al., 2009).

Examination of these initial compartments at a higher resolution has led to their subdivision – compartment A can be subdivided into two sub-compartments, and compartment B can be subdivided into four subcompartments (Rao et al., 2014). Subcompartment B1 is correlated with marks suggesting facultative heterochromatin, B2 contains a large percentage of pericentromeric heterochromatin and is enriched at the lamina and at nucleolus-associated domains (NADs). Subcompartment B3 is enriched at the lamina, but strongly depleted at NADs.

Of these different subcompartments of heterochromatin, chromatin associated with the nuclear lamina, known as lamin-associated domains (LADs), have been mapped using a technique called Dam-ID (Guelen et al., 2008; Pickersgill et al., 2006). LADs tend to be large and gene-poor, with lower average transcription (Guelen et al., 2008; Peric-Hupkes et al., 2010). Some LADs are constitutive, and remain associated with the lamina, while genes found in variable LADs can change their associations with the lamina based on transcription or cell-type. Examples of this behavior include the following genes: IgH (Kosak et al., 2002), CFTR (Zink et al., 2004), and casein (Ballester et al., 2008; Kress et al., 2011). Furthermore, cell-type specific genes move in and out of the lamina during development (Guelen et al., 2008; Peric-Hupkes et al., 2010). Loss of association with the lamina does not necessarily result in transcription, but rather “unlocks” genes for later transcription (Peric-Hupkes et al., 2010). Furthermore, a collective of work that artificially targets genes to the nuclear periphery show that genes at the periphery do not necessarily lose the ability to become transcriptionally active, but are generally more susceptible to silencing than the nuclear interior (Harr et al., 2015; Kumaran and Spector, 2008; Reddy et al., 2008; Zullo et al., 2012).

Interphase chromatin is highly dynamic (review in Gasser, 2002). In the spaces between chromosome territories, chromatin from different territories intermingle; inhibition of transcription changes intermingling patterns of some chromosomes (Branco and Pombo, 2006). Active genes dynamically colocalize in nuclear space to undergo transcription in shared transcription factories (Osborne et al., 2004), with some genes even looping out of their chromosome territories during gene activation (Chambeyron and Bickmore, 2004; Volpi et al., 2000). Interactions with the transcriptionally repressive nuclear periphery are also not static, with genes moving in and out of the lamina with transcriptional changes, as noted in the previous paragraph. Taken together, these studies show that chromatin is dynamic and that nuclear neighborhoods affects transcription.

#### Rationale: How does EBV interact with the 3D structure of the human genome?

The latent EBV genome is chromatinized, double-stranded DNA. Since the EBV genome has a similar structure to human chromatin and uses similar mechanisms to control transcription at the protein level (i.e. methylation, histone marks), we wondered whether the virus also uses the 3D

structure and functional organization of the nucleus to regulate gene expression and the genetic switch from latency to the lytic cycle. This investigation was the main topic of my thesis work and is presented in Chapter II.

### **BET proteins**

Lysine acetylation of histone tails is one of the markers of open chromatin. Acetylated lysines can be recognized by bromodomains. The bromodomain and extra-terminal domain (BET) family proteins (BRD2, BRD3, BRD4, and BRDT) are chromatin ‘readers’: they recognize acetylated lysines on histone tails via their bromodomain. Subsequently, they can recruit transcriptional regulator complexes and initiate transcription. Recently, a specific inhibitor of the BRD proteins, JQ1, has been described (Filippakopoulos et al., 2010). JQ1 binds in the acetyl-binding pocket of the BRD proteins, resulting in specific inhibition.

BRD4 plays a role in EBV enhancer (Lin et al., 2008) and promoter (Palermo et al., 2011) function. BET proteins have also been shown to play an important role in the lifecycles of other viruses. Viral proteins of both bovine papilloma virus (You et al., 2004) and Kaposi’s Sarcoma herpesvirus (KSHV) (You et al., 2006) bind BRD4 as a tether to host mitotic chromosomes to ensure equal segregation of viral genomes to daughter cells during cell division. BRD4 also plays an important role in the transcriptional activation of papillomaviruses (Ilves et al., 2006; McPhillips et al., 2006; Schweiger et al., 2006). Interestingly, opposite from what might be expected from inhibition of proteins that activate transcription, inhibition of BET proteins via treatment with BET inhibitors can reactivate HIV (Zhu et al., 2012), KSHV (Chen et al., 2017), and herpes simplex virus (Alfonso-Dunn et al., 2017; Ren et al., 2016).

BET inhibitors have also shown effectiveness in treating several forms of cancer (Asangani et al., 2014; Delmore et al., 2011; Jung et al., 2015; Mertz et al., 2011). MYC is involved in the pathogenesis of many cancers. Treatment with BET inhibitors decreases MYC expression, and subsequently decreases expression of MYC regulated genes (Delmore et al., 2011). As super enhancers such as those involved in the transcription of the *MYC* oncogene are more sensitive to treatment with JQ1 (Lovén et al., 2013), and tumor cells are often dependent on high levels of

expression of these oncogenes, tumor cells may be selectively more sensitive to JQ1 treatment compared to other somatic cells.

Rationale: How do BET inhibitors affect a ubiquitous latent virus?

The possible use of BET inhibitors as cancer treatment coupled with the knowledge that BET inhibitors can reactivate certain viruses led us to think about the possible implications of reactivating viruses from latency during cancer treatment. This led us to investigate the role of BET proteins in EBV reactivation. Contrary to many other viruses, we found that BET inhibitors inhibit EBV lytic reactivation at several distinct points in the EBV lifecycle. The results of these experiments are further discussed in Chapter III.

## **Chapter II: The EBV episome maneuvers between nuclear chromatin compartments during reactivation**

### **Introduction**

The chromatin of a human interphase nucleus is structurally and functionally organized at multiple scales. Chromosomes are subdivided into topologically associated domains (TADs), structural genomic units characterized by sharp boundaries that promote long-range interactions within but not between different domains (Dixon et al., 2012). TADs on average measure ~200 kb each (Rao et al., 2014) and fold into discrete globules in three-dimensional space (Boettiger et al., 2016). Each TAD may be classified into one of two large groups that correlate well with traditionally defined active euchromatin and inactive heterochromatin based on histone modifications, gene density, and polymerase occupancy (Kalhor et al., 2011; Lieberman-Aiden et al., 2009; Rao et al., 2014). Furthermore, TADs preferentially associate with other TADs of the same type within the same chromosome, resulting in two main compartments in the nucleus, termed compartment A and compartment B, which again roughly correspond to euchromatin and heterochromatin (Kalhor et al., 2011; Lieberman-Aiden et al., 2009; Rao et al., 2014). These two functionally distinct partitions of each chromosome are physically separated in the nucleus (Wang et al., 2016). Assembly mediated by long-range interactions also compacts individual chromosomes so that each occupies a discrete globular space known as a chromosome territory (Bolzer et al., 2005). These territories similarly partition into two main groups: gene-rich chromosomes found in the center of the nucleus and gene-poor chromosomes found at the periphery (Boyle et al., 2001). The organization of DNA does not necessarily proceed in a hierarchical manner but nonetheless spans scales of many orders of magnitude. Clearly, genome structure and function are linked on many levels.

Interphase chromatin is highly dynamic in a manner coupled to changes in transcription. As the transcriptional state of a TAD changes, that unit rearranges intrachromosomal contacts to associate with similarly active or inactive domains (Dixon et al., 2015). Reorganization is not, however, only restricted to changes in local interactions. Interchromosomal associations activate genes (Branco and Pombo, 2006; Ling et al., 2006; Lomvardas et al., 2006) and actively transcribed genes from different chromosomes colocalize (Fullwood et al., 2009; Osborne et al.,

2004). In many cases, genes move out of a chromosome territory when activated (Chambeyron and Bickmore, 2004; Lieberman-Aiden et al., 2009; Volpi et al., 2000). Such long-range contacts make the spaces between chromosome territories a dynamic interface. Inhibition of transcription changes intermingling patterns of chromosome pairs, suggesting that gene activity may drive these associations (Branco and Pombo, 2006). Taken together, these studies show that interchromosomal chromatin interactions are dynamic and that nuclear repositioning is often coupled with changes in transcription.

The human Epstein-Barr virus (EBV) is a double-stranded DNA herpesvirus that is maintained as an episome in the nucleus of a host cell. The viral genome is circular and chromatinized, resembling a small human chromosome in many molecular aspects. Like most herpesviruses, EBV establishes lifelong latency and occasionally undergoes spontaneous reactivation. The virus displays several different latent transcription programs in which different combinations of ~10 or fewer transcripts are expressed. During reactivation, transcription drastically increases to ~100 transcripts as the virus produces the proteins necessary for replication of the genome and packaging of new virions (Kenney, 2007). Latent gene expression patterns are regulated by three-dimensional intrachromosomal interactions within the viral genome (Arvey et al., 2012; Tempera et al., 2011), but how interchromosomal interactions between the virus and the human genome affect viral transcription is understudied for technical reasons.

Since the EBV genome has a similar structure to human chromatin and uses similar mechanisms to control transcription at the protein level, we wondered whether the virus also uses the 3D structure and functional organization of the nucleus to regulate gene expression and the genetic switch to a very transcriptionally active state. As a first step toward answering this question, we sought to understand the extent of engagement with this nuclear organization when double-stranded DNA viruses infect cells. Here we use *in situ* Hi-C (Rao et al., 2014) to measure interactions between the EBV genome and the human genome during latency and reactivation. We show that during latency, the EBV genome uses a small genetic element to interact with a network of repressive heterochromatin. Upon reactivation, the viral genome engages in different associations to leave this repressive environment and surround itself with active euchromatin.

## **Results**

### **Association of the EBV episome with the host genome depends on chromosome gene density**

We measured spatial DNA-DNA contacts with in situ Hi-C (Rao et al., 2014) to determine how the EBV episome interacts with human chromosomes and different nuclear compartments. To maximize signal for the transcriptionally quiescent form of the latent episome, we chose to examine Daudi, KemIII, RaeI, and Raji, Burkitt lymphoma cell lines that display very little spontaneous lytic reactivation capable of generating newly replicated linear genomes (Phan et al., 2016). Raji and Daudi cells contain ~60 and ~150 copies of the EBV episome, respectively (Pritchett et al., 1976). Our Hi-C data sets contain ~17–40 million valid paired end contacts after quality control filtering, of which ~4–9 million are interchromosomal and ~10,000–230,000 between the EBV episome and human genome.

First we examined interchromosomal interactions within the human genome at chromosome-level resolution by measuring observed interactions between different human chromosomes relative to random expectation. This metric normalizes for both random associations and chromosome length. We calculated robust and high-confidence ratios by obtaining similar sequencing depth as the original Hi-C protocol that first measured chromosome-level interchromosomal interactions (Lieberman-Aiden et al., 2009). The partitioning of gene-rich and gene-poor chromosomes into separate regions of nuclear space observed by Hi-C (Lieberman-Aiden et al., 2009) further validate the original observations detected with fluorescence *in situ* hybridization (Boyle et al., 2001). We ourselves detected small gene rich chromosomes such as 16, 17, 19, and 22 preferentially associating with each other, depicted by a cluster of red enriched nodes in the lower right of the heatmap (Figure 3A). We also detect the slightly weaker preferential association between large gene poor chromosomes such as 2–5, depicted by a second cluster of red enriched nodes in the upper left. The two groups of chromosomes tend to avoid one another as indicated by the cluster of blue depleted nodes in the upper right and lower left of the heatmap. We also note a few strong interactions that defy this pattern. For example, the artificially high interaction frequency between chromosomes 8 and 14 is due to the chromosomal translocation commonly found in Burkitt lymphoma (Engreitz et al., 2012) (Figure 3A, 3B, and 6A).

Next we examined interactions of the EBV episome with human chromosomes. Based on observed/expected chromosome association measurements, we discovered that the EBV episome avoids interaction with small gene rich chromosomes and preferentially interacts with large gene poor chromosomes (Figure 3A). This trend is conserved in the four cell lines we examined (Figure 3D). Although the exact order of the preferences varies slightly between cell lines, the strongest ratios are observed with the EBV episome avoiding chromosomes 16, 17, 19, 20, and 22 while interacting with 4 and 13. The observed trend does not correlate with size based on ratios calculated for chromosomes that defy the trend of gene density increasing as size decreases. The small but gene-poor chromosome 18 is not strongly avoided by the EBV episome; the large but gene-rich chromosome 1 is not strongly interacting with the EBV episome. EBV latency type, which varies between type I for RaeI and Daudi compared to type III for KemIII and Raji (Phan et al., 2016), also has no effect. To illustrate the suspected trend with statistical rigor, we plotted the observed/expected chromosome association preferences for EBV against gene density for each chromosome and calculated median slopes and 95% confidence intervals (CI) using Thiel-Sen linear regression (Sen, 1968). We found a negative slope in all Burkitt lymphoma cell lines (Figures 1D). The 95% CI completely falls in the negative range for all replicates (Figures 1A), demonstrating that the propensity of EBV to interact with a chromosome is strongly negatively correlated with the gene density of that chromosome.

### **Preferential EBV chromosome associations require episomal genomes**

To test whether viral chromosome preference is dependent on genome sequence or biophysical mobility, we performed in situ Hi-C on a cell line with integrated EBV. Namalwa cells contain an EBV genome with a sequence similar to others we examined, but it is integrated into chromosome 1. Gene expression predominantly consists of latent transcripts as measured by our RNA-seq experiments (Figure 3C), somewhat similar to the other Burkitt lymphoma lines studied. We found that integrated EBV does not show the same chromosome association preferences as episomal EBV and instead shows no correlation with gene density (Figure 3B), demonstrating that the viral genome must be episomal and less restricted to move around the nucleus in order to associate with chromosomes based on gene density. Furthermore, we note that the chromosome association preferences of integrated EBV in the Namalwa cell line are



similar to chromosome 1, suggesting that the local chromatin environment at the integration site cannot be overcome by the viral sequence.

### **Chromosome association preferences are conserved among some but not all episomal viruses**

We also performed in situ Hi-C on three cell lines containing other latent double-stranded DNA viruses to determine whether chromosome association preferences are a conserved feature of episomal vectors. Two lines contained different strains of human papillomavirus (HPV), HPV16 and HPV31, which are unrelated to EBV, and one line contained the Kaposi's sarcoma-associated herpesvirus (KSHV), which is closely related to EBV. We found that while KSHV does show a chromosome association preference similar to EBV, HPV16 and HPV31 do not (Figure 4). For KSHV, 95% CIs of calculated linear regression slopes fall within negative values, fitting a trend of lower chromosome association as a function of gene density. For HPV, regression slopes are close to 0 with the 95% CIs ambiguously spanning both negative and positive values. This demonstrates that while gene-density driven chromosome association preferences are not characteristic of all episomes, closely related gammaherpesviruses such as KSHV and EBV may use similar mechanisms to control their nuclear localization.

### **OriP and EBNA1 sufficiently reconstitute preferential EBV chromosome associations**

To obtain a higher resolution understanding of which regions in the viral genome contact the human genome, we analyzed a publicly available Hi-C data set of EBV-infected B cells where sequencing depth far exceeds any other experiment to date. The Hi-C data set obtained with GM12878 cells (Rao et al., 2014) contains ~5 billion pairwise contacts. We would have liked all of our experiments to have been performed with similar sequencing depth as the GM12878 data set, but this case represents an exceptional example in the field and is not tractably reproducible for financial reasons. We therefore complemented our own low-resolution experiments with the available high-resolution data. Our reanalysis that included the EBV genome sequence shows that viral chromosome preferences in this lymphoblastoid cell line are similar to that observed in Burkitt lymphoma lines (Figure 5A). We then measured contact frequencies between the EBV episome and human chromosomes and identified 117 significant interactions using the GOTHIC algorithm (Mifsud et al., 2015). Of these, 61 or 52.1% involved the 8-9 kb bin of the viral

genome (Figure 5B), which falls into a viral cis-regulatory element called OriP, genetically defined as bp 7315–9312.

To illuminate molecular properties of these intergenome loops, we applied the TargetFinder algorithm (Whalen et al., 2016), which was previously used to determine features that predict long-range intrachromosomal interactions. We extended TargetFinder to model interchromosomal loops by requiring that one region from each interacting pair of segments is in the human genome while the other is in the EBV genome. Features used to predict interchromosomal interactions accordingly included genomic marks on the human or EBV segment. Perhaps surprisingly, histone modification ChIP-seq signals did not significantly contribute to accurate modeling of interchromosomal loops. Known chromosome organizers such as CTCF and cohesin also do not contribute significantly. The top predictive feature on the viral episome is occupancy by the viral protein EBNA1. Identification of this feature is consistent with the fact that EBNA1 binds OriP to perform two functions: replication of circular episomes during S phase as well as tethering of the viral genome to human chromosomes during metaphase (Leight and Sugden, 2000). However, it is unknown whether EBNA1 mediates interactions between the viral episome and the human genome during interphase.

Considering that the majority of the significant interactions involved OriP, and that EBNA1 was a top predictor for significant human-viral contacts, we hypothesized that this assembly may be involved in interphase localization of the virus. To determine if OriP DNA and the EBNA1 protein are sufficient to reconstitute the chromosome association preferences of the entire virus, we performed in situ Hi-C on stably-transfected K562 cells containing pEBNA-DEST (pD), a plasmid that contains these two components. We found that pD showed similar preferences to the entire virus (Figure 5C), demonstrating that OriP and EBNA1 are sufficient to reconstitute preferential interactions with human chromosomes as seen with the full-length virus. Initial tests, however, imply that EBNA1 does not mediate chromosome preferences. We used shRNA to knockdown EBNA1 in Rael cells, which contain full-length virus. We did not see a change in chromosome preferences upon ~50-70% knockdown (Figure 6A). We also genetically deleted *EBNA1* from pD to generate pD $\Delta$ EBNA and transiently transfected both vectors into K562 cells. Transient transfections were necessary because *EBNA1* deletion precludes establishment of a

stably maintained episome. The experiment is technically more variable and requires greater sequencing depth. Nonetheless, we still did not see a difference in chromosome preferences upon deletion (Figure 6B). This preliminary data suggests that a protein other than EBNA1 binds to OriP to mediate these preferences.

### **EBV interacts with gene-poor human chromatin distant from transcription start sites**

To characterize the human side of chromatin interactions with latent EBV, we studied the genetic landscape of enriched sites. We again used the significant contacts from the GM12878 data set filtered through GOTHic. The 117 identified interactions localized to 91 unique 100 kb bins of human chromosomes. We used the Genomic Regions Enrichment of Annotations Tool (GREAT) (McLean et al., 2010) to measure gene density and distance to transcription start sites (TSSs). We compared the 91 significant regions to 100 sets of 91 randomly generated non-significant regions. Regions of the human genome that interact with the virus have ~20% lower gene density, empirical  $p=0.18$  (Figure 7A). Regions that interact with EBV are also farther from TSSs (Figure 7B). TSSs appear ~20% less frequently within 500 kb, empirical  $p<0.01$ , and ~250% more frequently beyond 500 kb, empirical  $p<0.01$ . We also used TargetFinder to ask which features were most predictive of viral-human interactions on the human side. We found that relative Hi-C coverage is the most predictive feature. In other words, regions of the human genome that interact with the viral episome have much higher Hi-C interaction frequencies in general compared to non-significant regions (Figure 7C). This result, however, does not imply some sort of non-specific technical artifact in our detection algorithm. We emphasize that peak-calling by the GOTHic algorithm normalizes for sequencing depth. Although the highest coverage portions of the human genome colocalize with EBV, these regions still do so with a frequency higher than random expectation. Together, our analysis argues that EBV preferentially associates with interactive gene-poor regions of human chromatin far from TSSs.

### **The EBV episome switches contacts from human heterochromatin to euchromatin during reactivation**

A single snapshot of nuclear organization is often incomplete, so we measured whether interactions between the viral and human genome were remodeled based on changes in transcription. To do so, we compared in situ Hi-C results between cells containing the latent viral

episome, which expresses ~1-10 transcripts, and cells containing the lytic viral episome, which expresses ~100 transcripts (Kenney, 2007). We used the Akata-Zta cell line, which contains the EBV genome and an additional plasmid with a doxycycline-inducible promoter that produces the viral protein BZLF1, which induces lytic gene expression, as well as non-functional LNGFR, which facilitates purification of reactivated cells (Ramasubramanian et al., 2015). We pre-treated Akata-Zta cells with acyclovir to block viral replication and ensure that we were examining interactions of episomes and not newly replicated linear genomes. DNA deep sequencing of acyclovir- and doxycycline-treated LNGFR- cells, which represent the latent population, estimate a viral genome copy number of ~20. Acyclovir indeed functions as intended; total EBV DNA content increased by only  $2.1 \pm 0.4$ -fold, much of which comes from abortive replication attempts near the lytic origins (Keck *et al.*, submitted). Comparison of EBV episomes in latent and lytic cells revealed that the chromosome association preferences are lost during reactivation (Figure 8A and 8B). In lytic cells, linear regression slopes are close to 0 instead of strongly negative. This loss of preferential association based on gene density was reproduced in five independent reactivation experiments (Figure 8C).

Since gene-poor chromosomes contain more heterochromatin than gene-rich chromosomes, we hypothesized that the preferential chromosome association is due to EBV localizing with specific types of host chromatin. We subsequently surmised that this interaction would change upon reactivation of the virus. For bioinformatic analysis, we used lamin-associated domains (LADs) mapped by DNA adenine methyltransferase identification (Guelen et al., 2008) as markers of heterochromatin. Different pieces of DNA in the same chromatin domain generally establish similar sets of long-range associations detectable by in situ Hi-C. We therefore classified bins of the human genome as either heterochromatin or euchromatin, calculated a characteristic interaction pattern for each type, and used logistic regression to determine which of these two classes the EBV genome more closely resembles. This algorithm differs from previous approaches (Dixon et al., 2015; Lieberman-Aiden et al., 2009; Rao et al., 2014) in that we explicitly consider interchromosomal interactions with the human genome instead of only intrachromosomal interactions. We therefore incorporate the role of the previously understudied yet prevalent associations between chromosomes and, in this case, genomes. Since heterochromatin is a transcriptionally repressive environment, we hypothesized that if viral

transcription increases, association with repressive heterochromatin would decrease. We indeed found that when compared to viral genomes in latent cells, episomes in reactivated cells showed a strong decrease in interactions with LADs (Figure 9), suggesting that the episome is leaving the transcriptionally repressive environment of heterochromatin and moving toward the transcriptionally permissive environment of euchromatin during reactivation.

## **Discussion**

Advances in high-throughput chromosome conformation capture technologies have now allowed us to quantitatively measure molecular interactions between host chromosomes and episomal pathogen genomes. While intrachromosomal interactions are well studied, interactions between chromosomes receive little scrutiny on the genome-wide level because previous methods were not sensitive enough to do thorough analysis. The original Hi-C assay performs proximity ligation with isolated protein-DNA complexes in dilute solution outside the context of a cell (Lieberman-Aiden et al., 2009), but the majority of interchromosomal associations detected result from spurious events instead of proximity-dependent intra-complex ligation (Nagano et al., 2015). Recent improvements to the original the Hi-C method structurally favor intra-complex ligation and yield lower rates of spurious events either through physical tethering to a surface, known as tethered Hi-C (Kalhor et al., 2011), or by performing the reaction within an intact nucleus, known as *in situ* Hi-C, (Nagano et al., 2013; Rao et al., 2014). In this study, we used the improved signal to noise ratio of *in situ* Hi-C to examine the interactions between host and pathogen genomes during viral infection. We also leveraged the copy number and high density transcriptional switching of the EBV episome to detect behavior not readily seen with autosomal loci. Our experiments reveal insight into the three-dimensional chromatin context of viral gene regulation as well general principles about the interplay of transcription and nuclear organization.

Very little was known about positioning of the viral genome within the nucleus or association with host chromosomes in three-dimensional space. Examining latent episomes, one previous study used three-dimensional fluorescence *in situ* hybridization after hypotonic chromosome condensation to detect possible colocalization between EBV episomes and human laminB1 (Deutsch et al., 2010; McLean et al., 2010) That observation is consistent with our own

molecular data. The same work showed EBV predominantly colocalizing with activating histone modifications, and to a lesser extent repressive modifications. While we did not examine localization with histone modifications directly, our Hi-C data detects interactions with repressive heterochromatin during latency, an apparent contradiction with the microscopy results. Our molecular Hi-C data is of higher resolution and also examined localization with better preservation of nuclear organization by avoiding possible artifacts resulting from the hypotonic treatment used to visualize chromatin for microscopy. Another study used live-cell imaging to track nuclear positioning of lytic viral genomes during and after DNA replication but not during latency (Chiu et al., 2013; Kenney, 2007). Our work specifically measures associations between EBV episomes with host chromosomes, comparing interactions during latency and reactivation.

We now know that even episomal viruses “integrate” into the network of human gene regulation. Here, we show that although EBV does not covalently integrate into the human genome, the virus noncovalently intermingles with the compartmentalized three-dimensional structure of the folded human genome. We determined that these interactions are non-random; the latent EBV episome preferentially interacts with gene-poor chromosomes and avoids gene-rich chromosomes. At higher resolution, the EBV episome associates with gene-poor regions of human chromatin distant from TSSs. The chromosome preferences can be reconstituted by OriP and EBNA1 alone. Surprisingly, initial results suggest that removal of EBNA1 does not change chromosome preferences, implying that another protein may be responsible for mediating these contacts.

The preferential association with human chromosomes during latency is not limited to EBV. We observe similar association patterns with KSHV. The strategy is not universally used by all episomal viruses, however, as we do not detect preferential interactions between HPV and human chromatin. The cause of this distinction, perhaps rooted in different selective pressures, remains to be elucidated.

We add another layer of understanding onto the sequence of molecular events coupled with viral reactivation. Much of what was previously known about the transition of EBV transcription from

latent to lytic involves binding of viral and host proteins to the episomal genome (Arvey et al., 2012; Kieff and Rickinson, 2013). Very little was known about positioning of the viral genome within the nucleus or association with host chromosomes in three-dimensional space. Here we show that the virus changes nuclear environments during reactivation, switching from interactions with heterochromatin during latency to interactions with euchromatin compartment during reactivation. As a result, in both the latent and lytic transcription states, the viral genome is surrounded with human chromatin of similar transcriptional activity.

The movement of an episome upon reactivation argues that reactivation can drive passage between chromatin compartments with changes in only a diffuse network of interchromosomal associations without strong intrachromosomal contacts. We know that transcriptional changes correlate with transitions between compartments (Dixon et al., 2015). This compartment switching, however, only identified changes in the predominantly detectable intrachromosomal contacts because previous computational methods did not consider contacts between chromosomes. Here, we show that the EBV episome changes compartments through changes in diffuse interchromosomal associations as transcription increases during reactivation. Previous examples of functional interchromosomal interactions involve single associations between two regions (Ling et al., 2006; Lomvardas et al., 2006). In contrast, the EBV episome forms a myriad of contacts with the heterochromatin compartment during latency and a different set of distributed contacts with euchromatin after transcriptional activation. The sum of many interchromosomal interactions may therefore contribute to gene regulation.

Future studies should involve tethering the viral episome to specific compartments, though recreating the network of interchromosomal interactions detected by Hi-C will be difficult. These experiments could elucidate the functional role of nuclear localization in EBV gene regulation: forcing connections with euchromatin may induce reactivation, while anchoring connections with heterochromatin may promote latency. The role of EBV chromatin in directing or responding to nuclear localization also requires clarification. The challenge still remains to determine whether transcriptional changes drive diffuse interchromosomal co-localization or vice versa.

## **Materials and methods**

### **Cell culture and plasmids**

EBV-positive Daudi, KemIII, RaeI, and Raji cells were maintained under standard conditions (Phan et al., 2016). K562 (Lozzio and Lozzio, 1975), EBV- and KSHV-positive BC-1 (Cesarman et al., 1995), and EBV-positive Namalwa (Klein et al., 1972) cells were maintained in RPMI-1640 with 25 mM HEPES and 2 g/L NaHCO<sub>3</sub> supplemented with 10% (v/v) fetal bovine serum (Invitrogen) in 5% CO<sub>2</sub> at 37 °C. EBV-positive Akata-Zta cells (Ramasubramanian et al., 2015) were maintained in RPMI-1640 with 25 mM HEPES and 2 g/L NaHCO<sub>3</sub> supplemented with 10% (v/v) Tet System Approved fetal bovine serum (Clontech). The HPV16-positive 20863 (Jeon et al., 1995) and HPV31-positive 9E (De Geest et al., 1993) keratinocyte cell lines were grown in F-medium, 3:1 (v/v) F-12-DMEM, 5% fetal bovine serum, 400 ng/ml hydrocortisone, 5 µg/ml insulin, 8.4 ng/ml cholera toxin, 10 ng/ml epidermal growth factor, 24 µg/ml adenine, 100 U/ml penicillin, and 100 µg/ml streptomycin, in the presence of irradiated 3T3-J2 feeder cells, as described previously (Chapman et al., 2014). Irradiated feeder cells were removed by versene treatment before the cells were harvested.

K562 cells were stably transfected with the pEBNA-DEST (pD) plasmid (Thermo Fisher Scientific) by a Nucleofector II device (Lonza) as directed, using solution V and program T-016. One day after transfection, 200 µg/ml hygromycin B was added and pD-positive K562 cells were selected for until transfected cells outgrew control cells and subsequently maintained in 200 µg/ml hygromycin B.

The *EBNA1* promoter and majority of the coding region were deleted from pD to generate pDΔEBNA by cutting with BsgI, filling in overhangs, and ligating blunt ends. Successful construction was verified by restriction digest mapping. For transient transfections, pD or pDΔEBNA plasmids were delivered into K562 cells using Fugene (Promega) at a 4:1 Fugene:DNA ratio using 20 µg DNA per 1 million cells. At 3 days post-transfection, 5 million cells were collected for Hi-C.



## **In situ Hi-C**

In situ Hi-C was performed with 5 million cells per experiment as described (Rao et al., 2014) with slight modifications. After end-repair and washes, Dynabeads (Thermo Fisher Scientific) with bound DNA were resuspended in 10 mM Tris, 0.1 mM EDTA pH 8.0 and transferred to new tubes. Sequencing libraries were created from bound DNA using the Ovation Ultralow Library System V2 kit (NuGEN) with one modification. After adapter ligation, because DNA is still attached to the beads, water instead of SPRI beads was added to the reaction. DNA bound to the beads was purified with a magnet, washed, and the beads were resuspended in 10 mM Tris, 0.1 mM EDTA pH 8.0. After library amplification, SPRI beads were added as directed to purify the amplified DNA. Quantitation and size distribution of libraries were performed using the Bioanalyzer High Sensitivity DNA Kit (Agilent). 50 base paired-end reads were sequenced on a HiSeq (Illumina).

Once sequenced, paired reads were aligned to combined human/viral reference genomes with HiCUP version 0.5.0 using default parameters (Wingett et al., 2015) to generate a set of interactions. We used the human hg19 sequence merged with the EBV NC\_007605.1, KSHV NC\_009333.1, HPV16 NC\_001526.2, or HPV31 J04353.1 sequence. The HiCUP processing steps remove PCR duplicates as well as invalid read pairs including those that are self-ligated or map to identical or adjacent fragments. Only alignments with mapq scores equal to or greater than 30 were retained. Data sets contained ~7–40 million valid paired end HiC contacts after quality control filtering, of which ~2–20 million were interchromosomal and ~400–230,000 between human and viral or plasmid sequences.

## **Analysis of interchromosomal interactions**

Chromosome-resolution heatmaps of interactions were determined from the HiCUP-filtered interchromosomal Hi-C interactions in sam format. Expected interactions were calculated using the following equation for each chromosome pair, where *chrA* represents the number of single end interchromosomal reads containing chrA, *chrB* represents the number of single end interchromosomal reads containing chrB, *totalPairs* represents the total number of interchromosomal paired end reads, and *all* represents the total number of interchromosomal single end reads, which is equal to  $2 \times totalPairs$ :

$$\left[\left(\frac{chrA}{all} * \frac{chrB}{all - chrA}\right) + \left(\frac{chrB}{all} * \frac{chrA}{all - chrB}\right)\right] * totalPairs$$

The chromosome association preference value for each combination was calculated by dividing the observed number of reads containing chrA and chrB by the expected value. Chromosome association preferences of viral genomes were plotted against gene density measured in genes per Mb (Naidoo et al., 2011). Data were fit to a line using the Thiel-Sen non-parametric linear regression median slope method (Sen, 1968) as implemented in the *zyp* R package.

### **ChIP-seq**

BZLF1 and EBNA1 chromatin immunoprecipitation deep sequencing (ChIP-seq) experiments were performed as previously described (Keck *et al.*, submitted) using 3 µg of the anti-BZLF1 antibody BZ1 (Santa Cruz, sc-53904) and 3 µg of the anti-EBNA1 antibody 0211 (Santa Cruz, sc-57719).

### **Analysis of viral-human contact regions**

A large Hi-C data set from GM12878 cells (Rao et al., 2014) was reanalyzed to identify the strongest interactions between the EBV episome and human chromosomes. Chromosome-resolution heatmaps of interactions and chromosome association preference plots were generated from the HIC001 library. Further reanalysis included all fastq files from the primary and replicate sets, libraries HIC001–HIC0029. Data were independently processed using HiCUP version 0.5.8 and significant looping interactions were called using a Python implementation of the GOTHic algorithm (Mifsud et al., 2015). Our specific parameters for performing the GOTHic algorithm were as follows: To increase statistical power, reads were first mapped to fixed resolution bins, 100 kb on the human genome and 1 kb on the viral genome, using pairToBed as packaged in BEDTools version 2.26 (Quinlan, 2014). Counts from the two biological replicates were merged to increase the signal to noise ratio. Next, the probability of a spurious ligation was computed as a function of the relative coverage of each bin. Relative coverage was defined as the number of reads mapping to the bin divided by the total number of reads. Finally, the probability of observing a given number of reads by chance between two bins was computed using a binomial test, resulting in a p-value for each pair of bins. Multiple testing correction was performed using the Benjamini-Hochberg procedure, resulting in a q-value for

each pair of bins. Bin pairs with a q-value of 0.1 or less, which corresponds to a 10% false discovery rate, were treated as statistically significant and identified as positive interacting samples.

Features that predict contacts between the EBV episome and human chromosomes were identified using the TargetFinder algorithm (Whalen et al., 2016). Average signals for all ENCODE GM12878 ChIP-seq data sets, as well as for the BZLF1 and EBNA1 ChIP-seq experiments performed by us, were computed for EBV and human bins. These features were used with interaction labels to train a gradient boosting classifier using the scikit-learn Python package (Pedregosa et al., 2011) with the following parameters: `n_estimators = 200`, `learning_rate = 0.01`, and `max_depth = 3`. Stratified 10-fold cross-validation was performed with scikit-learn to obtain scores for precision, recall, and F1, the harmonic mean of precision and recall.

We characterized the genetic landscape of human chromosomal regions that contact the viral episome with the Genomic Regions Enrichment of Annotations Tool (GREAT) (<http://bejerano.stanford.edu/great/public/html/>) (McLean et al., 2010). To measure gene density, the “basal plus extension” parameter was used, with a proximal extension of 50 kb upstream and 50 kb downstream, and a distal extension of 0 kb. Since GREAT chooses the midpoint of the 100 kb human bin as a reference, these settings allowed genes to overlap and permitted measurement of the total number of TSSs in each region. To determine distance to TSSs, the “single nearest gene” parameter was set to search within 1000 kb, allowing determination of the nearest TSS in either direction. Each of these two analyses were performed on the 91 significant bins, and on 100 sets of 91 random non-significant bins. An empirical p-value was measured to determine significance.

### **shRNA-mediated EBNA1 knockdown**

RaeI cells and the K562 line stably transfected with pD were transduced with shEBNA1 or control shRNA (Dheekollu et al., 2016) by spinoculation. Lentivirus with 8 ug/ml polybrene was added to cells and spun at 800 xg for 30 minutes at room temperature. The supernatant was aspirated and cells resuspended in fresh media. After 48-72 hours post-transduction, RaeI cells

were selected with 2 µg/ml puromycin to maintain the shRNA plasmid and K562 cells were selected with 2 µg/ml puromycin and 200 µg/ml hygromycin B to maintain both the shRNA plasmid and pD. At 7 days post-transduction, cells were collected for Western blotting and 5 million cells were collected for in situ Hi-C.

Western Blots were performed using standard techniques. EBNA1 was detected using the anti-EBNA1 antibody 1EB12 (Santa Cruz, sc-81581) at 1:100-200 dilution and goat anti-rabbit-HRP (Abcam ab721) at 1:2,000-5,000 dilution. For normalization, actin was detected using an anti- $\alpha$ -actin antibody (Abcam, ab8227) at 1:10,000-20,000 dilution and rabbit anti-mouse-HRP (Abcam ab6728) at 1:20,000-30,000 dilution. Signals were detected using the SuperSignal West Pico Chemiluminescent Substrate (Thermo-Fisher), and a ChemiDoc MP Imaging System (BioRad). ImageLab (BioRad) version 5.2.1 was used to measure knockdown.

### **Viral reactivation**

Log-phase cultures of Akata-Zta cells were pretreated with 200 µM acyclovir (Sigma-Aldrich, A4669) for 1 hour before reactivation of the lytic cycle with 500 ng/mL doxycycline (Sigma-Aldrich). These cells contain a doxycycline-inducible plasmid with a bi-directional promoter that produces non-functional LNGFR along with the immediate early protein BZLF1, which starts the lytic cycle gene expression cascade and reactivates the virus (Ramasubramanian et al., 2015). After 1 day, cells were magnetically sorted using LNGFR Microbeads and LS columns (Miltenyi Biotech).

EBV DNA quantitation was determined by deep sequencing total DNA. Genomic DNA was purified by silica-based membrane affinity with a DNeasy Blood & Tissue Kit (Qiagen). Libraries were constructed and the percentage of EBV reads from total measured (Keck *et al.*, submitted). Viral genome copy number was estimated based on observed ratios between the number of reads mapped to the EBV and human genome sequences compared to the expected value, which is calculated as the ratio between the viral episome length and the summed length of all human chromosomes.

### **LAD state predictions**

The set of lamin interacting domains from Tig3 cells (Guelen et al., 2008) was downloaded from the UCSC genome browser (Kent et al., 2002). Hi-C interactions identified by HiCUP were processed into a format readable by the HiTC package (Servant et al., 2012) using 1 Mb bins for the human genome and 1 kb bins for the viral genome. We performed further analyses on these interaction matrices in R (R Core Team, 2016). First a full interaction matrix for all autosomes was constructed. Next, for each bin, the mean of interaction counts with LAD bins was calculated as was the mean of interaction counts with non-LAD bins. This created two vectors of interaction means whose lengths were the number of bins in the autosomal genome. These vectors contained the primary source of information linking LAD state and interaction counts. Correlations were then performed across all autosomal bins with the LAD mean vector and the non-LAD mean vector. A LAD bin will have a high correlation in interactions with the LAD mean counts and a low correlation in interactions with the non-LAD mean counts. A logistic regression was therefore performed on the LAD and non-LAD correlation values to estimate the probability with which each genome region would interact with lamin. Next, we calculated the probability that each viral bin interacted with the lamin by applying the logistic regression model of the autosomal LAD correlations to the viral interaction data.

### **Accession codes**

Deep sequencing data was deposited in the Gene Expression Omnibus database under accession code GSE98123.

## Chapter III: BET inhibitors block the EBV lytic cycle at two distinct steps

### Introduction

Modern antiviral drugs generally share two characteristics: the target is a single protein and that target acts at one distinct step in the viral life cycle (De Clercq, 2002). Acyclovir treats herpes by inhibiting the DNA polymerase. Azidothymidine treats HIV by inhibiting the reverse transcriptase. Sofosbuvir treats hepatitis C by inhibiting the RNA polymerase. Despite tremendous success, single-target/single-mechanism antiviral drugs have key weaknesses. Acquisition of viral resistance occurs frequently. A single target provides only a single point of intervention and potency. How then, can we in the field improve upon the current paradigm of drug design? We take our cues from the success of two efforts: combination antiretroviral therapy and polypharmacology. HIV medication is now often delivered as a combination of single-target drugs (Dieffenbach and Fauci, 2011). Chemical biologists are also challenging the single-target/single-mechanism paradigm by systematically optimizing the broad spectrum of targets hit by a drug (Hopkins, 2008). Off-target effects are not avoided, but rather specifically chosen to generate additive or synergistic interactions with other known targets. Here we report the serendipitous discovery of polypharmacological activity by a small molecule epigenetic regulator that acts against the Epstein-Barr virus (EBV).

EBV maintains a lifelong infection in over 90% of adults worldwide. Like other herpesviruses, EBV infection cycles between latent (Young and Rickinson, 2004) and lytic (Kenney, 2007) forms. During the latent phase, the ~170 kb genome is maintained as an episome, and transcription is limited to a dozen or fewer latent genes. The lytic cycle involves expression of ~100 genes and leads to production of viral progeny through a sequential cascade. This stepwise process begins upon either initial infection or reactivation from latency (summarized in Figure 10). First, cellular signals lead to expression of immediate-early genes, among which *BZLF1* is necessary and sufficient to promote downstream events (Countryman and Miller, 1985). The encoded proteins drive expression of early genes, whose products allow for replication of the viral genome and finally expression of late genes. While latent infection is implicated in the development of many cancers such as Burkitt lymphoma and nasopharyngeal carcinoma (Young

and Rickinson, 2004), lytic infection causes infectious mononucleosis (Luzuriaga and Sullivan, 2010) and drives post-transplantation lymphoproliferative disorder (Chen et al., 2010).

Proteins in the bromodomain and extraterminal (BET) family regulate multiple stages of viral life cycles. The bovine papilloma virus protein E2 binds the human protein BRD4 directly and colocalizes on mitotic chromosomes to attach viruses for proper segregation (Baxter et al., 2005; You et al., 2004). Mutations in E2 that perturb BRD4 binding abrogate attachment. Similar observations have been made with the Kaposi sarcoma-associated herpesvirus protein LANA and BRD4 (You et al., 2006). BRD4 also activates EBV enhancer (Lin et al., 2008) and promoter (Palermo et al., 2011) function to modulate gene expression. In addition to promoting viral propagation, BET proteins can also inhibit production. BRD2 and BRD4 suppress reactivation of latent human immunodeficiency virus by antagonizing transcription elongation (Banerjee et al., 2012; Boehm et al., 2013; Li et al., 2013; Zhu et al., 2012).

JQ1 (Filippakopoulos et al., 2010) and I-BET (Nicodeme et al., 2010) are inhibitors of BET protein bromodomains that demonstrate strong affinity for the three family members widely expressed in human tissues: BRD2, BRD3, and BRD4. Competitive binding to the two tandem bromodomains prevents recognition of acetylated lysine substrates. While JQ1 targets both bromodomains with similar affinity (Filippakopoulos et al., 2010), the compound RVX-208 preferentially binds to the second bromodomain (Picaud et al., 2013). Given multiple host protein targets and multiple functions in viral life cycles, JQ1 and other BET inhibitors present intriguing potential for polypharmacological inhibition of viral replication. We tested this hypothesis with EBV and discovered two different points of intervention.

## **Results**

**BET inhibitors block immediate-early transcription** — Here we present evidence that BET inhibitors block the EBV lytic cycle at two distinct steps, the first occurring before immediate-early transcription. We measured expression of BZLF1, the immediate-early transactivator that serves as a marker for the lytic cycle, using flow cytometry. With MutuI, an EBV-positive Burkitt lymphoma line, only ~1% of cells display background spontaneous reactivation (Figure 11a). Cells treated with 1  $\mu$ M JQ1, I-BET, or RVX-208 alone similarly yield a low percentage of

cells positive for BZLF1. Antibodies raised against human immunoglobulin crosslink the B cell receptor and reactivate EBV from latency (Tovey et al., 1978). For cells grown in the presence of antibody, pretreatment with BET inhibitors instead of vehicle decreases the percentage of BZLF1-positive cells, which indicates fewer cells containing lytic EBV. JQ1 and I-BET both reduce antibody-induced BZLF1 expression to approximately the level seen without antibody treatment. Used at the same concentration as JQ1, RVX-208 results in slightly less inhibition, implicating bromodomain 1 of the BET proteins in initiation of the EBV lytic cycle. To measure dose-dependent inhibition by JQ1, we treated cells with the cytotoxic chemotherapy drug gemcitabine, which also induces lytic progression (Feng et al., 2004). We measured an approximate  $IC_{50}$  of  $20 \pm 9$  nM (Figure 11b), a concentration consistent with the affinity of the small molecule for BET bromodomains (Filippakopoulos et al., 2010). We therefore chose to perform future experiments at a BET inhibitor concentration of 1  $\mu$ M, the approximate lowest dose that yields maximum efficacy.

JQ1 blocking BZLF1 protein production should also prevent downstream transcription of lytic genes and replication of viral DNA. To confirm this inhibition of transcription, we performed RNA-seq on cells induced by antibody with or without 1  $\mu$ M JQ1 pretreatment (Figure 11c). We controlled for pleiotropic toxicity by verifying that JQ1-treated cells show similar growth,  $97 \pm 12\%$ , and viability,  $102 \pm 1\%$ , compared to untreated cells. Vehicle-treated lines display a transcription profile consisting predominantly of low abundance lytic gene signals from background spontaneous reactivation (Fernandez and Miranda, 2016; Phan et al., 2016). Cells grown in the presence of antibody show increased transcription throughout the EBV genome, similar to induction previously observed (Fernandez and Miranda, 2016). The highest peaks correspond to lytic genes, some of which are labeled in Figure 11c. In contrast, cells pretreated with JQ1 before antibody exposure yield an overall profile similar to that from cells not treated with antibody, confirming that JQ1-mediated inhibition of BZLF1 expression also prevents increased transcription of downstream lytic genes. Similar to the rest of the transcriptome, *BZLF1* expression only increases above background levels in cells incubated with antibody alone (Figure 11c inset). Thus, we know that the lack of BZLF1 protein induction detected by flow cytometry after JQ1 treatment (Figure 11a) is due to lack of *BZLF1* gene expression rather than post-transcriptional regulation. We also confirmed that replication of viral DNA is inhibited



upon JQ1 pretreatment by deep sequencing all DNA extracted from cells and calculating the increase in viral genomes. The pattern of the results is similar to that seen with lytic gene transcription: viral DNA increases with antibody exposure but decreases back to background levels with JQ1 pretreatment prior to antibody exposure (Figure 11d). Thus, JQ1 completely suppresses the EBV lytic cycle even at downstream readouts, speaking to the strong efficacy of inhibition.

**BET proteins localize to the lytic origins of replication** — Our first hint that BET inhibitors act at multiple steps in the viral life cycle came when we discovered that BET proteins bind the EBV genome at the two lytic origin of replication (OriLyt) elements. Given that BET inhibitors prevent *BZLF1* expression, we suspected that BET proteins would localize to the *BZLF1* promoter. To test this possibility, and to simultaneously check for potential binding elsewhere, we probed the entire EBV genome for BRD2, BRD3, and BRD4 occupancy with ChIP-seq (Figure 12a). Contrary to our suspicion, we did not detect noticeable enrichment in the region near the *BZLF1* transcription start site at ~90 kb on the EBV genome. Much to our surprise, however, we detected strong signals of occupancy for all three BET proteins at ~41 and ~144 kb, within the 3' edge of the two OriLyt elements (Hammerschmidt and Sugden, 1988) genetically defined as 40301-41293 and 143207-144444. Histone modifications that colocalize with BET proteins in these regions (Figure 12a) are also consistent with bromodomain function. Acetylated H3K9 and H3K27, which may serve as bromodomain binding partners, are enriched at these sites. The BET protein-bound regions lack peaks of H3K4 trimethylation, suggesting the assembly of enhancer-like as opposed to promoter-like chromatin (Wang et al., 2008).

We also measured the effect of JQ1 on BRD4 occupancy at the OriLyt elements. Although our initial ChIP-seq protocol readily detected BRD4 occupancy on the high copy number EBV episome, we could not readily identify occupancy on the human genome. To improve sensitivity so that we could compare binding in response to BET inhibitor treatment between sites on both genomes, we increased the number of cells processed and repeated the ChIP-seq experiment. Among many other sites, BRD4 has been shown to bind super-enhancers of the *POUF2AF1* and *BCL6* genes in B cell lymphoma lines (Chapuy et al., 2013). In our own experiments, as expected, 1  $\mu$ M JQ1 substantially reduces BRD4 occupancy both at these super-enhancers and at

associated promoter proximal regions (Figure 12b). JQ1 also reduces BRD4 binding to the viral OriLyt elements ~2-fold. Although this reduction of occupancy in the EBV genome is weaker than effects observed in the human genome, similar behavior at the viral OriLyt elements further validates our identification of this enriched occupancy as BET protein binding events.

If BET proteins do not directly bind the *BZLF1* promoter to drive expression, then we surmise that BET inhibitor activity at that site occurs through an indirect mechanism involving other host proteins. Our RNA-seq data identified ~3000 differentially regulated human genes in response to 1  $\mu$ M JQ1 treatment. Pathway analysis reveals 10 enriched groups of genes either known or predicted to be controlled by the transcription factors FOXP3, STAT6, SPI1, KLF1, E2F4, EBF1, BACH1, YY1, NFE2L2, and TAL1. We followed up on these leads by depleting individual proteins and measuring the effect on viral reactivation. Lentivirus shRNA reduces BACH1 expression by ~70% compared to a control non-targeting shRNA (Figure 11e). This BACH1 knockdown reduces the increase in BZLF1 expression induced by gemcitabine ~2-fold (Figure 11f). Other candidate factors may also mediate the effect of BET inhibitors on viral transcription, but our preliminary results suggest that JQ1 perturbs BACH1 function to decrease immediate-early protein production.

**BET inhibitors prevent lytic DNA replication** — To demonstrate that BET inhibitors act at a second step in the viral life cycle, we determined that JQ1 blocks EBV DNA replication despite ectopic *BZLF1* expression. Because BRD2, BRD3, and BRD4 bind the lytic origins of replication, we hypothesize that BET inhibitors could perturb the function of that genetic element. Prevention of *BZLF1* expression in MutuI cells by JQ1 precludes testing for this effect because blocking immediate-early transcription abrogates all downstream events, including lytic DNA replication (Figure 11). To perform a classical epistasis experiment and ask if JQ1 treatment regulates viral transcription downstream of *BZLF1* expression, we studied Akata-Zta (Ramasubramanian et al., 2015), an EBV-positive cell line with a doxycycline-inducible and plasmid-borne *BZLF1* gene. If the effect of BET protein inhibition by JQ1 were only upstream of *BZLF1* transcription, then ectopic expression of *BZLF1* should cause reactivation of EBV even in the presence of JQ1. First we ensured that BET inhibitors did not reduce ectopic *BZLF1* expression by verifying that pretreatment before addition of doxycycline did not affect the

percentage of BZLF1-positive cells (Figure 13a). RNA-seq verified that, as expected, incubation with doxycycline and consequent lytic cycle induction causes transcription to increase throughout the EBV genome (Figure 13b).

If DNA replication were perturbed by JQ1, the sequential ordering of EBV transcription predicts that late gene expression would be reduced without affecting early gene expression. When Akata-Zta cells are pretreated with 1  $\mu$ M JQ1 before exposure to doxycycline, total transcription of *BZLF1* does not change (Figure 13b inset) whereas expression is reduced at many other genes (Figure 13b). Again, we controlled for pleiotropic toxicity by verifying that JQ1-treated cells showed similar growth,  $79 \pm 23\%$ , and viability,  $101 \pm 1\%$ , compared to untreated cells. The overlapping nature of EBV gene organization often confounds analysis, so we measured expression only at non-overlapping RNA segments. We found that while none of 18 early genes are perturbed by JQ1 pretreatment, 12 out of 18 late genes show significantly decreased expression (Table 1). RNA levels for 11 of the 12 differentially regulated genes change by greater than 2-fold. Similar yet less pronounced effects are observed with I-BET pretreatment. None of 18 early genes but 4 out of 18 late genes show significantly decreased expression (Table 2), but the RNA level change was less than 2-fold. We also verified that viral transcripts needed for OriLyt function were not disturbed. In addition to *BZLF1*, 8 genes are necessary for lytic DNA replication (Fixman et al., 1992). Of these 8, overlapping transcripts precluded unambiguous measurement of *BMRF1* and *BMLF1* expression. Levels of the 6 other genes, *BALF5*, *BALF2*, *BSLF1*, *BBLF4*, *BBLF2/3*, and *BRLF1*, however, do not decrease upon treatment with either JQ1 or I-BET (Tables 1 and 2). Down-regulation of expression specific to late genes even in the presence of the transcripts required for OriLyt function points to a blockade of lytic DNA replication.

To directly verify a replication defect, we measured the viral DNA content of cells. We found that 1  $\mu$ M JQ1 pretreatment reduced the percentage of EBV DNA in cells by  $\sim 3$ -fold compared to doxycycline treatment alone (Figure 13c). I-BET pretreatment reduced EBV DNA content by  $\sim 2$ -fold, and this weaker inhibition of DNA replication relative to that by JQ1 is consistent with the smaller RNA-seq perturbations. RVX-208 yields no reduction, again emphasizing the primary role of bromodomain 1 in inhibition of the EBV life cycle.

We further probed the step at which lytic replication is blocked by measuring the appearance of newly synthesized portions in preparations of bulk DNA. Akata-Zta cells contain the LNGFR gene under control of the same bidirectional tetracycline-inducible promoter that expresses the BZLF1 protein. Magnetic purification of this cell surface marker allows for separation of cells containing latent and reactivated EBV. When Akata-Zta cells are pretreated with acyclovir before exposure to doxycycline, we detect more DNA content near both OriLyt elements in cells containing lytic episomes (Figure 14a). The signal arises from abortive DNA replication that initiates prior to incorporation of acyclovir and consequent chain termination during elongation. When 1  $\mu$ M JQ1 pretreatment is added, this abortive replication is not detected. Thus, JQ1 blocks the initiation of lytic DNA replication.

Although JQ1 reduces BRD4 binding to the OriLyt elements during latency (Figure 12b), we suspected that larger perturbations may occur during reactivation. We therefore measured differences in BRD4 occupancy between latent and lytic episomes with ChIP-seq (Figure 14b). Akata-Zta cells were reactivated with doxycycline but also pretreated with acyclovir to prevent lytic synthesis of linear genomes that may confound measurement of protein binding to circular episomes. Populations containing latent and lytic EBV were separated based on LNGFR expression. In the absence of JQ1, BRD4 occupancy increases  $\sim$ 4–12-fold at the lytic origins of replication upon reactivation. In the presence of JQ1, occupancy increases only  $\sim$ 1–2-fold. JQ1 reduces the change in enrichment by  $\sim$ 4–5-fold. This prevention of BRD4 recruitment may underlie the defect in lytic DNA replication initiation.

## **Discussion**

BET inhibitors display specific activity against EBV. Dual-action transcriptional inhibition does not appear to be the result of a nonspecific antiviral host response against episomal DNA viruses. JQ1 reduces replication of the JC polyomavirus through inhibition of BRD4-mediated NF- $\kappa$ B coactivation (Wollebo et al., 2016). Opposite effects are observed with the herpes simplex virus, as BET inhibitors promote lytic infection (Ren et al., 2016) and stimulate reactivation from latency (Alfonso-Dunn et al., 2017) by enhancing levels of P-TEFb on viral promoters. Results with the Kaposi sarcoma-associated herpesvirus depend on context. JQ1 does not induce lytic

replication usually observed during Myc depletion (Tolani et al., 2014), but BET inhibitors also disrupt cohesion-dependent DNA loops to activate lytic reactivation (Chen et al., 2017). We observe distinct effects of BET inhibitors on EBV transcription.

We propose a model (Figure 10) wherein BET inhibitors control the EBV life cycle at two distinct points: before immediate-early gene expression and at initiation of lytic DNA replication. We suspect that the first block occurs indirectly because BET proteins do not themselves bind the *BZLF1* promoter (Figure 12). JQ1 alters expression of genes controlled by the host protein BACH1, and BACH1 knockdown reduces viral reactivation (Figure 11f). The second block likely occurs by directly preventing lytic DNA replication (Figure 13), an association supported by binding of BRD2, BRD3, and BRD4 to the lytic origins of replication (Figure 12). We favor the interpretation that JQ1 reduces BRD4 recruitment at the OriLyt elements to prevent replication initiation (Figure 14), but we cannot formally rule out uncharacterized indirect effects. Although inhibition at the second block (Figure 13c) is not as robust as inhibition at the first block (Figure 11a), the combined effects result in complete suppression of all stages of the EBV lytic cycle (Figure 11c and 11d). Such dual-action inhibitors may be more effective than current drugs and result in a decreased risk of resistance. Many BET inhibitors are currently in clinical trials for cancer, and repurposing them against EBV may be useful in treating lytic replication during infectious mononucleosis and post-transplantation lymphoproliferative disorder.

Systems pharmacology approaches attempt to target key nodes in a network to most efficiently disrupt a biological process. The EBV lytic cycle progresses as a sequential cascade. Immediate-early expression of transcription factors to bind multiple viral promoters serves as an initial amplification step to activate early genes. DNA replication drives a second amplification step necessary for the transcription of late genes. Our studies of viral chromatin led to the serendipitous discovery that BET inhibitors target both key nodes in the EBV lytic cascade. These small molecules have several properties that may underlie the ability to perturb multiple steps in a viral pathway: nanomolar affinity for different complexes, involvement in epigenetics that disregulates diverse genes, and binding to a host rather than a viral protein. Only a few other similar lead compounds also exist. GNF-2 targets both the Abl kinase and viral glycoprotein E to

inhibit dengue virus replication (Clark et al., 2016). 17-DMAG reduces EBV replication in both a BGLF4-dependent and BGLF4-independent manner (Sun et al., 2013). Identifying even more compounds with multiple modes of inhibition would greatly increase our repertoire for treatment. We hope that BET inhibitors will serve as another prototype success to encourage directed polypharmacological discovery of next generation drugs.

## **Materials and methods**

**Cell culture and treatment** — MutuI (Gregory et al., 1990) cells were grown under standard conditions (Fernandez and Miranda, 2016). Akata-Zta (Ramasubramanian et al., 2015) cells were obtained from Alison Sinclair (University of Sussex) and maintained in RPMI-1640 with 25 mM HEPES and 2 g/L NaHCO<sub>3</sub> supplemented with 10% (v/v) Tet System Approved fetal bovine serum (Clontech) in 5% CO<sub>2</sub> at 37 °C. Growth was measured with a hemocytometer and viability was measured by trypan blue exclusion.

To induce reactivation of the lytic cycle, log phase cultures were treated with 10 µg/mL goat anti-human IgG, IgM, IgA secondary antibody (Thermo Scientific), 500 ng/mL doxycycline (Sigma-Aldrich), or vehicle for 1 day. Where BET inhibitor pretreatment is noted, 1 µM JQ1 (EMD Millipore), I-BET/GSK525762A (EMD Millipore), RVX-208 (Cayman Chemical), or vehicle was added for 1 hour before induction. Where lytic genome replication elongation is specifically prevented, 200 µM acyclovir (Sigma-Aldrich) was added for 1 hour before induction. The JQ1 dose response was determined by performing pretreatment with vehicle, 10 nM, 100 nM, 1 µM, or 10 µM for 1 hour before induction with 1 µg/mL gemcitabine (Sigma-Aldrich) or vehicle for 3 days. Data were fit to the sigmoidal equation  $a+(b-a)/(1+(x/c)^d)$ , where  $c = IC_{50}$ , using KaleidaGraph version 4.5.2.

Lentivirus shRNA was used to deplete BACH1 from MutuI cells. pLKO.1-hPGK-Puro-CMV-tGFP plasmids contained either a BACH1 targeting shRNA of the sequence CCGGCCAGCAAGAATGCCCAAGAACTCGAGTTTCTTGGGCATTCTTGCTGGTTTTT (Sigma-Aldrich, TRCN0000013596) or a non-targeting control shRNA of the sequence CCGGGCGCGATAGCGCTAATAATTTCTC GAGAAATTATTAGCGCTATCGCGCTTTTTT (Sigma-Aldrich, custom order). Lentiviruses were produced by transfecting plasmids into 293T

cells and infection-based titers measured with GFP expression (Wang and McManus, 2009) (UCSF ViraCore). MutuI cells were transduced at a multiplicity of infection of 3 for 1 day, spun down, and resuspended in RPMI-1640 with 25 mM HEPES, 2 g/L NaHCO<sub>3</sub>, 10% (v/v) fetal bovine serum, and 2 µg/µL puromycin in 5% CO<sub>2</sub> at 37 °C.

To enrich for Akata-Zta cells containing latent or lytic EBV episomes, populations were separated based on cell surface marker expression. Reactivated cells were magnetically purified using MACSelect LNGFR MicroBeads and LS Columns (Miltenyi Biotec).

**Staining and flow cytometry** — EBV immediate-early gene expression was measured by flow cytometry on a FACSCalibur (BD Biosciences) after staining for BZLF1 (Phan et al., 2016).

**Western blotting** — Protein knockdown was measured with Western blots using the SuperSignal West Pico Chemiluminescent Substrate (Thermo-Fisher), a ChemiDoc MP Imaging System (BioRad), and ImageLab version 5.2.1 (BioRad). BACH1 was detected using the F-9 antibody (Santa Cruz Biotechnology, sc-271211) at 1:300 dilution and rabbit anti-mouse-HRP (abcam, ab6728) at 1:5,000 dilution. For normalization, actin was detected using anti-β-actin (abcam, ab8227) at 1:10,000 dilution and rabbit anti-mouse-HRP (abcam, ab6728) at 1:10,000 dilution.

**RNA-seq** — RNA-seq libraries were prepared and sequenced as described (Phan et al., 2016). EBV transcriptome profiles were determined by mapping reads to the viral genome (Phan et al., 2016). Every experimental condition was measured with three independent biological replicates and yielded ~10–110 million mapped sequences per sample.

Differential expression of viral genes upon drug treatment was calculated by comparing independent triplicate experiments where Akata-Zta cells were induced with 500 ng/mL doxycycline for 1 day following 1 hour pretreatment with either 1 µM JQ1, 1 µM I-BET, or vehicle. Transcriptional changes were calculated by measuring normalized nucleotide counts for each lytic transcript integrated over only exons spanning regions that did not overlap with any other transcript (Phan et al. in press). The significance threshold was set at a p-value < 0.05.

Differential expression of human genes (Williams et al., 2014) upon drug treatment was calculated by comparing independent triplicate experiments where MutuI cells were treated with 1  $\mu$ M JQ1 or vehicle for 1 day. Adaptors and low-quality portions of reads were trimmed with Fastq-mcf, sequence quality control assessed with FastQC and RSeQC, and spliced and unspliced reads aligned to the hg19 reference human genome with Tophat 2.0.13 and Bowtie 2.2.4, respectively. Reads were assigned to genes as annotated by Ensembl using featureCounts. Genes yielding counts per million expression below 0.5 or above 5000 in more than one sample were excluded from analysis. Re-normalization of all other genes and calculation of differential expression p-values were performed with edgeR. Pathway enrichment analysis was performed with GO-Elite 1.2.5 and a cut-off p-value of 0.05. Transcription factors predicted to control enriched groups of genes were identified using a Z-score threshold of 2 from the MergedTFTargets gene set.

**ChIP-seq** — ChIP-seq methods were based on standard protocols (Aparicio et al., 2005) with the following modifications.  $3.6 \times 10^7$  treated cells were crosslinked by adding formaldehyde to 1% (v/v) at room temperature for 10 minutes. Cells were then washed, lysed, and the resulting nuclei frozen. Upon thawing, volumes were adjusted to 36% to reflect the starting cell number. Chromatin was digested with MNase for 5 minutes prior to shearing using a Bioruptor water bath sonicator (Diagenode). After sonication, tubes were vortexed and spun down for 10 minutes at 4°C and  $18,000 \times g$ . Aliquots of input samples with 10 mM Tris, 1 mM EDTA, pH 7.5 added to 80  $\mu$ L were combined with 100  $\mu$ L 50 mM Tris-HCl, pH 7.5, 10 mM EDTA, 1% (w/v) SDS, and 20  $\mu$ L 20 mg/mL Pronase in 100 mM Tris, 150 mM NaCl, pH 7.5 for reverse crosslinking. 10–15  $\mu$ L epitope-specific antibodies per ChIP were preincubated with 150  $\mu$ L protein G Dynabeads (Invitrogen) and 450  $\mu$ L of Buffer A containing 10 mM Tris-HCl, 1 mM EDTA, 150 mM NaCl, 5% (v/v) glycerol, 0.1% (w/v) sodium deoxycholate, 0.1% (w/v) SDS, 1% (v/v) Triton X-100, pH 8.0 rotating at 4°C for 1 hour. ChIP antibodies used recognized BRD4 (Bethyl, A301-985A), BRD2 (Cell Signaling, 5848S), BRD3 (Bethyl, A302-368A), H3K27ac (Abcam, ab4729), H3K9ac (Abcam, ab4441) and H3K4me3 (Abcam, ab8580). Dynabeads were transferred to 2.5 mL cold Buffer A without SDS but supplemented with 25  $\mu$ L Halt Protease Inhibitor Cocktail (Thermo Scientific). 277.5  $\mu$ L of chromatin, the proportion equivalent to  $1.5 \times 10^7$  cells, was added to the beads in buffer and incubated on a rotator for 4 hours at 4°C. Beads were collected



on a magnetic rack and washed consecutively with the following ice cold buffers: Buffer A with Halt Protease Inhibitor Cocktail, then Buffer A with 500 mM NaCl and Halt Protease Inhibitor Cocktail, and finally 20 mM Tris-HCl, 1 mM EDTA, 250 mM LiCl, 0.5% (v/v) NP-40, 0.5% (w/v) sodium deoxycholate, Halt Protease Inhibitor Cocktail, pH 8.0. Complexes were eluted from the beads in 300  $\mu$ L 10 mM Tris, 1 mM EDTA, 0.7% (w/v) SDS, pH 8.0 at room temperature. For reverse crosslinking, the eluate was added to 450  $\mu$ L of 50 mM Tris, 10 mM EDTA, 0.45% (w/v) SDS, pH 7.0 and 82.5  $\mu$ L 20 mg/mL Pronase in 100 mM Tris, 150 mM NaCl, pH 7.5. Reverse crosslinking of input and CHIP eluate samples was performed by incubation at 42°C for 2 hours and then 65°C overnight. DNA was purified by silica-based membrane affinity with a MinElute PCR Purification Kit (Qiagen). CHIP-seq libraries were prepared with either the Ovation Ultralow Library System (NuGen) or Ovation Ultralow Library System V2 (NuGen). Quantification and size distribution of libraries were observed using the Bioanalyzer High Sensitivity DNA Kit (Agilent). Size selection of the predominant DNA peak between ~200–400 bp was performed either by gel extraction or magnetic bead purification. For gel extraction, the band from a 1% agarose gel in Tris-acetate-EDTA was excised and purified with silica-based membrane affinity using a MinElute Gel Extraction Kit (Qiagen). For magnetic bead purification, solutions were treated with two steps of solid phase reversible immobilization using Agencourt RNAClean XP beads (Nugen). Libraries were sequenced on a HiSeq (Illumina).

For immunoprecipitation experiments measuring the effect of JQ1 treatment on BRD4 occupancy in the MutuI line,  $1 \times 10^8$  treated cells were processed per CHIP. Initial buffer volumes were scaled up accordingly, but purification occurred with 10  $\mu$ g BRD4-specific antibody preincubated with 100  $\mu$ L protein G Dynabeads. Other steps were identical to the protocol performed with fewer cells.

Sequence fragments were trimmed to 50 bp and mapped to an index containing both the human hg19 and the EBV reference (Genbank ID:NC\_007605.1) genomes using Bowtie 0.12.8 (Langmead et al., 2009) allowing for up to 2 mismatches and 2 alignments. Peaks on the EBV genome in MutuI cells were visualized after normalization to the background baseline (Holdorf et al., 2011). Peaks on the human genome in MutuI cells and EBV genome in Akata-Zta cells were visualized after normalization to the total number of mapped reads. We processed data

from Akata-Zta cells treated with doxycycline differently to control for the emergence of lytic linear genomes that may confound determination of the background baseline representing circular episomes. Every experimental condition was measured with two independent biological replicates and yielded ~20–80 million mapped sequences each data set.

**EBV DNA quantitation** — EBV genome abundance was determined by deep sequencing of total chromatin. Input chromatin was purified, libraries were prepared, and DNA was sequenced as described for ChIP-seq. The percentage of EBV reads was calculated as a proportion of viral reads that mapped to an index containing both the human hg19 and the EBV reference (Genbank ID:NC\_007605.1) genomes using Bowtie 0.12.8 (Langmead et al., 2009) allowing for up to 2 mismatches and 1 alignment. EBV genome abundance upon lytic induction and/or drug pretreatment was normalized to the vehicle control in each individual set of experiments. Every experimental condition was measured with three independent biological replicates and yielded ~10–30 million mapped sequences each data set.

**Replication fragment mapping** — DNA content distribution across the EBV genome upon induction of lytic replication was measured by deep sequencing of total DNA. Total DNA was purified by silica-based membrane affinity as packaged in the DNeasy Blood & Tissue Kit (Qiagen) and subsequently sheared using an S2 Focused-ultrasonicator (Covaris) to obtain fragments ~200 bp in length. Libraries were prepared, DNA sequenced, and reads mapped as described for ChIP-seq. Peaks on the EBV genome were visualized after normalization to the total number of mapped reads. Every experimental condition was measured with two independent biological replicates and yielded ~30–40 million mapped sequences each data set.

**Accession codes** — Deep sequencing data was deposited in the Gene Expression Omnibus database under accession code GSE84214

## Chapter IV: Discussion

This work has uncovered novel aspects of chromatin dynamics in EBV reactivation – movement of the viral genome from one chromatin compartment to another during reactivation, and a role for the chromatin-reading protein BRD4. We have shown that the EBV genome interacts with repressive chromatin during latency, and leaves this repressive compartment during reactivation. Surprisingly, we found that EBNA1 is not responsible for mediating EBV chromosome preferences – which is contrary to what we expected. Previously, it was known that EBNA1 binds to OriP and tethers the viral genome to the human genome during metaphase to ensure equal division of genomes among daughter cells (Frappier, 2015); however, it was unknown whether EBNA1 played a role in contacting human chromatin during interphase. Considering that the majority of the significant viral-human Hi-C interactions involved OriP, and that EBNA1 was a top predictor for these significant human-viral contacts, we believed EBNA1 was a strong candidate. However, after removal of EBNA1 using several different methods, we do not find a difference in chromosome preferences. We hypothesize that another protein that binds to OriP may be responsible for mediating these preferences.

Recent studies have begun to determine the factors important for recruitment of human sequences to the lamina. Targeted recruitment of YY1 to ectopic sequences facilitates recruitment to the lamina, but this is dependent on H3K27me3 and H3K9me2/3 (Harr et al., 2015). We do not see enrichment of either of these marks along the viral genome, and YY1 binding is only enriched in the W repeats (Arvey et al., 2013). We hypothesize that a different mechanism than the one used in human recruitment to the lamina is involved in EBV localization to the periphery and subsequent movement away from the periphery during reactivation. Interestingly, EBV encodes a viral kinase, BGLF4, which phosphorylates a wide variety of proteins including lamin A/C, which results in disruption of the lamina (Lee et al., 2008). This is thought to help mediate escape of viral capsids from the nucleus. It is tempting to speculate that this kinase may be involved in release of the viral genome from the periphery during reactivation. Future experiments determining the mechanism behind recruitment to the nuclear periphery as well as release from the periphery will have implications not only for the EBV field but also for the field of chromatin biology.

We found that EBV leaves the repressive compartment during reactivation; however, the opposite seems to be true for the alphaherpesvirus herpes simplex I (HSV). HSV1 associates with the lamina, resulting in decreased heterochromatin on the viral genome and increased immediate early gene expression (Silva et al., 2011; 2008). In lamin A/C<sup>-/-</sup> cells, viral transcription is reduced, viral replication compartments are smaller, and there are more heterochromatic marks on the viral genome (Silva et al., 2008), demonstrating that lamin A/C plays an important role in the reactivation of HSV1. Determining the role of the lamina in the lifecycle of different viruses and conducting experiments that tether the viral genome to the periphery, as previously done with human genes (Finlan et al., 2008; Reddy et al., 2008) will help clarify whether nuclear localization is sufficient to regulate transcription.

Understanding how nuclear localization of viral genomes affect their transcription could have implications in treating disease. For example, forcing genomes away from the nuclear periphery could increase reactivation of viruses during lytic induction therapy. Conversely, tethering genomes to the nuclear periphery could prevent reactivation of viruses. Though these strategies may be applicable for regulating gammaherpesviruses such as EBV and KSHV, it remains to be seen how many viruses use this mechanism to regulate their transcription.

Furthermore, the possible use of BET inhibitors as cancer treatment coupled with the knowledge that BET inhibitors can reactivate certain viruses led us to think about the possible implications of reactivating viruses from latency during cancer treatment. Contrary to several other viruses that have been studied, we found that the BET inhibitor JQ1 blocks the EBV lytic cycle. Opposite to what we expected, we did not find BRD4 bound to the immediate early BZLF1 promoter. Instead, we found that inhibition of BZLF expression was upstream, and likely a result of indirect effects of JQ1 on human genes such as BACH1. We also found that BRD4 was bound to the lytic origins of replication on the viral genome and that during reactivation, BRD4 occupancy increases 4-12 fold, and this increase is inhibited by treatment with JQ1. This inhibition of binding is concomitant with inhibition of viral replication, indicating that JQ1 blocks EBV replication at two distinct steps, by indirect upstream blocking of transcription of the immediate early protein BZLF1, and by blocking replication. Interestingly, when we performed BRD4 ChIP-seq with a greater number of cells, several smaller peaks became apparent. Further

investigations into these peaks may lead to a better understanding of the EBV lifecycle and how BET inhibitors interrupt it. These discoveries have implications in treating disease, as targeting two steps is more effective than monotherapy and provides less chance for development of resistance. JQ1 could be used as a treatment for infectious mononucleosis or post-transplant lymphoproliferative disorder.

In conclusion, these studies have not only led to a better understanding of how the latent-lytic switch of EBV is regulated, but have created a broader understanding of the definition of chromatin compartments and have led to the understanding that, in addition to intrachromosomal interactions, interchromosomal interactions can contribute to gene regulation. Further studies involving tethering the viral genome to specific regions will help elucidate the functional role of nuclear localization in EBV gene regulation. The challenge still remains to determine whether transcriptional changes drive changes in nuclear localization or vice-versa.

## References

- Ahmed, W., Philip, P.S., Tariq, S., and Khan, G. (2014). Epstein-Barr virus-encoded small RNAs (EBERs) are present in fractions related to exosomes released by EBV-transformed cells. *PLoS ONE* *9*, e99163.
- Alber, G., Kim, K.M., Weiser, P., Riesterer, C., Carsetti, R., and Reth, M. (1993). Molecular mimicry of the antigen receptor signalling motif by transmembrane proteins of the Epstein-Barr virus and the bovine leukaemia virus. *Curr. Biol.* *3*, 333–339.
- Alfonso-Dunn, R., Turner, A.-M.W., Jean Beltran, P.M., Arbuckle, J.H., Budayeva, H.G., Cristea, I.M., and Kristie, T.M. (2017). Transcriptional Elongation of HSV Immediate Early Genes by the Super Elongation Complex Drives Lytic Infection and Reactivation from Latency. *Cell Host & Microbe* *21*, 507–517.e5.
- Altmann, M., and Hammerschmidt, W. (2005). Epstein-Barr virus provides a new paradigm: a requirement for the immediate inhibition of apoptosis. *PLoS Biol* *3*, e404.
- Ambinder, R.F., Robertson, K.D., Moore, S.M., and Yang, J. (1996). Epstein-Barr virus as a therapeutic target in Hodgkin's disease and nasopharyngeal carcinoma. *Seminars in Cancer Biology* *7*, 217–226.
- Aparicio, O., Geisberg, J.V., Sekinger, E., Yang, A., Moqtaderi, Z., and Struhl, K. (2005). Chromatin immunoprecipitation for determining the association of proteins with specific genomic sequences in vivo. *Curr Protoc Mol Biol Chapter 21*, Unit21.3.
- Arvey, A., Tempera, I., and Lieberman, P. (2013). Interpreting the Epstein-Barr Virus (EBV) Epigenome Using High-Throughput Data. *Viruses* *5*, 1042–4254.
- Arvey, A., Tempera, I., Tsai, K., Chen, H.-S., Tikhmyanova, N., Klichinsky, M., Leslie, C., and Lieberman, P.M. (2012). An Atlas of the Epstein-Barr Virus Transcriptome and Epigenome Reveals Host-Virus Regulatory Interactions. *Cell Host & Microbe* *12*, 233–245.
- Asangani, I.A., Dommeti, V.L., Wang, X., Malik, R., Cieslik, M., Yang, R., Escara-Wilke, J., Wilder-Romans, K., Dhanireddy, S., Engelke, C., et al. (2014). Therapeutic targeting of BET bromodomain proteins in castration-resistant prostate cancer. *Nature* *510*, 278–282.

- Babcock, G.J., Decker, L.L., Volk, M., and Thorley-Lawson, D.A. (1998). EBV persistence in memory B cells in vivo. *Immunity* 9, 395–404.
- Ballester, M., Kress, C., Hue-Beauvais, C., Kiêu, K., Lehmann, G., Adenot, P., and Devinoy, E. (2008). The nuclear localization of WAP and CSN genes is modified by lactogenic hormones in HC11 cells. *J Cell Biochem* 105, 262–270.
- Banerjee, C., Archin, N., Michaels, D., Belkina, A.C., Denis, G.V., Bradner, J., Sebastiani, P., Margolis, D.M., and Montano, M. (2012). BET bromodomain inhibition as a novel strategy for reactivation of HIV-1. *J. Leukoc. Biol.* 92, 1147–1154.
- Baxter, M.K., McPhillips, M.G., Ozato, K., and McBride, A.A. (2005). The mitotic chromosome binding activity of the papillomavirus E2 protein correlates with interaction with the cellular chromosomal protein, Brd4. *Journal of Virology* 79, 4806–4818.
- Bellows, D.S., Howell, M., Pearson, C., Hazlewood, S.A., and Hardwick, J.M. (2002). Epstein-Barr virus BALF1 is a BCL-2-like antagonist of the herpesvirus antiapoptotic BCL-2 proteins. *Journal of Virology* 76, 2469–2479.
- Ben-Sasson, S.A., and Klein, G. (1981). Activation of the Epstein-Barr virus genome by 5-azacytidine in latently infected human lymphoid lines. *Int J Cancer* 28, 131–135.
- Bernheim, A., Berger, R., and Lenoir, G. (1980). [Translocations t(2;8) and t(8;22) in continuous cell lines of African Burkitt's lymphoma]. *C. R. Acad. Sci., D, Sci. Nat.* 291, 237–239.
- Bhende, P.M., Seaman, W.T., Delecluse, H.-J., and Kenney, S.C. (2004). The EBV lytic switch protein, Z, preferentially binds to and activates the methylated viral genome. *Nat Genet* 36, 1099–1104.
- Bochkarev, A., Barwell, J.A., Pfuetzner, R.A., Furey, W., Edwards, A.M., and Frappier, L. (1995). Crystal structure of the DNA-binding domain of the Epstein-Barr virus origin-binding protein EBNA 1. *Cell* 83, 39–46.
- Boehm, D., Calvanese, V., Dar, R.D., Xing, S., Schroeder, S., Martins, L., Aull, K., Li, P.-C., Planelles, V., Bradner, J.E., et al. (2013). BET bromodomain-targeting compounds reactivate

HIV from latency via a Tat-independent mechanism. *Cell Cycle* 12, 452–462.

Boettiger, A.N., Bintu, B., Moffitt, J.R., Wang, S., Beliveau, B.J., Fudenberg, G., Imakaev, M., Mirny, L.A., Wu, C.-T., and Zhuang, X. (2016). Super-resolution imaging reveals distinct chromatin folding for different epigenetic states. *Nature* 529, 418–422.

Bolzer, A., Kreth, G., Solovei, I., Koehler, D., Saracoglu, K., Fauth, C., Müller, S., Eils, R., Cremer, C., Speicher, M.R., et al. (2005). Three-dimensional maps of all chromosomes in human male fibroblast nuclei and prometaphase rosettes. *PLoS Biol* 3, e157.

Boyle, S., Gilchrist, S., Bridger, J.M., Mahy, N.L., Ellis, J.A., and Bickmore, W.A. (2001). The spatial organization of human chromosomes within the nuclei of normal and emerin-mutant cells. *Hum Mol Genet* 10, 211–219.

Branco, M.R., and Pombo, A. (2006). Intermingling of chromosome territories in interphase suggests role in translocations and transcription-dependent associations. *PLoS Biol* 4, e138.

Caldwell, R.G., Wilson, J.B., Anderson, S.J., and Longnecker, R. (1998). Epstein-Barr virus LMP2A drives B cell development and survival in the absence of normal B cell receptor signals. *Immunity* 9, 405–411.

Cancer Genome Atlas Research Network (2014). Comprehensive molecular characterization of gastric adenocarcinoma. *Nature* 513, 202–209.

Cesarman, E., Moore, P.S., Rao, P.H., Inghirami, G., Knowles, D.M., and Chang, Y. (1995). In vitro establishment and characterization of two acquired immunodeficiency syndrome-related lymphoma cell lines (BC-1 and BC-2) containing Kaposi's sarcoma-associated herpesvirus-like (KSHV) DNA sequences. *Blood* 86, 2708–2714.

Chambeyron, S., and Bickmore, W.A. (2004). Chromatin decondensation and nuclear reorganization of the *HoxB* locus upon induction of transcription. *Genes & Development* 18, 1119–1130.

Chapman, S., McDermott, D.H., Shen, K., Jang, M.K., and McBride, A.A. (2014). The effect of Rho kinase inhibition on long-term keratinocyte proliferation is rapid and conditional. *Stem Cell*



Res Ther 5, 60.

Chapuy, B., McKeown, M.R., Lin, C.Y., Monti, S., Roemer, M.G.M., Qi, J., Rahl, P.B., Sun, H.H., Yeda, K.T., Doench, J.G., et al. (2013). Discovery and Characterization of Super-Enhancer-Associated Dependencies in Diffuse Large B Cell Lymphoma. *Cancer Cell* 24, 777–790.

Chau, C.M., Zhang, X.Y., McMahon, S.B., and Lieberman, P.M. (2006). Regulation of Epstein-Barr Virus Latency Type by the Chromatin Boundary Factor CTCF. *Journal of Virology* 80, 5723–5732.

Chen, H.-L., Peng, J., Zhu, X.-B., Gao, J., Xue, J.-L., Wang, M.-W., and Xia, H.-S. (2010). Detection of EBV in nasopharyngeal carcinoma by quantum dot fluorescent in situ hybridization. *Experimental and Molecular Pathology* 89, 367–371.

Chen, H.-S., De Leo, A., Wang, Z., Kerekovic, A., Hills, R., and Lieberman, P.M. (2017). BET-Inhibitors Disrupt Rad21-Dependent Conformational Control of KSHV Latency. *PLoS Pathog* 13, e1006100.

Cheng, Y.C., Grill, S.P., Dutschman, G.E., Nakayama, K., and Bastow, K.F. (1983). Metabolism of 9-(1,3-dihydroxy-2-propoxymethyl)guanine, a new anti-herpes virus compound, in herpes simplex virus-infected cells. *J. Biol. Chem.* 258, 12460–12464.

Chiu, Y.-F., Sugden, A.U., and Sugden, B. (2013). Epstein-Barr viral productive amplification reprograms nuclear architecture, DNA replication, and histone deposition. *Cell Host & Microbe* 14, 607–618.

Clark, M.J., Miduturu, C., Schmidt, A.G., Zhu, X., Pitts, J.D., Wang, J., Potisophon, S., Zhang, J., Wojciechowski, A., Hann Chu, J.J., et al. (2016). GNF-2 Inhibits Dengue Virus by Targeting Abl Kinases and the Viral E Protein. *Cell Chem Biol* 23, 443–452.

Countryman, J., and Miller, G. (1985). Activation of expression of latent Epstein-Barr herpesvirus after gene transfer with a small cloned subfragment of heterogeneous viral DNA. *Proc. Natl. Acad. Sci. U.S.A.* 82, 4085–4089.

Davie, J.R. (2003). Inhibition of histone deacetylase activity by butyrate. *J. Nutr.* 133, 2485S–

2493S.

Day, L.L., Chau, C.M.C., Nebozhyn, M.M., Rennekamp, A.J.A., Showe, M.M., and Lieberman, P.M.P. (2007). Chromatin profiling of Epstein-Barr virus latency control region. *Journal of Virology* *81*, 6389–6401.

De Clercq, E. (2002). Strategies in the design of antiviral drugs. *Nat Rev Drug Discov* *1*, 13–25.

De Geest, K., Turyk, M.E., Hosken, M.I., Hudson, J.B., Laimins, L.A., and Wilbanks, G.D. (1993). Growth and differentiation of human papillomavirus type 31b positive human cervical cell lines. *Gynecol Oncol* *49*, 303–310.

Delmore, J.E., Issa, G.C., Lemieux, M.E., Rahl, P.B., Shi, J., Jacobs, H.M., Kastiris, E., Gilpatrick, T., Paranal, R.M., Qi, J., et al. (2011). BET bromodomain inhibition as a therapeutic strategy to target c-Myc. *Cell* *146*, 904–917.

Deutsch, M.J., Ott, E., Papior, P., and Schepers, A. (2010). The latent origin of replication of Epstein-Barr virus directs viral genomes to active regions of the nucleus. *Journal of Virology* *84*, 2533–2546.

Dheekollu, J., Wiedmer, A., Sentana-Lledo, D., Cassel, J., Messick, T., and Lieberman, P.M. (2016). HCF1 and OCT2 Cooperate with EBNA1 To Enhance OriP-Dependent Transcription and Episome Maintenance of Latent Epstein-Barr Virus. *Journal of Virology* *90*, 5353–5367.

di Renzo, L., Altiock, A., Klein, G., and Klein, E. (1994a). Endogenous TGF-beta contributes to the induction of the EBV lytic cycle in two Burkitt lymphoma cell lines. *Int J Cancer* *57*, 914–919.

di Renzo, L., Altiock, A., Klein, G., and Klein, E. (1994b). Endogenous TGF-beta contributes to the induction of the EBV lytic cycle in two Burkitt lymphoma cell lines. *Int J Cancer* *57*, 914–919.

Dieffenbach, C.W., and Fauci, A.S. (2011). Thirty years of HIV and AIDS: future challenges and opportunities. *Ann. Intern. Med.* *154*, 766–771.

Dixon, J.R., Jung, I., Selvaraj, S., Shen, Y., Antosiewicz-Bourget, J.E., Lee, A.Y., Ye, Z., Kim, A., Rajagopal, N., Xie, W., et al. (2015). Chromatin architecture reorganization during stem cell differentiation. *Nature* 518, 331–336.

Dixon, J.R., Selvaraj, S., Yue, F., Kim, A., Li, Y., Shen, Y., Hu, M., Liu, J.S., and Ren, B. (2012). Topological domains in mammalian genomes identified by analysis of chromatin interactions. *Nature* 485, 376–380.

Djavadian, R., Chiu, Y.-F., and Johannsen, E. (2016). An Epstein-Barr Virus-Encoded Protein Complex Requires an Origin of Lytic Replication In Cis to Mediate Late Gene Transcription. *PLoS Pathog* 12, e1005718.

Engreitz, J.M., Agarwala, V., and Mirny, L.A. (2012). Three-dimensional genome architecture influences partner selection for chromosomal translocations in human disease. *PLoS ONE* 7, e44196.

Erikson, J., ar-Rushdi, A., Drwinga, H.L., Nowell, P.C., and Croce, C.M. (1983). Transcriptional activation of the translocated c-myc oncogene in burkitt lymphoma. *Proc. Natl. Acad. Sci. U.S.a.* 80, 820–824.

Faggioni, A., Zompetta, C., Grimaldi, S., Barile, G., Frati, L., and Lazdins, J. (1986). Calcium modulation activates Epstein-Barr virus genome in latently infected cells. *Science* 232, 1554–1556.

Fahmi, H., Cochet, C., Hmama, Z., Opolon, P., and Joab, I. (2000). Transforming growth factor beta 1 stimulates expression of the Epstein-Barr virus BZLF1 immediate-early gene product ZEBRA by an indirect mechanism which requires the MAPK kinase pathway. *Journal of Virology* 74, 5810–5818.

Feng, W.-H., Hong, G., Delecluse, H.-J., and Kenney, S.C. (2004). Lytic induction therapy for Epstein-Barr virus-positive B-cell lymphomas. *Journal of Virology* 78, 1893–1902.

Feng, W.-H., Israel, B., Raab-Traub, N., Busson, P., and Kenney, S.C. (2002a). Chemotherapy induces lytic EBV replication and confers ganciclovir susceptibility to EBV-positive epithelial cell tumors. *Cancer Research* 62, 1920–1926.

Feng, W.-H., Westphal, E., Mauser, A., Raab-Traub, N., Gulley, M.L., Busson, P., and Kenney, S.C. (2002b). Use of adenovirus vectors expressing Epstein-Barr virus (EBV) immediate-early protein BZLF1 or BRLF1 to treat EBV-positive tumors. *Journal of Virology* 76, 10951–10959.

Fernandez, S.G., and Miranda, J.J.L. (2016). Bendamustine reactivates latent Epstein-Barr virus. *Leuk. Lymphoma* 57, 1208–1210.

Filippakopoulos, P., Qi, J., Picaud, S., Shen, Y., Smith, W.B., Fedorov, O., Morse, E.M., Keates, T., Hickman, T.T., Felletar, I., et al. (2010). Selective inhibition of BET bromodomains. *Nature* 468, 1067–1073.

Finlan, L.E., Sproul, D., Thomson, I., Boyle, S., Kerr, E., Perry, P., Ylstra, B., Chubb, J.R., and Bickmore, W.A. (2008). Recruitment to the Nuclear Periphery Can Alter Expression of Genes in Human Cells. *PLoS Genet* 4, e1000039.

Fixman, E.D., Hayward, G.S., and Hayward, S.D. (1992). trans-acting requirements for replication of Epstein-Barr virus ori-Lyt. *Journal of Virology* 66, 5030–5039.

Frappier, L. (2015). EBNA1. In *Current Topics in Microbiology and Immunology*, (Cham: Springer International Publishing), pp. 3–34.

Freeman, S.M., Abboud, C.N., Whartenby, K.A., Packman, C.H., Koeplin, D.S., Moolten, F.L., and Abraham, G.N. (1993). The “bystander effect”: tumor regression when a fraction of the tumor mass is genetically modified. *Cancer Research* 53, 5274–5283.

Fullwood, M.J., Liu, M.H., Pan, Y.F., Liu, J., Xu, H., Mohamed, Y.B., Orlov, Y.L., Velkov, S., Ho, A., Mei, P.H., et al. (2009). An oestrogen-receptor-alpha-bound human chromatin interactome. *Nature* 462, 58–64.

Furman, P.A., St Clair, M.H., Fyfe, J.A., Rideout, J.L., Keller, P.M., and ELION, G.B. (1979). Inhibition of herpes simplex virus-induced DNA polymerase activity and viral DNA replication by 9-(2-hydroxyethoxymethyl)guanine and its triphosphate. *Journal of Virology* 32, 72–77.

Gahn, T.A., and Sugden, B. (1995). An EBNA-1-dependent enhancer acts from a distance of 10 kilobase pairs to increase expression of the Epstein-Barr virus LMP gene. *Journal of Virology*

69, 2633–2636.

Gao, X., Ikuta, K., Tajima, M., and Sairenji, T. (2001). 12-O-tetradecanoylphorbol-13-acetate induces Epstein-Barr virus reactivation via NF-kappaB and AP-1 as regulated by protein kinase C and mitogen-activated protein kinase. *Virology* 286, 91–99.

Gasser, S.M. (2002). Visualizing chromatin dynamics in interphase nuclei. *Science* 296, 1412–1416.

Gregory, C.D., Rowe, M., and Rickinson, A.B. (1990). Different Epstein-Barr virus-B cell interactions in phenotypically distinct clones of a Burkitt's lymphoma cell line. *J. Gen. Virol.* 71 (Pt 7), 1481–1495.

Guelen, L., Pagie, L., Brasset, E., Meuleman, W., Faza, M.B., Talhout, W., Eussen, B.H., de Klein, A., Wessels, L., de Laat, W., et al. (2008). Domain organization of human chromosomes revealed by mapping of nuclear lamina interactions. *Nature* 453, 948–951.

Gutiérrez, M.I., Judde, J.G., Magrath, I.T., and Bhatia, K.G. (1996). Switching viral latency to viral lysis: a novel therapeutic approach for Epstein-Barr virus-associated neoplasia. *Cancer Research* 56, 969–972.

Hammerschmidt, W., and Sugden, B. (1988). Identification and characterization of oriLyt, a lytic origin of DNA replication of Epstein-Barr virus. *Cell* 55, 427–433.

Harr, J.C., Luperchio, T.R., Wong, X., Cohen, E., Wheelan, S.J., and Reddy, K.L. (2015). Directed targeting of chromatin to the nuclear lamina is mediated by chromatin state and A-type lamins. *J Cell Biol* 208, 33–52.

Hausen, zur, A., van Rees, B.P., van Beek, J., Craanen, M.E., Bloemena, E., Offerhaus, G.J.A., Meijer, C.J.L.M., and van den Brule, A.J.C. (2004). Epstein-Barr virus in gastric carcinomas and gastric stump carcinomas: a late event in gastric carcinogenesis. *J. Clin. Pathol.* 57, 487–491.

Henderson, A., Ripley, S., Heller, M., and Kieff, E. (1983). Chromosome site for Epstein-Barr virus DNA in a Burkitt tumor cell line and in lymphocytes growth-transformed in vitro. *Proc. Natl. Acad. Sci. U.S.a.* 80, 1987–1991.

- Henderson, S., Huen, D., Rowe, M., Dawson, C., Johnson, G., and Rickinson, A. (1993). Epstein-Barr virus-coded BHRF1 protein, a viral homologue of Bcl-2, protects human B cells from programmed cell death. *Proc. Natl. Acad. Sci. U.S.a.* *90*, 8479–8483.
- Holdorf, M.M., Cooper, S.B., Yamamoto, K.R., and Miranda, J.J.L. (2011). Occupancy of chromatin organizers in the Epstein-Barr virus genome. *Virology* *415*, 1–5.
- Hong, G.K., Kumar, P., Wang, L., Damania, B., Gulley, M.L., Delecluse, H.J., Polverini, P.J., and Kenney, S.C. (2005a). Epstein-Barr Virus Lytic Infection Is Required for Efficient Production of the Angiogenesis Factor Vascular Endothelial Growth Factor in Lymphoblastoid Cell Lines. *Journal of Virology* *79*, 13984–13992.
- Hong, G.K., Gulley, M.L., Feng, W.-H., Delecluse, H.-J., Holley-Guthrie, E., and Kenney, S.C. (2005b). Epstein-Barr virus lytic infection contributes to lymphoproliferative disease in a SCID mouse model. *Journal of Virology* *79*, 13993–14003.
- Hopkins, A.L. (2008). Network pharmacology: the next paradigm in drug discovery. *Nat. Chem. Biol.* *4*, 682–690.
- Hsu, C.-Y., Yi, Y.-H., Chang, K.-P., Chang, Y.-S., Chen, S.-J., and Chen, H.-C. (2014). The Epstein-Barr virus-encoded microRNA MiR-BART9 promotes tumor metastasis by targeting E-cadherin in nasopharyngeal carcinoma. *PLoS Pathog* *10*, e1003974.
- Hsu, D.H., de Waal Malefyt, R., Fiorentino, D.F., Dang, M.N., Vieira, P., de Vries, J., Spits, H., Mosmann, T.R., and Moore, K.W. (1990). Expression of interleukin-10 activity by Epstein-Barr virus protein BCRF1. *Science* *250*, 830–832.
- Hung, S.C., Kang, M.S., and Kieff, E. (2001). Maintenance of Epstein-Barr virus (EBV) oriP-based episomes requires EBV-encoded nuclear antigen-1 chromosome-binding domains, which can be replaced by high-mobility group-I or histone H1. *Proc. Natl. Acad. Sci. U.S.a.* *98*, 1865–1870.
- Iempridee, T., Das, S., Xu, I., and Mertz, J.E. (2011). Transforming growth factor beta-induced reactivation of Epstein-Barr virus involves multiple Smad-binding elements cooperatively activating expression of the latent-lytic switch BZLF1 gene. *Journal of Virology* *85*, 7836–7848.

Ilves, I., Mäemets, K., Silla, T., Janikson, K., and Ustav, M. (2006). Brd4 is involved in multiple processes of the bovine papillomavirus type 1 life cycle. *Journal of Virology* 80, 3660–3665.

Imai, S., Koizumi, S., Sugiura, M., Tokunaga, M., Uemura, Y., Yamamoto, N., Tanaka, S., Sato, E., and Osato, T. (1994). Gastric carcinoma: monoclonal epithelial malignant cells expressing Epstein-Barr virus latent infection protein. *Proc. Natl. Acad. Sci. U.S.a.* 91, 9131–9135.

Imai, S., Nishikawa, J., and Takada, K. (1998). Cell-to-cell contact as an efficient mode of Epstein-Barr virus infection of diverse human epithelial cells. *Journal of Virology* 72, 4371–4378.

Iwakiri, D., and Takada, K. (2010). Role of EBERs in the pathogenesis of EBV infection. *Adv. Cancer Res.* 107, 119–136.

Jeon, S., Allen-Hoffmann, B.L., and Lambert, P.F. (1995). Integration of human papillomavirus type 16 into the human genome correlates with a selective growth advantage of cells. *Journal of Virology* 69, 2989–2997.

Jia, W.-H., and Qin, H.-D. (2012). Non-viral environmental risk factors for nasopharyngeal carcinoma: a systematic review. *Seminars in Cancer Biology* 22, 117–126.

Jiang, J.-H., Wang, N., Li, A., Liao, W.-T., Pan, Z.-G., Mai, S.-J., Li, D.-J., Zeng, M.-S., Wen, J.-M., and Zeng, Y.-X. (2006). Hypoxia can contribute to the induction of the Epstein-Barr virus (EBV) lytic cycle. *J. Clin. Virol.* 37, 98–103.

Johannsen, E., Luftig, M., Chase, M.R., Weicksel, S., Cahir-McFarland, E., Illanes, D., Sarracino, D., and Kieff, E. (2004). Proteins of purified Epstein-Barr virus. *Proc. Natl. Acad. Sci. U.S.a.* 101, 16286–16291.

Jung, M., Gelato, K.A., Fernández-Montalván, A., Siegel, S., and Haendler, B. (2015). Targeting BET bromodomains for cancer treatment. *Epigenomics* 7, 487–501.

Kalhor, R., Tjong, H., Jayathilaka, N., Alber, F., and Chen, L. (2011). Genome architectures revealed by tethered chromosome conformation capture and population-based modeling. *Nat Biotechnol* 30, 90–98.

- Kalla, M., Gobel, C., and Hammerschmidt, W. (2011). The Lytic Phase of Epstein-Barr Virus Requires a Viral Genome with 5-Methylcytosine Residues in CpG Sites. *Journal of Virology* *86*, 447–458.
- Kanda, T., Horikoshi, N., Murata, T., Kawashima, D., Sugimoto, A., Narita, Y., Kurumizaka, H., and Tsurumi, T. (2013). Interaction between Basic Residues of Epstein-Barr Virus EBNA1 Protein and Cellular Chromatin Mediates Viral Plasmid Maintenance. *Journal of Biological Chemistry* *288*, 24189–24199.
- Kanda, T., Miyata, M., Kano, M., Kondo, S., Yoshizaki, T., and Iizasa, H. (2015). Clustered microRNAs of the Epstein-Barr virus cooperatively downregulate an epithelial cell-specific metastasis suppressor. *Journal of Virology* *89*, 2684–2697.
- Kang, D., Skalsky, R.L., and Cullen, B.R. (2015). EBV BART MicroRNAs Target Multiple Pro-apoptotic Cellular Genes to Promote Epithelial Cell Survival. *PLoS Pathog* *11*, e1004979.
- Kaye, K.M., Izumi, K.M., and Kieff, E. (1993). Epstein-Barr virus latent membrane protein 1 is essential for B-lymphocyte growth transformation. *Proc. Natl. Acad. Sci. U.S.a.* *90*, 9150–9154.
- Kelly, G.L., Long, H.M., Stylianou, J., Thomas, W.A., Leese, A., Bell, A.I., Bornkamm, G.W., Mautner, J., Rickinson, A.B., and Rowe, M. (2009). An Epstein-Barr virus anti-apoptotic protein constitutively expressed in transformed cells and implicated in burkitt lymphomagenesis: the Wp/BHRF1 link. *PLoS Pathog* *5*, e1000341.
- Kenney, S., Ge, J.Q., Westphal, E.M., and Olsen, J. (1998). Gene therapy strategies for treating Epstein-Barr virus-associated lymphomas: comparison of two different Epstein-Barr virus-based vectors. *Hum. Gene Ther.* *9*, 1131–1141.
- Kenney, S.C. (2007). Reactivation and lytic replication of EBV. In *Human Herpesviruses: Biology, Therapy, and Immunoprophylaxis*, A. Arvin, G. Campadelli-Fiume, E. Mocarski, P.S. Moore, B. Roizman, R. Whitley, K. Yamanishi, and S.C. Kenney, eds. (Cambridge: Cambridge University Press).
- Kenney, S.C., and Mertz, J.E. (2014). *Seminars in Cancer Biology*. *Seminars in Cancer Biology* *26*, 60–68.



Kent, W.J., Sugnet, C.W., Furey, T.S., Roskin, K.M., Pringle, T.H., Zahler, A.M., and Haussler, D. (2002). The human genome browser at UCSC. *Genome Res* 12, 996–1006.

Kieff, E., and Rickinson, A.B. (2013). Epstein-Barr Virus and Its Replication. In *Fields Virology*, D.M. Knipe, and P.M. Howley, eds. (Philadelphia: Lippincott Williams & Wilkins), pp. 2603–2654.

Klein, G. (1983). Specific chromosomal translocations and the genesis of B-cell-derived tumors in mice and men. *Cell* 32, 311–315.

Klein, G., Dombos, L., and Gothoskar, B. (1972). Sensitivity of Epstein-Barr virus (EBV) producer and non-producer human lymphoblastoid cell lines to superinfection with EB-virus. *Int J Cancer* 10, 44–57.

Kosak, S.T., Skok, J.A., Medina, K.L., Riblet, R., Le Beau, M.M., Fisher, A.G., and Singh, H. (2002). Subnuclear compartmentalization of immunoglobulin loci during lymphocyte development. *Science* 296, 158–162.

Kozomara, A., and Griffiths-Jones, S. (2014). miRBase: annotating high confidence microRNAs using deep sequencing data. *Nucleic Acids Res* 42, D68–D73.

Kress, C., Kiêu, K., Droineau, S., Galio, L., and Devinoy, E. (2011). Specific positioning of the casein gene cluster in active nuclear domains in luminal mammary epithelial cells. *Chromosome Res* 19, 979–997.

Kumaran, R.I., and Spector, D.L. (2008). A genetic locus targeted to the nuclear periphery in living cells maintains its transcriptional competence. *J Cell Biol* 180, 51–65.

Laichalk, L.L., and Thorley-Lawson, D.A. (2005). Terminal differentiation into plasma cells initiates the replicative cycle of Epstein-Barr virus in vivo. *Journal of Virology* 79, 1296–1307.

Langmead, B., Trapnell, C., Pop, M., and Salzberg, S.L. (2009). Ultrafast and memory-efficient alignment of short DNA sequences to the human genome. *Genome Biol* 10, R25.

Lee, C.P., Chen, J.Y., Wang, J.T., Kimura, K., Takemoto, A., Lu, C.C., and Chen, M.R. (2007).

- Epstein-Barr Virus BGLF4 Kinase Induces Premature Chromosome Condensation through Activation of Condensin and Topoisomerase II. *Journal of Virology* *81*, 5166–5180.
- Lee, C.P., Huang, Y.H., Lin, S.F., Chang, Y., Chang, Y.H., Takada, K., and Chen, M.R. (2008). Epstein-Barr Virus BGLF4 Kinase Induces Disassembly of the Nuclear Lamina To Facilitate Virion Production. *Journal of Virology* *82*, 11913–11926.
- Lee, H.S., Chang, M.S., Yang, H.-K., Lee, B.L., and Kim, W.H. (2004). Epstein-barr virus-positive gastric carcinoma has a distinct protein expression profile in comparison with epstein-barr virus-negative carcinoma. *Clin Cancer Res* *10*, 1698–1705.
- Lei, T., Yuen, K.-S., Xu, R., Tsao, S.-W., Chen, H., Li, M., Kok, K.-H., and Jin, D.-Y. (2013). Targeting of DICE1 tumor suppressor by Epstein-Barr virus-encoded miR-BART3\* microRNA in nasopharyngeal carcinoma. *Int J Cancer* *133*, 79–87.
- Leight, E.R., and Sugden, B. (2000). EBNA-1: a protein pivotal to latent infection by Epstein-Barr virus. *Rev. Med. Virol.* *10*, 83–100.
- Levitskaya, J., Coram, M., Levitsky, V., Imreh, S., Steigerwald-Mullen, P.M., Klein, G., Kurilla, M.G., and Masucci, M.G. (1995). Inhibition of antigen processing by the internal repeat region of the Epstein-Barr virus nuclear antigen-1. *Nature* *375*, 685–688.
- Levitskaya, J., Sharipo, A., Leonchiks, A., Ciechanover, A., and Masucci, M.G. (1997). Inhibition of ubiquitin/proteasome-dependent protein degradation by the Gly-Ala repeat domain of the Epstein-Barr virus nuclear antigen 1. *Proc. Natl. Acad. Sci. U.S.a.* *94*, 12616–12621.
- Li, Z., Guo, J., Wu, Y., and Zhou, Q. (2013). The BET bromodomain inhibitor JQ1 activates HIV latency through antagonizing Brd4 inhibition of Tat-transactivation. *Nucleic Acids Res* *41*, 277–287.
- Lieberman-Aiden, E., van Berkum, N.L., Williams, L., Imakaev, M., Ragoczy, T., Telling, A., Amit, I., Lajoie, B.R., Sabo, P.J., Dorschner, M.O., et al. (2009). Comprehensive mapping of long-range interactions reveals folding principles of the human genome. *Science* *326*, 289–293.
- Lin, A., Wang, S., Nguyen, T., Shire, K., and Frappier, L. (2008). The EBNA1 protein of

Epstein-Barr virus functionally interacts with Brd4. *Journal of Virology* 82, 12009–12019.

Lin, J.C., SMITH, M.C., and Pagano, J.S. (1984). Prolonged Inhibitory Effect of 9-(1,3-Dihydroxy-2-Propoxymethyl)Guanine Against Replication of Epstein-Barr Virus. *Journal of Virology* 50, 50–55.

Ling, J.Q., Li, T., Hu, J.F., Vu, T.H., Chen, H.L., Qiu, X.W., Cherry, A.M., and Hoffman, A.R. (2006). CTCF mediates interchromosomal colocalization between Igf2/H19 and Wsb1/Nf1. *Science* 312, 269–272.

Lomvardas, S., Barnea, G., Pisapia, D.J., Mendelsohn, M., Kirkland, J., and Axel, R. (2006). Interchromosomal interactions and olfactory receptor choice. *Cell* 126, 403–413.

Lovén, J., Hoke, H.A., Lin, C.Y., Lau, A., Orlando, D.A., Vakoc, C.R., Bradner, J.E., Lee, T.I., and Young, R.A. (2013). Selective Inhibition of Tumor Oncogenes by Disruption of Super-Enhancers. *Cell* 153, 320–334.

Lozzio, C.B., and Lozzio, B.B. (1975). Human Chronic Myelogenous Leukemia Cell-Line with Positive Philadelphia Chromosome. *Blood* 45, 321–334.

Luzuriaga, K., and Sullivan, J.L. (2010). Infectious mononucleosis. *N. Engl. J. Med.* 362, 1993–2000.

Ma, S.-D., Hegde, S., Young, K.H., Sullivan, R., Rajesh, D., Zhou, Y., Jankowska-Gan, E., Burlingham, W.J., Sun, X., Gulley, M.L., et al. (2011). A new model of Epstein-Barr virus infection reveals an important role for early lytic viral protein expression in the development of lymphomas. *Journal of Virology* 85, 165–177.

Marquitz, A.R., and Raab-Traub, N. (2012). The role of miRNAs and EBV BARTs in NPC. *Seminars in Cancer Biology* 22, 166–172.

Marshall, W.L., Yim, C., Gustafson, E., Graf, T., Sage, D.R., Hanify, K., Williams, L., Fingerhuth, J., and Finberg, R.W. (1999). Epstein-Barr virus encodes a novel homolog of the bcl-2 oncogene that inhibits apoptosis and associates with Bax and Bak. *Journal of Virology* 73, 5181–5185.

- Masood, R., Zhang, Y., Bond, M.W., Scadden, D.T., Moudgil, T., Law, R.E., Kaplan, M.H., Jung, B., Espina, B.M., and Lunardi-Iskandar, Y. (1995). Interleukin-10 is an autocrine growth factor for acquired immunodeficiency syndrome-related B-cell lymphoma. *Blood* 85, 3423–3430.
- McLean, C.Y., Bristor, D., Hiller, M., Clarke, S.L., Schaar, B.T., Lowe, C.B., Wenger, A.M., and Bejerano, G. (2010). GREAT improves functional interpretation of cis-regulatory regions. *Nat Biotechnol* 28, 495–501.
- McPhillips, M.G., Oliveira, J.G., Spindler, J.E., Mitra, R., and McBride, A.A. (2006). Brd4 is required for e2-mediated transcriptional activation but not genome partitioning of all papillomaviruses. *Journal of Virology* 80, 9530–9543.
- Mentzer, S.J., Fingerhuth, J., Reilly, J.J., Perrine, S.P., and Faller, D.V. (1998). Arginine butyrate-induced susceptibility to ganciclovir in an Epstein-Barr-virus-associated lymphoma. *Blood Cells, Molecules, and Diseases* 24, 114–123.
- Mentzer, S.J., Perrine, S.P., and Faller, D.V. (2001). Epstein--Barr virus post-transplant lymphoproliferative disease and virus-specific therapy: pharmacological re-activation of viral target genes with arginine butyrate. *Transpl Infect Dis* 3, 177–185.
- Mertz, J.A., Conery, A.R., Bryant, B.M., Sandy, P., Balasubramanian, S., Mele, D.A., Bergeron, L., and Sims, R.J. (2011). Targeting MYC dependence in cancer by inhibiting BET bromodomains. *Proc Natl Acad Sci U S A* 108, 16669–16674.
- Mettenleiter, T.C. (2002). Herpesvirus assembly and egress. *Journal of Virology* 76, 1537–1547.
- Mifsud, B., Martincorena, I., Darbo, E., Sugar, R., Schoenfelder, S., Fraser, P., and Luscombe, N. (2015). GOTHic, a simple probabilistic model to resolve complex biases and to identify real interactions in Hi-C data (bioRxiv).
- Mosialos, G., Birkenbach, M., Yalamanchili, R., VanArsdale, T., Ware, C., and Kieff, E. (1995). The Epstein-Barr virus transforming protein LMP1 engages signaling proteins for the tumor necrosis factor receptor family. *Cell* 80, 389–399.

- Moss, D.J., Misko, I.S., Burrows, S.R., Burman, K., McCarthy, R., and Sculley, T.B. (1988). Cytotoxic T-cell clones discriminate between A- and B-type Epstein-Barr virus transformants. *Nature* 331, 719–721.
- Nagano, T., Lubling, Y., Stevens, T.J., Schoenfelder, S., Yaffe, E., Dean, W., Laue, E.D., Tanay, A., and Fraser, P. (2013). Single-cell Hi-C reveals cell-to-cell variability in chromosome structure. *Nature* 502, 59–64.
- Nagano, T., Várnai, C., Schoenfelder, S., Javierre, B.-M., Wingett, S.W., and Fraser, P. (2015). Comparison of Hi-C results using in-solution versus in-nucleus ligation. *Genome Biol* 16, 1068.
- Naidoo, N., Pawitan, Y., Soong, R., Cooper, D.N., and Ku, C.-S. (2011). Human genetics and genomics a decade after the release of the draft sequence of the human genome. *Hum. Genomics* 5, 577–622.
- Newman, C., and Polk, B.F. (1987). Resolution of oral hairy leukoplakia during therapy with 9-(1,3-dihydroxy-2-propoxymethyl)guanine (DHPG). *Ann. Intern. Med.* 107, 348–350.
- Nicodeme, E., Jeffrey, K.L., Schaefer, U., Beinke, S., Dewell, S., Chung, C.-W., Chandwani, R., Marazzi, I., Wilson, P., Coste, H., et al. (2010). Suppression of inflammation by a synthetic histone mimic. *Nature* 468, 1119–1123.
- Nilsson, T., Zetterberg, H., Wang, Y.C., and Rymo, L. (2001). Promoter-proximal regulatory elements involved in oriP-EBNA1-independent and -dependent activation of the Epstein-Barr virus C promoter in B-lymphoid cell lines. *Journal of Virology* 75, 5796–5811.
- Norseen, J., Johnson, F.B., and Lieberman, P.M. Role for G-quadruplex RNA binding by Epstein-Barr virus nuclear antigen 1 in DNA replication and metaphase chromosome attachment. *Journal of Virology* 83, 10336–10346.
- Osborne, C.S., Chakalova, L., Brown, K.E., Carter, D., Horton, A., Debrand, E., Goyenechea, B., Mitchell, J.A., Lopes, S., Reik, W., et al. (2004). Active genes dynamically colocalize to shared sites of ongoing transcription. *Nat Genet* 36, 1065–1071.
- Palermo, R.D., Webb, H.M., and West, M.J. (2011). RNA Polymerase II Stalling Promotes

Nucleosome Occlusion and pTEFb Recruitment to Drive Immortalization by Epstein-Barr Virus. *PLoS Pathog* 7, e1002334.

Pallesen, G., Hamilton-Dutoit, S.J., Rowe, M., and Young, L.S. (1991). Expression of Epstein-Barr virus latent gene products in tumour cells of Hodgkin's disease. *Lancet* 337, 320–322.

Pearson, G.R., Luka, J., Petti, L., Sample, J., Birkenbach, M., Braun, D., and Kieff, E. (1987). Identification of an Epstein-Barr virus early gene encoding a second component of the restricted early antigen complex. *Virology* 160, 151–161.

Pedregosa, F., Varoquaux, G., Gramfort, A., Michel, V., Thirion, B., Grisel, O., Blondel, M., Prettenhofer, P., Weiss, R., Dubourg, V., et al. (2011). Scikit-learn: Machine Learning in Python. *Journal of Machine Learning Research* 2835–2830.

Peric-Hupkes, D., Meuleman, W., Pagie, L., Bruggeman, S.W.M., Solovei, I., Brugman, W., Gräf, S., Flicek, P., Kerkhoven, R.M., van Lohuizen, M., et al. (2010). Molecular maps of the reorganization of genome-nuclear lamina interactions during differentiation. *Mol Cell* 38, 603–613.

Perrine, S.P., Hermine, O., Small, T., Suarez, F., O'Reilly, R., Boulad, F., Fingerhuth, J., Askin, M., Levy, A., Mentzer, S.J., et al. (2007). A phase 1/2 trial of arginine butyrate and ganciclovir in patients with Epstein-Barr virus-associated lymphoid malignancies. *Blood* 109, 2571–2578.

Phan, A.T., Fernandez, S.G., Somberg, J.J., Keck, K.M., and Miranda, J.L. (2016). Biochemical and Biophysical Research Communications. *Biochem Biophys Res Commun* 474, 71–75.

Picaud, S., Wells, C., Felletar, I., Brotherton, D., Martin, S., Savitsky, P., Diez-Dacal, B., Philpott, M., Bountra, C., Lingard, H., et al. (2013). RVX-208, an inhibitor of BET transcriptional regulators with selectivity for the second bromodomain. *Proc Natl Acad Sci U S A* 110, 19754–19759.

Pickersgill, H., Kalverda, B., de Wit, E., Talhout, W., Fornerod, M., and van Steensel, B. (2006). Characterization of the *Drosophila melanogaster* genome at the nuclear lamina. *Nat Genet* 38, 1005–1014.

Price, A.M., and Luftig, M.A. (2015). To be or not IIb: a multi-step process for Epstein-Barr virus latency establishment and consequences for B cell tumorigenesis. *PLoS Pathog* *11*, e1004656.

Pritchett, R., Pedersen, M., and Kieff, E. (1976). Complexity of EBV homologous DNA in continuous lymphoblastoid cell lines. *Virology* *74*, 227–231.

Puglielli, M.T., Woisetschlaeger, M., and Speck, S.H. (1996). oriP is essential for EBNA gene promoter activity in Epstein-Barr virus-immortalized lymphoblastoid cell lines. *Journal of Virology* *70*, 5758–5768.

Quinlan, A.R. (2014). BEDTools: The Swiss-Army Tool for Genome Feature Analysis. *Bioinformatics* *26*, 841–842.

Ramasubramanian, S., Osborn, K., Al-Mohammad, R., Naranjo Perez-Fernandez, I.B., Zuo, J., Balan, N., Godfrey, A., Patel, H., Peters, G., Rowe, M., et al. (2015). Epstein-Barr virus transcription factor Zta acts through distal regulatory elements to directly control cellular gene expression. *Nucleic Acids Res* *43*, 3563–3577.

Rao, S.S.P., Huntley, M.H., Durand, N.C., Stamenova, E.K., Bochkov, I.D., Robinson, J.T., Sanborn, A.L., Machol, I., Omer, A.D., Lander, E.S., et al. (2014). A 3D map of the human genome at kilobase resolution reveals principles of chromatin looping. *Cell* *159*, 1665–1680.

Reddy, K.L., Zullo, J.M., Bertolino, E., and Singh, H. (2008). Transcriptional repression mediated by repositioning of genes to the nuclear lamina. *Nature* *452*, 243–247.

Ren, K., Zhang, W., Chen, X., Ma, Y., Dai, Y., Fan, Y., Hou, Y., Tan, R.X., and Li, E. (2016). An Epigenetic Compound Library Screen Identifies BET Inhibitors That Promote HSV-1 and -2 Replication by Bridging P-TEFb to Viral Gene Promoters through BRD4. *PLoS Pathog* *12*, e1005950.

Resnick, L., Herbst, J.S., Ablashi, D.V., Atherton, S., Frank, B., Rosen, L., and Horwitz, S.N. (1988). Regression of oral hairy leukoplakia after orally administered acyclovir therapy. *Jama* *259*, 384–388.

- Roychowdhury, S., Peng, R., Baiocchi, R.A., Bhatt, D., Vourganti, S., Grecula, J., Gupta, N., Eisenbeis, C.F., Nuovo, G.J., Yang, W., et al. (2003). Experimental treatment of Epstein-Barr virus-associated primary central nervous system lymphoma. *Cancer Research* 63, 965–971.
- Scala, G., Quinto, I., Ruocco, M.R., Arcucci, A., Mallardo, M., Caretto, P., Forni, G., and Venuta, S. (1990). Expression of an exogenous interleukin 6 gene in human Epstein Barr virus B cells confers growth advantage and in vivo tumorigenicity. *J. Exp. Med.* 172, 61–68.
- Schneider, B.G., Gulley, M.L., Eagan, P., Bravo, J.C., Mera, R., and Geradts, J. (2000). Loss of p16/CDKN2A tumor suppressor protein in gastric adenocarcinoma is associated with Epstein-Barr virus and anatomic location in the body of the stomach. *Human Pathology* 31, 45–50.
- Schweiger, M.-R., You, J., and Howley, P.M. (2006). Bromodomain protein 4 mediates the papillomavirus E2 transcriptional activation function. *Journal of Virology* 80, 4276–4285.
- Sears, J., Ujihara, M., Wong, S., Ott, C., Middeldorp, J., and Aiyar, A. (2004). The amino terminus of Epstein-Barr Virus (EBV) nuclear antigen 1 contains AT hooks that facilitate the replication and partitioning of latent EBV genomes by tethering them to cellular chromosomes. *Journal of Virology* 78, 11487–11505.
- Sen, P.K. (1968). Estimates of the Regression Coefficient Based on Kendall's Tau. *J Am Stat Assoc* 63, 1379–1389.
- Servant, N., Lajoie, B.R., Nora, E.P., Giorgetti, L., Chen, C.-J., Heard, E., Dekker, J., and Barillot, E. (2012). HiTC: exploration of high-throughput “C” experiments. *Bioinformatics* 28, 2843–2844.
- Seto, E., Yang, L., Middeldorp, J., Sheen, T.-S., Chen, J.-Y., Fukayama, M., Eizuru, Y., Ooka, T., and Takada, K. (2005). Epstein-Barr virus (EBV)-encoded BARF1 gene is expressed in nasopharyngeal carcinoma and EBV-associated gastric carcinoma tissues in the absence of lytic gene expression. *J. Med. Virol.* 76, 82–88.
- Shannon-Lowe, C., and Rowe, M. (2011). Epstein-Barr virus infection of polarized epithelial cells via the basolateral surface by memory B cell-mediated transfer infection. *PLoS Pathog* 7, e1001338.



- Shinozaki-Ushiku, A., Kunita, A., Isogai, M., Hibiya, T., Ushiku, T., Takada, K., and Fukayama, M. (2015). Profiling of Virus-Encoded MicroRNAs in Epstein-Barr Virus-Associated Gastric Carcinoma and Their Roles in Gastric Carcinogenesis. *Journal of Virology* *89*, 5581–5591.
- Silva, L., Oh, H.S., Chang, L., Yan, Z., Triezenberg, S.J., and Knipe, D.M. (2011). Roles of the Nuclear Lamina in Stable Nuclear Association and Assembly of a Herpesviral Transactivator Complex on Viral Immediate-Early Genes. *mBio* *3*, e00300–11–e00300–11.
- Silva, L., Cliffe, A., Chang, L., and Knipe, D.M. (2008). Role for A-Type Lamins in Herpesviral DNA Targeting and Heterochromatin Modulation. *PLoS Pathog* *4*, e1000071.
- Sun, X., Bristol, J.A., Iwahori, S., Hagemeyer, S.R., Meng, Q., Barlow, E.A., Fingerroth, J.D., Tarakanova, V.L., Kalejta, R.F., and Kenney, S.C. (2013). Hsp90 inhibitor 17-DMAG decreases expression of conserved herpesvirus protein kinases and reduces virus production in Epstein-Barr virus-infected cells. *Journal of Virology* *87*, 10126–10138.
- Tempera, I., and Lieberman, P.M. (2010). Chromatin organization of gammaherpesvirus latent genomes. *BBA - Gene Regulatory Mechanisms* *1799*, 236–245.
- Tempera, I., Klichinsky, M., and Lieberman, P.M. (2011). EBV latency types adopt alternative chromatin conformations. *PLoS Pathog* *7*, e1002180.
- Tempera, I., Wiedmer, A., Dheekollu, J., and Lieberman, P.M. (2010). CTCF Prevents the Epigenetic Drift of EBV Latency Promoter Qp. *PLoS Pathog* *6*, e1001048.
- Thompson, M.P., and Kurzrock, R. (2004). Epstein-Barr virus and cancer. *Clin Cancer Res* *10*, 803–821.
- Tolani, B., Gopalakrishnan, R., Punj, V., Matta, H., and Chaudhary, P.M. (2014). Targeting Myc in KSHV-associated primary effusion lymphoma with BET bromodomain inhibitors. *Oncogene* *33*, 2928–2937.
- Tomicic, M.T., Thust, R., and Kaina, B. (2002). Ganciclovir-induced apoptosis in HSV-1 thymidine kinase expressing cells: critical role of DNA breaks, Bcl-2 decline and caspase-9 activation. *Oncogene* *21*, 2141–2153.

Tomkinson, B., Robertson, E., and Kieff, E. (1993). Epstein-Barr virus nuclear proteins EBNA-3A and EBNA-3C are essential for B-lymphocyte growth transformation. *Journal of Virology* *67*, 2014–2025.

Torgbor, C., Awuah, P., Deitsch, K., Kalantari, P., Duca, K.A., and Thorley-Lawson, D.A. (2014). A multifactorial role for *P. falciparum* malaria in endemic Burkitt's lymphoma pathogenesis. *PLoS Pathog* *10*, e1004170.

Tovey, M.G., Lenoir, G., and Begon-Lours, J. (1978). Activation of latent Epstein-Barr virus by antibody to human IgM. *Nature* *276*, 270–272.

Tsao, S.-W., Tsang, C.M., To, K.-F., and Lo, K.-W. (2015). The role of Epstein-Barr virus in epithelial malignancies. *J. Pathol.* *235*, 323–333.

Ushiku, T., Chong, J.-M., Uozaki, H., Hino, R., Chang, M.-S., Sudo, M., Rani, B.R., Sakuma, K., Nagai, H., and Fukayama, M. (2007). p73 gene promoter methylation in Epstein-Barr virus-associated gastric carcinoma. *Int J Cancer* *120*, 60–66.

van Rees, B.P., Caspers, E., Hausen, zur, A., van den Brule, A., Drillenburger, P., Weterman, M.A.J., and Offerhaus, G.J.A. (2002). Different pattern of allelic loss in Epstein-Barr virus-positive gastric cancer with emphasis on the p53 tumor suppressor pathway. *The American Journal of Pathology* *161*, 1207–1213.

Vereide, D.T., Seto, E., Chiu, Y.-F., Hayes, M., Tagawa, T., Grundhoff, A., Hammerschmidt, W., and Sugden, B. (2014). Epstein-Barr virus maintains lymphomas via its miRNAs. *Oncogene* *33*, 1258–1264.

Vockerodt, M., Haier, B., Buttgereit, P., Tesch, H., and Kube, D. (2001). The Epstein-Barr virus latent membrane protein 1 induces interleukin-10 in Burkitt's lymphoma cells but not in Hodgkin's cells involving the p38/SAPK2 pathway. *Virology* *280*, 183–198.

Volpi, E.V., Chevret, E., Jones, T., Vatcheva, R., Williamson, J., Beck, S., Campbell, R.D., Goldsworthy, M., Powis, S.H., Ragoussis, J., et al. (2000). Large-scale chromatin organization of the major histocompatibility complex and other regions of human chromosome 6 and its response to interferon in interphase nuclei. *Journal of Cell Science* *113*, 1565–1576.

Walling, D.M., Flaitz, C.M., and Nichols, C.M. (2003). Epstein-Barr virus replication in oral hairy leukoplakia: response, persistence, and resistance to treatment with valacyclovir. *J Infect Dis* 188, 883–890.

Wang, D., Liebowitz, D., and Kieff, E. (1985). An EBV membrane protein expressed in immortalized lymphocytes transforms established rodent cells. *Cell* 43, 831–840.

Wang, K., Yuen, S.T., Xu, J., Lee, S.P., Yan, H.H.N., Shi, S.T., Siu, H.C., Deng, S., Chu, K.M., Law, S., et al. (2014). Whole-genome sequencing and comprehensive molecular profiling identify new driver mutations in gastric cancer. *Nat Genet* 46, 573–582.

Wang, S., Su, J.-H., Beliveau, B.J., Bintu, B., Moffitt, J.R., Wu, C.-T., and Zhuang, X. (2016). Spatial organization of chromatin domains and compartments in single chromosomes. *Science* 353, 598–602.

Wang, X., and McManus, M. (2009). Lentivirus production. *JoVE*.

Wang, Z., Zang, C., Rosenfeld, J.A., Schones, D.E., Barski, A., Cuddapah, S., Cui, K., Roh, T.-Y., Peng, W., Zhang, M.Q., et al. (2008). Combinatorial patterns of histone acetylations and methylations in the human genome. *Nat Genet* 40, 897–903.

Wei, M.X., and Ooka, T. (1989). A transforming function of the BARF1 gene encoded by Epstein-Barr virus. *Embo J* 8, 2897–2903.

Wei, M.X., Moulin, J.C., Decaussin, G., Berger, F., and Ooka, T. (1994). Expression and tumorigenicity of the Epstein-Barr virus BARF1 gene in human Louckes B-lymphocyte cell line. *Cancer Research* 54, 1843–1848.

Wen, W., Iwakiri, D., Yamamoto, K., Maruo, S., Kanda, T., and Takada, K. (2007). Epstein-Barr virus BZLF1 gene, a switch from latency to lytic infection, is expressed as an immediate-early gene after primary infection of B lymphocytes. *Journal of Virology* 81, 1037–1042.

Westphal, E.M., Blackstock, W., Feng, W., Israel, B., and Kenney, S.C. (2000). Activation of lytic Epstein-Barr virus (EBV) infection by radiation and sodium butyrate in vitro and in vivo: a potential method for treating EBV-positive malignancies. *Cancer Research* 60, 5781–5788.

Whalen, S., Truty, R.M., and Pollard, K.S. (2016). Enhancer-promoter interactions are encoded by complex genomic signatures on looping chromatin. *Nat Genet* 48, 488–496.

Wildeman, M.A., Novalic, Z., Verkuijlen, S.A.W.M., Juwana, H., Huitema, A.D.R., Tan, I.B., Middeldorp, J.M., de Boer, J.P., and Greijer, A.E. (2012). Cytolytic virus activation therapy for Epstein-Barr virus-driven tumors. *Clin Cancer Res* 18, 5061–5070.

Williams, A.G., Thomas, S., Wyman, S.K., and Holloway, A.K. (2014). RNA-seq Data: Challenges in and Recommendations for Experimental Design and Analysis. *Curr Protoc Hum Genet* 83, 11.13.1–13.20.

Wingett, S., Ewels, P., Furlan-Magaril, M., Nagano, T., Schoenfelder, S., Fraser, P., and Andrews, S. (2015). HiCUP: pipeline for mapping and processing Hi-C data. *F1000Res* 4.

Wollebo, H.S., Bellizzi, A., Cossari, D.H., Salkind, J., Safak, M., and White, M.K. (2016). The Brd4 acetyllysine-binding protein is involved in activation of polyomavirus JC. *J. Neurovirol.* 22, 615–625.

You, J., Croyle, J.L., Nishimura, A., Ozato, K., and Howley, P.M. (2004). Interaction of the bovine papillomavirus E2 protein with Brd4 tethers the viral DNA to host mitotic chromosomes. *Cell* 117, 349–360.

You, J., Srinivasan, V., Denis, G.V., Harrington, W.J., Ballestas, M.E., Kaye, K.M., and Howley, P.M. (2006). Kaposi's sarcoma-associated herpesvirus latency-associated nuclear antigen interacts with bromodomain protein Brd4 on host mitotic chromosomes. *Journal of Virology* 80, 8909–8919.

Young, L.S., Dawson, C.W., Clark, D., Rupani, H., Busson, P., Tursz, T., Johnson, A., and Rickinson, A.B. (1988). Epstein-Barr virus gene expression in nasopharyngeal carcinoma. *J. Gen. Virol.* 69 (Pt 5), 1051–1065.

Young, L.S., Lau, R., Rowe, M., Niedobitek, G., Packham, G., Shanahan, F., Rowe, D.T., Greenspan, D., Greenspan, J.S., and Rickinson, A.B. (1991). Differentiation-associated expression of the Epstein-Barr virus BZLF1 transactivator protein in oral hairy leukoplakia. *Journal of Virology* 65, 2868–2874.

Young, L.S., and Rickinson, A.B. (2004). Epstein–Barr virus: 40 years on. *Nat Rev Cancer* 4, 757–768.

Young, L.S., Yap, L.-F., and Murray, P.G. (2016). Epstein–Barr virus: more than 50 years old and still providing surprises. *Nature Publishing Group* 16, 789–802.

Zhu, J., Gaiha, G.D., John, S.P., Pertel, T., Chin, C.R., Gao, G., Qu, H., Walker, B.D., Elledge, S.J., and Brass, A.L. (2012). Reactivation of latent HIV-1 by inhibition of BRD4. *Cell Rep* 2, 807–816.

Zink, D., Amaral, M.D., Englmann, A., Lang, S., Clarke, L.A., Rudolph, C., Alt, F., Luther, K., Braz, C., Sadoni, N., et al. (2004). Transcription-dependent spatial arrangements of CFTR and adjacent genes in human cell nuclei. *J Cell Biol* 166, 815–825.

Zullo, J.M., Demarco, I.A., Piqué-Regi, R., Gaffney, D.J., Epstein, C.B., Spooner, C.J., Luperchio, T.R., Bernstein, B.E., Pritchard, J.K., Reddy, K.L., et al. (2012). DNA sequence-dependent compartmentalization and silencing of chromatin at the nuclear lamina. *Cell* 149, 1474–1487.

TABLE 1

<b>EBV genes differentially regulated by JQ1 during viral reactivation<sup>a</sup></b>			
<b>Gene</b>	<b>Coordinates</b>	<b>Log<sub>2</sub> fold change</b>	<b>P-value</b>
<b>Late (12 out of 18 change expression level)</b>			
BNRF1	1691-5407	-1.50	0.010
BCRF1	9631-10262	-0.88	0.004
BOLF1	59905-62728	+0.12	0.837
BORF1	63035-63880	+0.07	0.908
BSRF1	74594-75316	-0.02	0.739
BLRF1	76232-76574	-1.41	0.031
BLLF1	77764-79904	-1.79	0.001
BZLF2	89483-89828	-1.90	0.004
BRRF2	93955-95631	-1.44	0.009
BKRF2	97655-98064	-1.71	0.015
BBRF1	101972-103659	-0.70	0.064
BBRF3	106751-108075	-1.37	0.032
BGRF1/BDRF1	112826-113190, 117017-118064	-1.08	0.028
BDLF1	120189-121018	-1.52	0.003
BcLF1	121099-125072	-1.79	0.004
BXRF1	132847-133012	-0.73	0.098
BVRF2	135628-136330	-1.42	0.010
BILF2	137464-138282	-0.74	0.080
<b>Early (0 out of 18 change expression level)</b>			
BHLF1	38014-40529	-0.92	0.069
BHRF1	41471-43251	-1.14	0.129
BFLF1	44794-46235	-0.68	0.139
BaRF1	66601-67551	-0.31	0.377
BSLF1 <sup>b</sup>	72069-74593	-0.48	0.208
BLLF3	75320-76218	-0.31	0.330
BRLF1 <sup>b</sup>	90907-92727	-0.03	0.713
BRRF1	92898-93827	-0.35	0.255
BBLF4 <sup>b</sup>	99537-101587	-0.35	0.258
BBLF2_3 <sup>b</sup>	104503-105098, 105227-106692	+0.03	0.793
BcRF1	125423-127415	-0.39	0.324
BXLF1	131022-132570	+0.11	0.859
LF3	140692-143711	-0.25	0.306
BALF5 <sup>b</sup>	152642-155265	-0.28	0.214
BALF3	160532-160549	-0.47	0.209
BALF2 <sup>b</sup>	160909-164356	-0.42	0.269
BALF1	164388-164984	-0.82	0.239
BARF1	165008-165712	-0.71	0.166
<b>Unassigned (0 out of 6 change expression level)</b>			
BCLT1	5868-6136	-0.66	0.157
BCLT2	6172-6475	-0.51	0.216
BFRF1A	46281-46543	-0.49	0.158
BGLF3	111830-112649	-0.95	0.079
BDLF3.5	116767-116926	-0.86	0.064
BVLF1	134887-135431	-0.44	0.332

<sup>a</sup> Row shading indicates differentially regulated genes with a p-value < 0.05.

<sup>b</sup> Protein product required for lytic DNA replication.

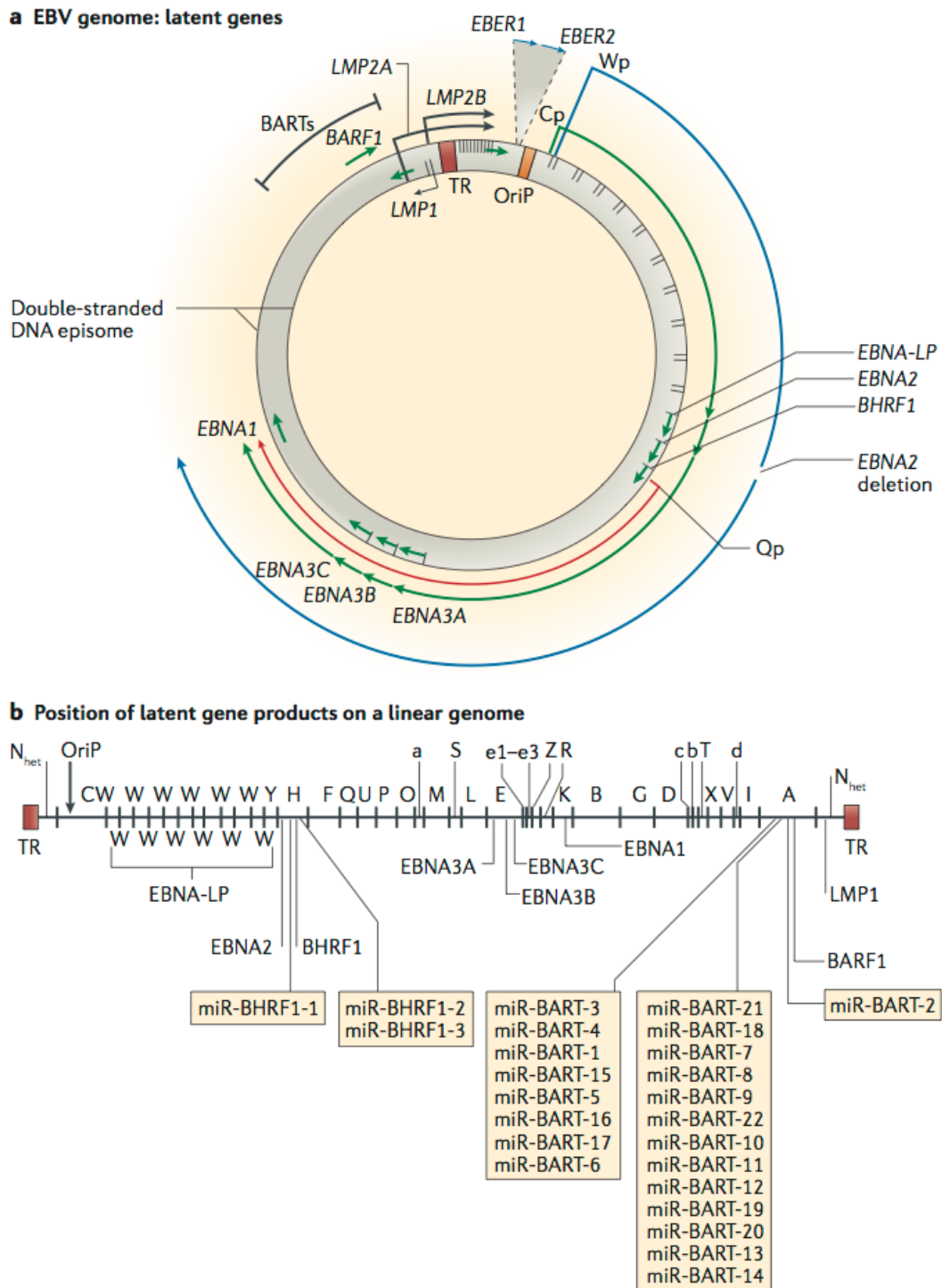
**Table 1. EBV genes differentially regulated by JQ1 during viral reactivation.**

TABLE 2

**EBV genes differentially regulated by I-BET during viral reactivation<sup>a</sup>**

Gene	Coordinates	Log <sub>2</sub> fold change	P-value
<b>Late (4 out of 18 change expression level)</b>			
BNRF1	1691-5407	-0.68	0.038
BCRF1	9631-10262	+0.03	0.929
BOLF1	59905-62728	-0.29	0.485
BORF1	63035-63880	-0.22	0.621
BSRF1	74594-75316	+0.27	0.418
BLRF1	76232-76574	-0.54	0.127
BLLF1	77764-79904	-0.73	0.112
BZLF2	89483-89828	-0.94	0.233
BRRF2	93955-95631	-0.54	0.115
BKRF2	97655-98064	-0.78	0.009
BBRF1	101972-103659	-0.11	0.504
BBRF3	106751-108075	-0.48	0.088
BGRF1/BDRF1	112826-113190, 117017-118064	-0.43	0.008
BDLF1	120189-121018	-0.60	0.333
BcLF1	121099-125072	-0.80	0.075
BXRF1	132847-133012	-0.14	0.611
BVRF2	135628-136330	-0.65	0.095
BILF2	137464-138282	-0.28	0.017
<b>Early (0 out of 18 change expression level)</b>			
BHLF1	38014-40529	-0.45	0.297
BHRF1	41471-43251	-0.56	0.054
BFLF1	44794-46235	-0.28	0.473
BaRF1	66601-67551	-0.23	0.445
BSLF1 <sup>b</sup>	72069-74593	-0.20	0.578
BLLF3	75320-76218	-0.21	0.458
BRLF1 <sup>b</sup>	90907-92727	+0.07	0.796
BRRF1	92898-93827	-0.10	0.689
BBLF4 <sup>b</sup>	99537-101587	-0.19	0.180
BBLF2/BBLF3 <sup>b</sup>	104503-105098, 105227-106692	+0.10	0.653
BcRF1	125423-127415	+0.04	0.801
BXLF1	131022-132570	+0.22	0.618
LF3	140692-143711	-0.10	0.667
BALF5 <sup>b</sup>	152642-155265	-0.22	0.311
BALF3	160532-160549	-0.59	0.216
BALF2 <sup>b</sup>	160909-164356	-0.38	0.375
BALF1	164388-164984	-0.24	0.356
BARF1	165008-165712	-0.38	0.078
<b>Unassigned (0 out of 6 change expression level)</b>			
BCLT1	5868-6136	+0.26	0.995
BCLT2	6172-6475	+0.18	0.827
BFRF1A	46281-46543	-0.13	0.794
BGLF3	111830-112649	-0.30	0.348
BDLF3.5	116767-116926	-0.11	0.764
BVLF1	134887-135431	-0.22	0.512

<sup>a</sup> Row shading indicates differentially regulated genes with a p-value < 0.05.<sup>b</sup> Protein product required for lytic DNA replication.**Table 2. EBV genes differentially regulated by I-BET during viral reactivation.**



**Figure 1. EBV and its latent genes in 2016.** (A) Location and transcription of Epstein–Barr virus (EBV) latent genes on the double-stranded viral DNA episome. The origin of plasmid replication (OriP) is shown in orange. The short thick green arrows represent exons encoding



latent proteins: six Epstein–Barr nuclear antigens (EBNAs 1, 2, 3A, 3B and 3C, and EBNA-LP), latent membrane proteins (LMPs 1, 2A and 2B), BamHI fragment H rightward open reading frame (BHRF1) and BamHI-A fragment rightward reading frame (BARF1). The short blue arrows at the top represent the highly transcribed non-polyadenylated EBV-encoded RNAs (*EBER1* and *EBER2*). The middle long green arrow represents EBV transcription during latency III, in which all the EBNAs are transcribed from either the Cp or Wp promoter; the different EBNAs are encoded by individual mRNAs that are generated by differential splicing of the same long primary transcript. The inner red arrow represents the *EBNA1* transcript, which originates from the Qp promoter during latency I and latency II. Latency II is characterized by expression of EBNA1 together with the LMPs. Wp-restricted latency is initiated from the Wp promoter and there is expression of all the EBNAs, except EBNA2, which is deleted in this form of latency (outer long blue arrow). (B) Location of open reading frames for EBV latent proteins on the BamHI restriction map of the prototype EBV B95-8 genome including the viral microRNAs (miRs) in sequence order. The BamHI fragments are named according to size, with A being the largest. Lower-case letters indicate the smallest fragments. TR refers to the terminal repeats at each end of the genome. This region was often referred to as  $N_{het}$  to indicate heterogeneity in this region according to the number of TRs within different virus isolates. BART, BamHI-A rightward transcript.

Reprinted from (Young et al., 2016)

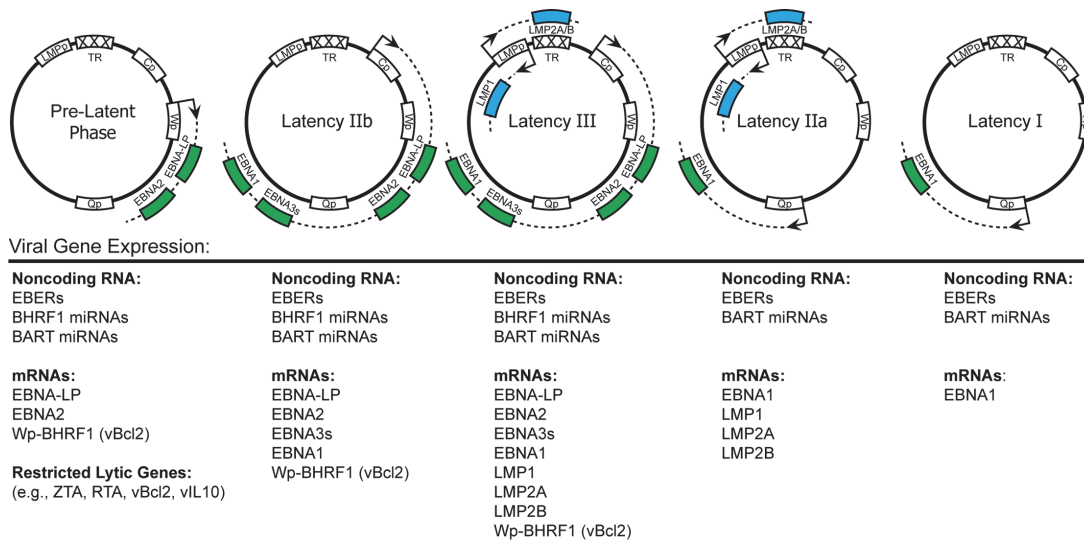


**Figure 2. EBV latency gene expression in different latency states.** This figure depicts, from left to right, the theoretical progression of EBV latency gene expression from initial infection to true latency. The EBV genome is shown in episomal form closed at the terminal repeats (TR). Promoters are shown as white boxes and include the EBNA promoters Cp, Wp, and Qp as well as the bidirectional LMPp. Primary mRNA transcripts are shown as dotted lines, while coding regions have been simplified as colored boxes. An expanded list of viral genes expressed in each latency state is listed directly underneath the representative schematic.

Reprinted from (Price and Luftig, 2015)

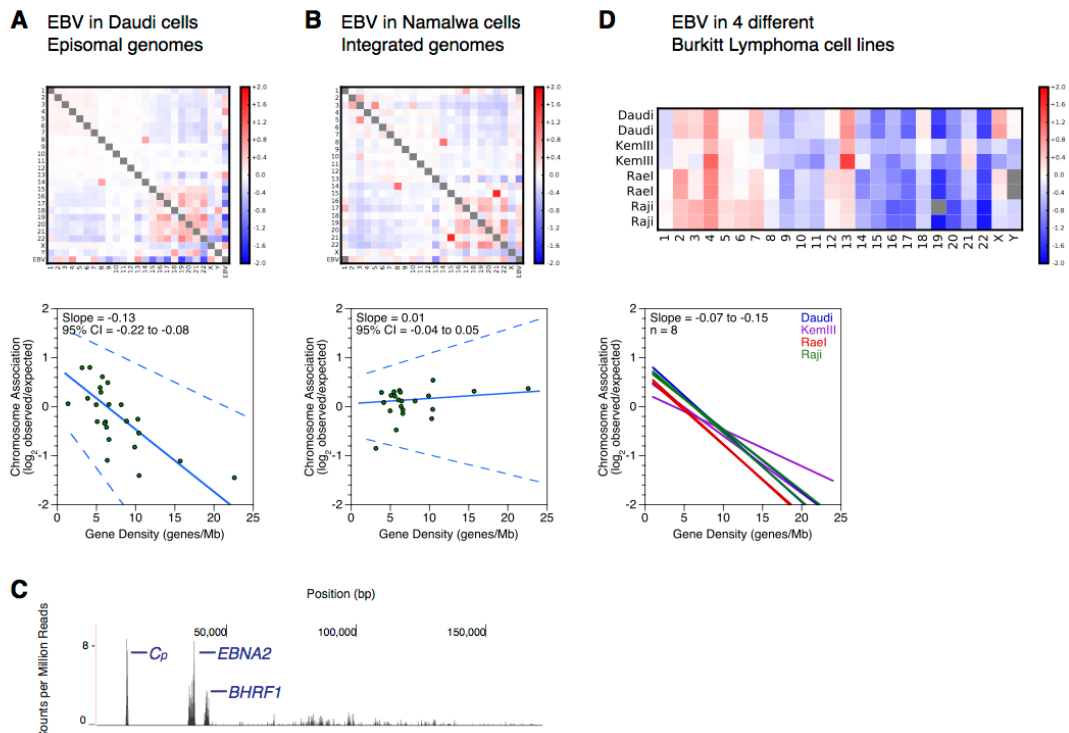


**Figure 3. Episomal EBV genomes associate with the human genome in correlation with chromosomal gene density.** (A, B) Interchromosomal contacts involving the EBV and human genomes in the Daudi and Namalwa cell lines measured by Hi-C. Heatmaps of chromosome association between chromosomes and between each human chromosome and the EBV genome. Observed counts are normalized against random expectation and shown on a log<sub>2</sub> scale. Red indicates enrichment and blue indicates depletion. Below, scatterplots depict virus-human chromosome association plotted against gene density of each chromosome. Solid line indicates the Thiel-Sen fit and the dashed lines indicate the 95% confidence interval. (C) Deep sequencing of EBV transcription in the Namalwa cell line. The X axis denotes nucleotide position and the Y axis denotes the number of counts per million mapped reads. RNA signals with unambiguously assignable annotations are marked. *BHRF1*, *Cp*, and *EBNA2* are latent transcripts labeled blue. One representative transcriptome from two independent replicates is shown. (D) Interchromosomal contacts between the EBV and human genomes in Burkitt lymphoma cell lines measured by Hi-C. Heatmaps of chromosome association between each human chromosome and the EBV genome in different Burkitt lymphoma cell lines. Shown are two replicates of four different cell lines: Daudi, KemII, Rael, and Raji. Observed counts are

normalized against random expectation and shown on a log<sub>2</sub> scale. Red indicates enrichment and blue indicates depletion. Gray boxes represent either Y chromosomes not present in the female RaeI cell line or a score with absolute value greater than 2. Below, solid lines indicate the Thiel-Sen fit of virus-human chromosome association plotted against gene density of each chromosome. Each line represents one of two independent biological replicates for four different cell lines. See also Figure S1.

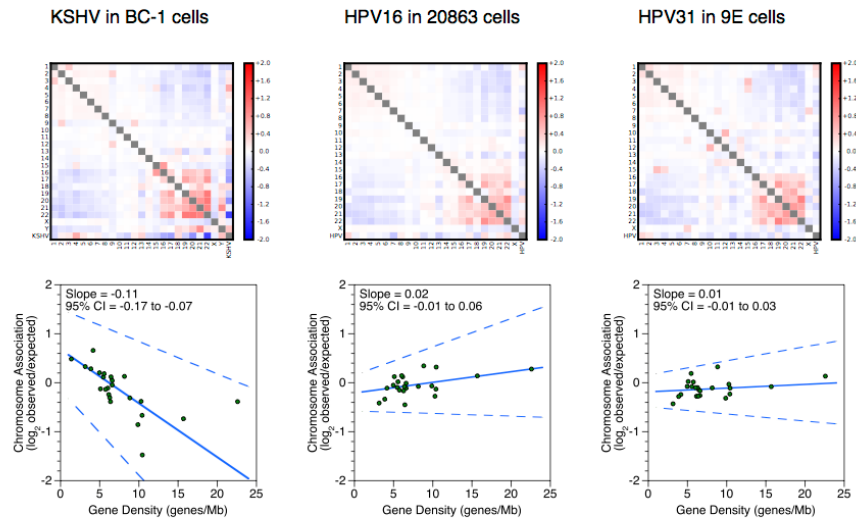


**Figure 4. KSHV but not HPV genomes associate with the human genome in correlation with chromosomal gene density.** Interchromosomal contacts involving the KSHV, HPV, and human genomes in the BC-1, 20863, and 9E cell lines measured by Hi-C. Heatmaps of chromosome association between chromosomes and between each human chromosome and the KSHV or HPV genome. Observed counts are normalized against random expectation and shown on a log<sub>2</sub> scale. Red indicates enrichment and blue indicates depletion. Scatterplot shows the correlation between gene density of each chromosome and the virus-human chromosome association. Solid line indicates the Thiel-Sen fit and the dashed lines indicate the 95% confidence interval.

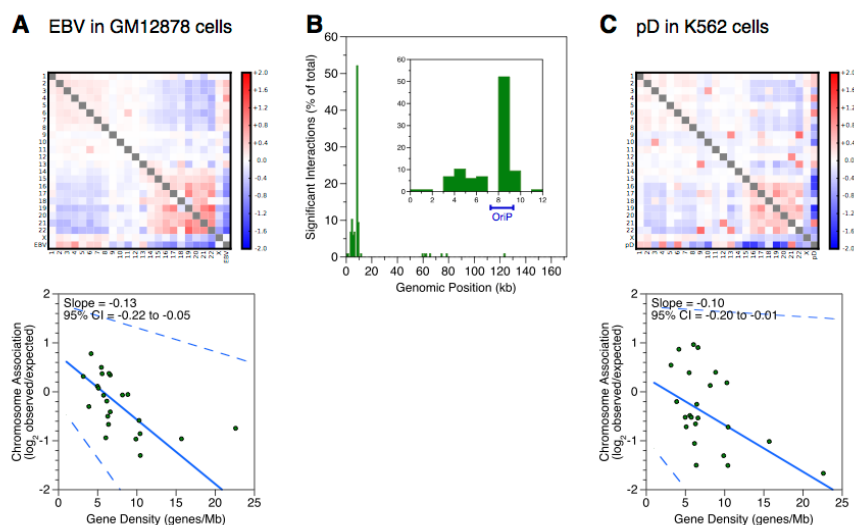


**Figure 5. OriP-bound EBNA1 is sufficient to reconstitute chromosome association**

**preferences of full-length EBV.**

(A, C) Interchromosomal contacts involving EBV genomes, the pD plasmid, and human genomes in the reanalyzed GM12878 data set and K562 cell line measured by Hi-C. Heatmap of chromosome association between chromosomes and between each human chromosome and the EBV genome or pD plasmid. Observed counts are normalized against random expectation and shown on a log<sub>2</sub> scale. Red indicates enrichment and blue indicates depletion. Scatterplot shows the correlation between gene density of each chromosome and the plasmid-human chromosome association. Solid line indicates the Thiel-Sen fit and the dashed lines indicate the 95% confidence interval. (B) Localization within the EBV genome of significant interchromosomal contacts involving human chromosomes in the reanalyzed GM12878 data set. Histogram of unique significant interactions between human chromosomes and the EBV episome. The percentage of total interactions are plotted against position on the EBV genome in 1 kb bins. Inset depicts a zoom view of the first 10 kb of the viral genome.

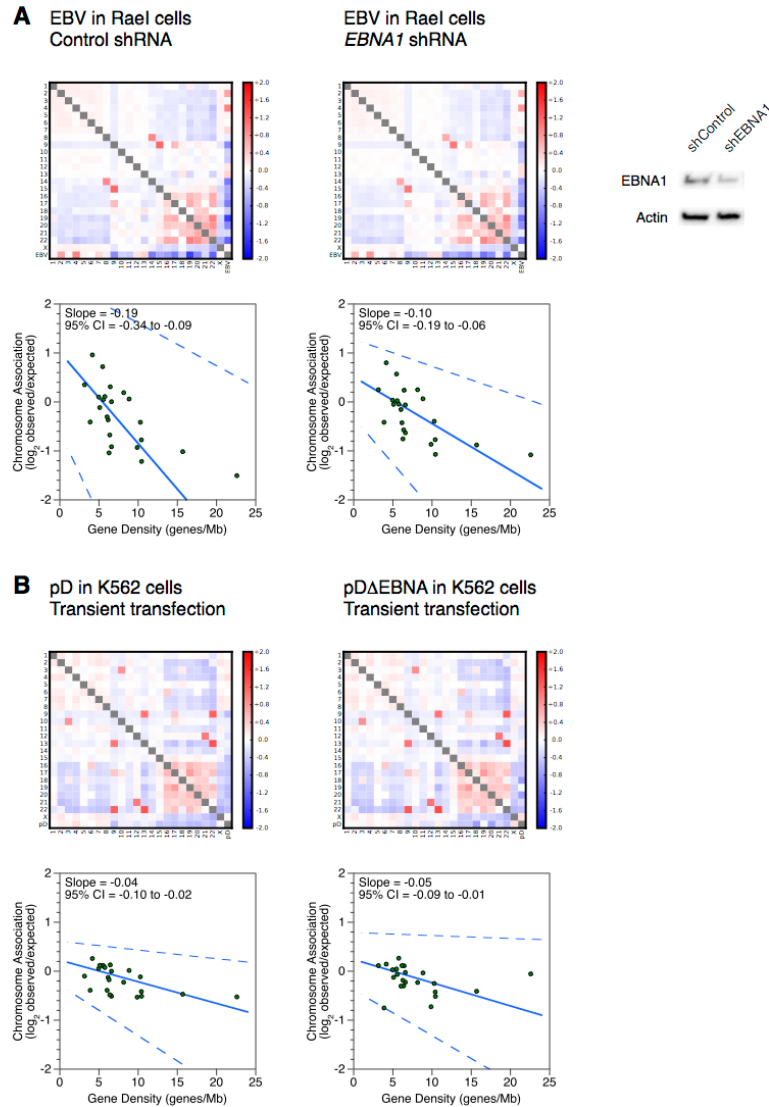


**Figure 6. EBNA1 is not necessary to reconstitute chromosome association preferences of full length EBV.** (A, B) Interchromosomal contacts involving the pD plasmid, pDΔEBNA plasmid, EBV genomes, and human genomes in the RaelI and K562 cell lines measured by Hi-C. Heatmap of chromosome association between chromosomes and between each human chromosome and the EBV genome, pD plasmid, or pDΔEBNA plasmid. Observed counts are normalized against random expectation and shown on a log<sub>2</sub> scale. Red indicates enrichment and blue indicates depletion. Scatterplot shows the correlation between gene density of each chromosome and the plasmid human chromosome association. Solid line indicates the Thiel-Sen fit and the dashed lines indicate the 95% confidence interval. (A) Lentivirus mediated shRNA depletion of the EBV EBNA1 protein in the RaelI cell line. Western blots depict EBNA1 and β

actin expression levels in whole cell lysates after control or EBNA1 knockdown. (B) Deletion of the EBV EBNA1 gene in the pD $\Delta$ EBNA plasmid in the K562 cell line. pD and pD $\Delta$ EBNA are transiently transfected prior to measurement of interchromosomal contacts by Hi-C.



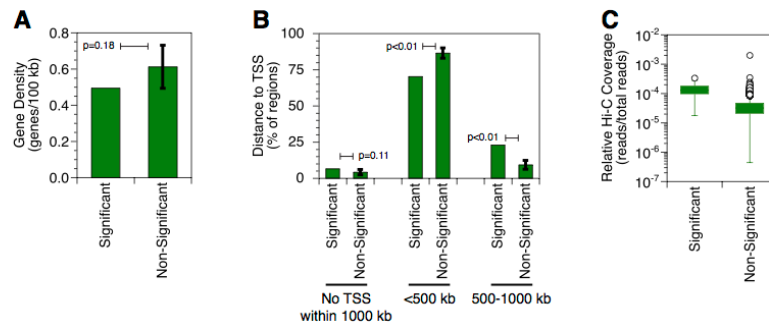


**Figure 7. EBV episomes contact gene-poor human chromatin distant from transcription**

**start sites.** (A) Gene density of human genome regions that interact with the EBV episome in the reanalyzed GM12878 data set. The single set of significant interacting regions are compared to randomly chosen and equally large subsets of non-significant interacting regions. Error bar represents the standard deviation of 100 replicates resulting in an empirical p-value. (B) Distance to nearest TSS from human genome regions that interact with the EBV episome in the reanalyzed GM12878 data set. The single set of significant interacting regions are compared to randomly chosen and equally large subsets of non-significant interacting regions. Error bars represent the standard deviation of 100 replicates resulting in an empirical p-value. (C) Gene density of human genome regions that interact with the EBV episome in the reanalyzed GM12878 data set. Box and whisker plots for relative Hi-C coverage of human genome regions that interact significantly with the EBV genome compared to background. All significant interacting regions are compared to all non-significant interacting regions. Each box depicts 50% of the data. Whiskers extend 150% of the interquartile distance from the upper and lower quartiles with outliers shown as circles.

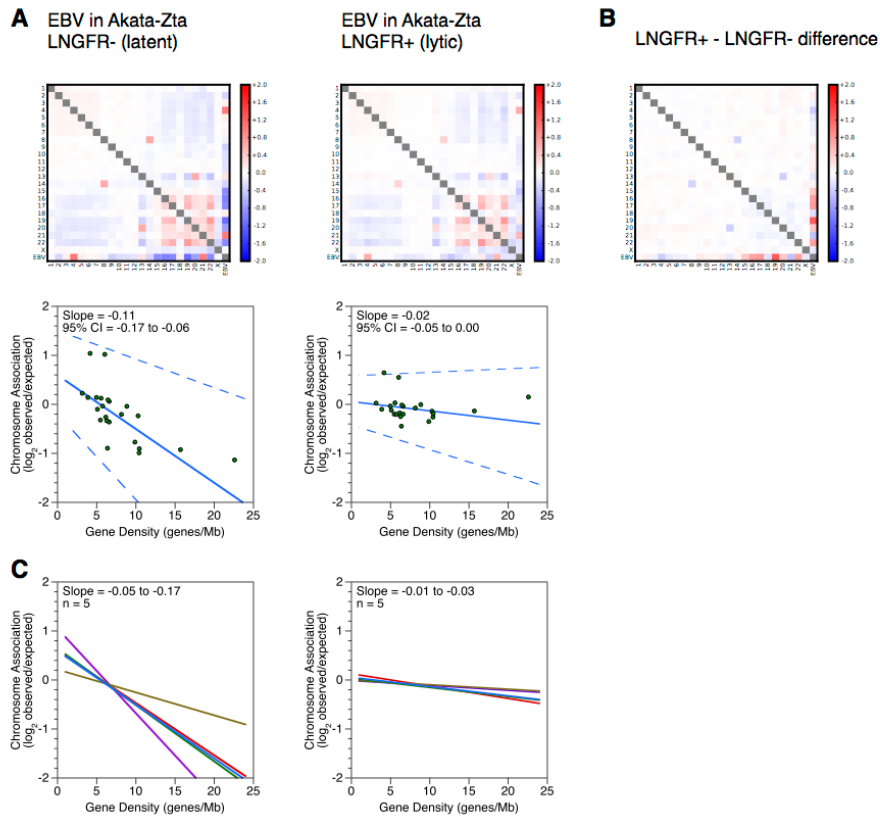


**Figure 8. Chromosome association preferences of EBV episomes restructure during**

**reactivation.** (A) Interchromosomal contacts involving the EBV and human genomes in the Akata ZTA cell line measured by Hi-C. LNGFR and LNGFR+ cells contain latent and lytic episomes, respectively. Heatmaps of chromosome association between chromosomes and between each human chromosome and the EBV genome during latency and reactivation. Observed counts are normalized against random expectation and shown on a log<sub>2</sub> scale. Red indicates enrichment and blue indicates depletion. Below, scatterplots depict virus human chromosome association plotted against gene density of each chromosome. Solid line indicates the Thiel-Sen fit and the dashed lines indicate the 95% confidence interval. Results are representative of five independent and paired biological replicates. (B) Changes in interchromosomal contacts involving the EBV and human genomes in the Akata ZTA cell line upon reactivation measured by Hi-C. Subtraction heatmap depicting differences between latent and lytic chromosome associations shown in (A). Chromosome association values during latency were subtracted from values during reactivation. Results are representative of

five independent and paired biological replicates. (C) Interchromosomal contacts between the EBV and human genomes in the Akata ZTA cell line measured by Hi-C. LNGFR and LNGFR+ cells contain latent and lytic episomes, respectively. Solid lines indicate the Thiel-Sen fit of virus human chromosome association plotted against gene density of each chromosome. Each line represents one of five independent biological replicates. Paired comparisons are matched by color.

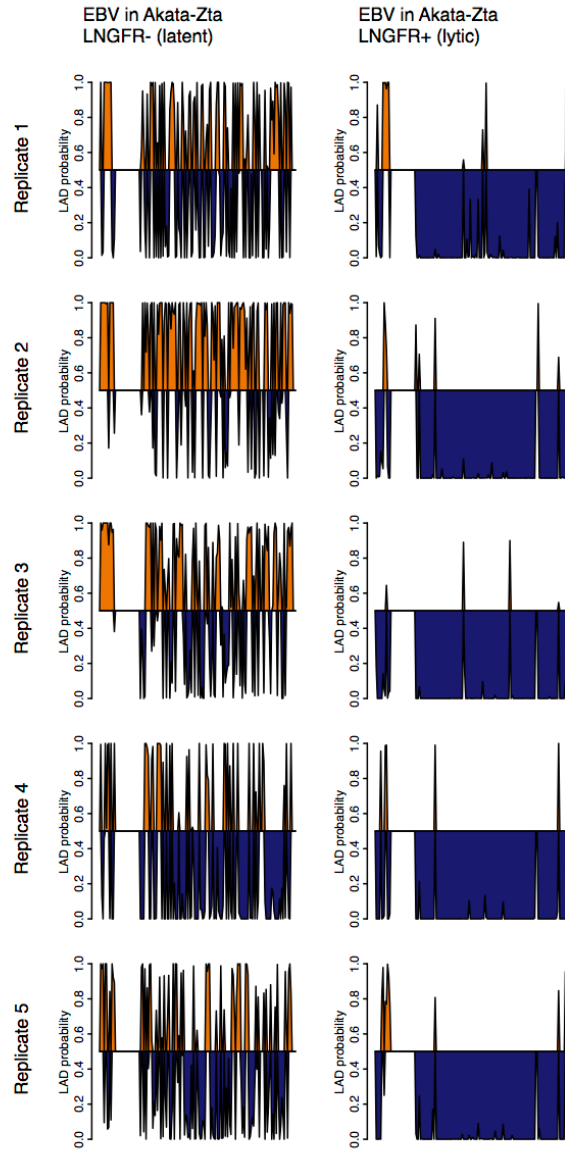


**Figure 9. Predicted association of the EBV genome with LADs during latency and reactivation in the Akata ZTA cell line.** LNGFR and LNGFR+ cells contain latent and lytic episomes, respectively. The probability of LAD association is plotted against position on the viral genome divided into 1 kb bins. Probabilities greater than 0.5 are shaded orange; probabilities less than 0.5 are shaded blue. Shown are five independent and paired biological replicates.

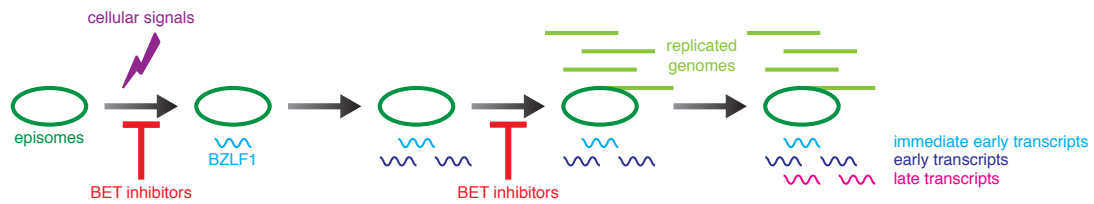


**Figure 10. Schematic of the EBV lytic cycle and BET inhibitor points of intervention.** Each arrow indicates one sequential step in the cascade: cellular signals induce immediate-early gene expression, immediate-early proteins transactivate early genes, early gene products license lytic DNA replication, and lytic DNA replication promotes late gene expression. Data presented in this paper provide evidence that BET inhibitors suppress immediate-early gene expression and lytic DNA replication.

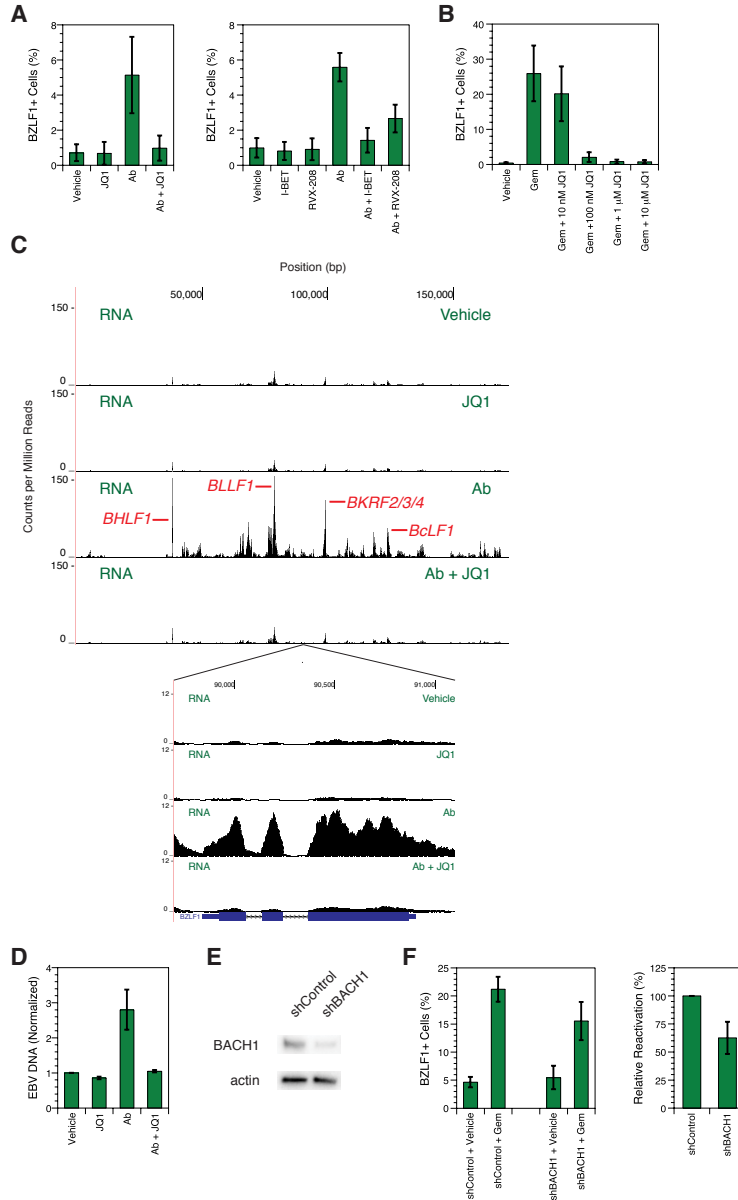


**Figure 11. BET inhibitors suppress BZLF1 expression.** (A) flow cytometry analysis of BZLF1 staining in MutuI cells treated with antibody (Ab). Error bars show the standard deviation of  $n = 8$  (left) or  $n = 4$  (right) replicates. (B) flow cytometry of BZLF1 staining in MutuI cells treated with gemcitabine. Error bars show the standard deviation of  $n = 4$  replicates. (C) RNA-seq profiles of treated MutuI cells showing the entire EBV genome (top) or the region containing the *BZLF1* gene (inset). Axes denote genomic position in basepairs and counts per million mapped reads. Some major peaks corresponding to lytic gene expression are labeled. Below the inset, the *BZLF1* gene is shown in schematic form where blocks represent exons and lines with arrows represent introns. Results are

representative of three independent biological replicates. (D) fold change in EBV DNA from treated MutuI cells based on deep sequencing of chromatin. EBV content was calculated as a percentage of total sequenced DNA, and for each set, EBV DNA percentage was normalized to that in the vehicle-treated sample. Error bars represent the standard deviation of  $n = 3$  replicates. (E) Western blots of BACH1 expression levels in MutuI cells after shRNA-mediated knockdown.  $\beta$ -actin expression levels are shown as normalization controls. (F) flow cytometry of BZLF1 staining in MutuI cells treated with gemcitabine during BACH1 knockdown. Relative reactivation is calculated as the increase in BZLF1-positive cell percentage relative to the control. Error bars show the standard deviation of  $n = 5$  replicates.

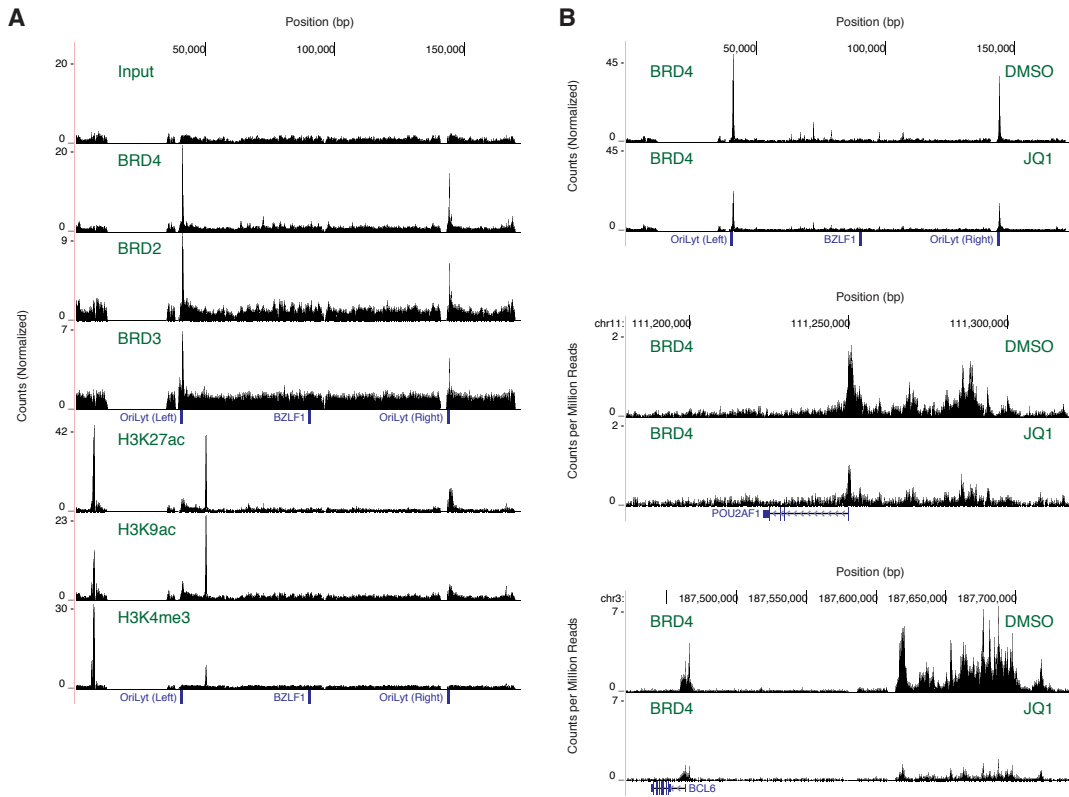


**Figure 12. BET proteins bind the lytic origins of replication.** (A) ChIP-seq mapping of BET protein and histone modification occupancy on the EBV genome in untreated MutuI cells. Input DNA (top) serves as a control reference. Results are representative of two independent biological replicates. (B) ChIP-seq mapping of BRD4 occupancy on the EBV and human genomes in MutuI cells treated with JQ1. Results are representative of two independent biological replicates. For the EBV genome, location of the *BZLF1* gene and the left and right OriLyt elements are indicated. Occupancy is calculated as enrichment over the background baseline. For the human genome, the *POU2AF1* and *BCL6* genes are shown in schematic form where blocks represent exons and lines with arrows represent introns. Occupancy is calculated as counts per million mapped reads.



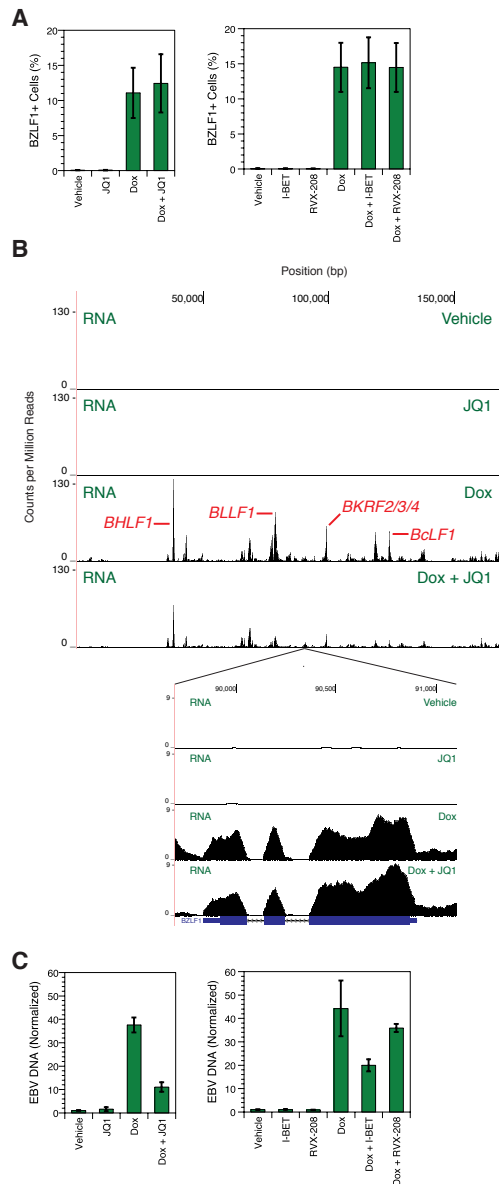


**Figure 13. BET inhibitors suppress lytic DNA replication.** (A) flow cytometry analysis of BZLF1 staining in Akata-Zta cells treated with doxycycline (Dox). Error bars show the standard deviation of n = 4 replicates. (B) RNA-seq profiles of treated Akata-Zta cells showing the entire EBV genome (top) or the region containing the *BZLF1* gene (inset). Axes denote genomic position in basepairs and counts per million mapped reads. Some major peaks corresponding to lytic gene expression are labeled. Below the inset, the *BZLF1* gene is shown in schematic form where blocks represent exons and lines with arrows represent introns. Results are representative

of three independent biological replicates. (C) fold change in EBV DNA from treated Akata-Zta cells based on deep sequencing of chromatin. EBV content was calculated as a percentage of total sequenced DNA, and for each set, EBV DNA was normalized to that in the vehicle-treated sample. Error bars represent the standard deviation of  $n = 3$  replicates.

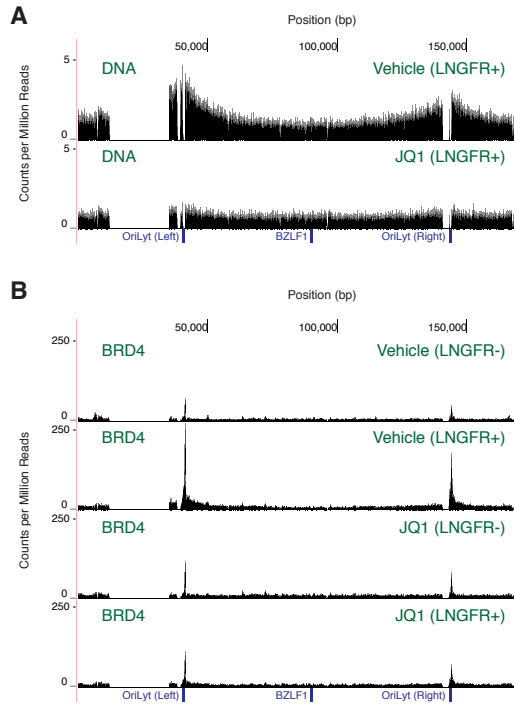



**Figure 14. JQ1 prevents BRD4 recruitment to the lytic origins of replication.** (A) EBV DNA content based on deep sequencing of chromatin from Akata-Zta cells treated with JQ1. Results are representative of two independent biological replicates. (B) ChIP-seq mapping of BRD4 occupancy on the EBV genome in Akata-Zta cells treated with JQ1. Results are representative of two independent biological replicates. All conditions include acyclovir pretreatment and reactivation with doxycycline. Cells containing lytic EBV were purified based on positive LNGFR expression. For the EBV genome, location of the *BZLF1* gene and the left and right OriLyt elements are indicated. Occupancy is calculated as counts per million mapped reads.

**Publishing Agreement**

*It is the policy of the University to encourage the distribution of all theses, dissertations, and manuscripts. Copies of all UCSF theses, dissertations, and manuscripts will be routed to the library via the Graduate Division. The library will make all theses, dissertations, and manuscripts accessible to the public and will preserve these to the best of their abilities, in perpetuity.*

**Please sign the following statement:**

*I hereby grant permission to the Graduate Division of the University of California, San Francisco to release copies of my thesis, dissertation, or manuscript to the Campus Library to provide access and preservation, in whole or in part, in perpetuity.*

  
Author Signature

8/31/17  
Date